

ผลของพอลิเมอร์ต่อสมบัติเจลอิเล็กโทรไลต์ในแบตเตอรี่ชนิดตะกั่ว-กรด

นางสาวอมรรัตน์ ชัยสิทธิ์

วิทยานิพนธ์นี้เป็นส่วนหนึ่งของการศึกษาตามหลักสูตรปริญญาวิทยาศาสตรมหาบัณฑิต

สาขาวิชาปิโตรเคมีและวิทยาศาสตร์พอลิเมอร์

คณะวิทยาศาสตร์ จุฬาลงกรณ์มหาวิทยาลัย

ปีการศึกษา 2551

ลิขสิทธิ์ของจุฬาลงกรณ์มหาวิทยาลัย

EFFECT OF POLYMERS ON GEL ELECTROLYTE PROPERTIES IN LEAD-
ACID BATTERY

Miss Amornrat Chaiyasit

A Thesis Submitted in Partial Fulfillment of the Requirements
for the Degree of Master of Science Program in Petrochemistry and Polymer Science
Faculty of Science
Chulalongkorn University
Academic Year 2008
Copyright of Chulalongkorn University

Thesis Title EFFECT OF POLYMERS ON GEL ELECTROLYTE
 PROPERTIES IN LEAD-ACID BATTERY
By Miss Amornrat Chaiyasit
Field of Study Petrochemistry and Polymer Science
Advisor Associate Professor Orawon Chailapakul, Ph.D.

Accepted by the Faculty of Science, Chulalongkorn University in
Partial Fulfillment of the Requirements for the Master's Degree

.....Dean of the Faculty of Science
(Professor Supot Hannongbua, Dr.rer.nat.)

THESIS COMMITTEE

.....Chairman
(Associate Professor Supawan Tantayanon, Ph.D.)

.....Advisor
(Associate Professor Orawon Chailapakul, Ph.D.)

.....Examiner
(Associate Professor Nuanphun Chantarasiri, Ph.D.)

.....Examiner
(Passapol Ngamukot, Ph.D.)

.....External Examiner
(Weena Siangproh, Ph.D.)

อมรรัตน์ ชัยสิทธิ์: ผลของพอลิเมอร์ต่อสมบัติเจลอิเล็กโทรไลต์ในแบตเตอรี่ชนิดตะกั่ว-กรด.
(EFFECT OF POLYMERS ON GEL ELECTROLYTE PROPERTIES IN LEAD-
ACID BATTERY) อ.ที่ปรึกษาวิทยานิพนธ์หลัก : รศ.ดร. อรวรรณ ชัยลภากุล, 110 หน้า.

งานวิจัยนี้ศึกษาผลของสารเติมแต่งต่อประสิทธิภาพของเจลอิเล็กโทรไลต์ด้วยวิธีวัดค่าการนำไฟฟ้าและค่าความสามารถในการคายประจุของแบตเตอรี่ชนิดตะกั่ว-กรดแบบวาล์วเจลอิเล็กโทรไลต์ที่ประกอบด้วยพุ่มซิลิกา ร้อยละ 2 โดยมีมวลต่อปริมาตร และกรดซัลฟิวริก ร้อยละ 35 โดยมีมวลต่อปริมาตร ให้ค่าการนำไฟฟ้าที่อุณหภูมิ 25 องศาเซลเซียส สูงถึง 838 มิลลิซีเมนตต่อเซนติเมตร เจลอิเล็กโทรไลต์นี้ถูกนำไปศึกษาต่อโดยการเติมสารเติมแต่งชนิดต่างๆ เพื่อเพิ่มประสิทธิภาพในการอัดประจุซ้ำ และ/หรือ กรดฟอสฟอริก เพื่อขยายพื้นผิวของสารไวปฏิกิริยาที่แผ่นบวก อีกทั้งช่วยปรับปรุงอายุการใช้งานให้นานขึ้น และเพื่อเพิ่มค่าการนำไฟฟ้าของเจลอิเล็กโทรไลต์ สารเติมแต่งชนิดต่างๆที่ศึกษาได้แก่ โซเดียมซัลเฟต กรดฟอสฟอริก และพอลิเมอร์นำไฟฟ้า ประกอบด้วย พอลิเอनीลีน พอลิพิโรล และพอลิเพนีสินซัลไฟด์ นอกจากนี้ได้ทำการทดสอบเวลาในการเกิดเจลอิเล็กโทรไลต์ และกระบวนการรวมตัวของออกซิเจน ในเจลอิเล็กโทรไลต์ที่แตกต่างกัน และมีการเปรียบเทียบค่าความสามารถในการคายประจุ (เวลา 1 ชั่วโมง อุณหภูมิ 25 องศาเซลเซียส) กับค่ามาตรฐานของแบตเตอรี่ชนิดเดียวกันที่บรรจุอิเล็กโทรไลต์แบบน้ำกรด

ผลการทดลองแสดงให้เห็นว่าพุ่มซิลิกา กรดซัลฟิวริก และสารเติมแต่ง ส่งผลต่อ ค่าการนำไฟฟ้า และเวลาในการเกิดเจลของเจลอิเล็กโทรไลต์ โดยพบว่าค่าการนำไฟฟ้ามีความสัมพันธ์ต่อความสามารถในการคายประจุของแบตเตอรี่ชนิดตะกั่ว-กรดแบบวาล์วที่บรรจุเจลอิเล็กโทรไลต์ เจลอิเล็กโทรไลต์ที่ประกอบด้วยพอลิพิโรล และพอลิพิโรลกับโซเดียมซัลเฟต ให้ค่าความสามารถในการคายประจุสูงที่สุดและเกิดการสูญเสียน้ำน้อยที่สุด นอกจากนี้เจลอิเล็กโทรไลต์ที่ประกอบด้วยพอลิเอनीลีน พอลิพิโรล พอลิเพนีสินซัลไฟด์ และ/หรือโซเดียมซัลเฟต และที่ไม่เติมสารเติมแต่ง ให้ค่าความสามารถในการคายประจุที่สูงกว่ามาตรฐานของแบตเตอรี่ชนิดเดียวกันที่บรรจุอิเล็กโทรไลต์แบบน้ำกรด (2.3 แอมป์ชั่วโมง) ในทางตรงกันข้ามพบว่าเจลอิเล็กโทรไลต์ที่ประกอบด้วยกรดฟอสฟอริก ให้ค่าการนำไฟฟ้าและค่าความสามารถในการคายประจุที่ต่ำที่สุด

สาขาวิชาปิโตรเคมีและวิทยาศาสตร์พอลิเมอร์

ลายมือชื่อ.....

ปีการศึกษา.....2551.....

ลายมือชื่ออ.ที่ปรึกษาวิทยานิพนธ์หลัก.....

4972570123 : MAJOR PETROCHEMISTRY AND POLYMER SCIENCE

KEYWORDS : LEAD-ACID BATTERY/ VALVE-REGULATED LEAD ACID BATTERY / GELLED ELECTROLYTE / ADDITIVE / CONDUCTING POLYMER

AMORN RAT CHAIYASIT : EFFECT OF POLYMERS ON GEL ELECTROLYTE PROPERTIES IN LEAD-ACID BATTERY. ADVISOR : ASSOC. PROF. ORAWON CHAILAPAKUL, Ph.D., 110 pp.

This thesis studied the effects of additives on the performance of gelled-electrolyte by measuring the conductivity values and discharge capacities of valve-regulated lead-acid (VRLA) batteries. The gelled-electrolyte containing 2%(w/v) of fumed silica and 35%(w/v) of sulfuric acid provided the highest conductivity (σ) of 838 mS/cm at 25°C. This gelled electrolyte was selected for development by adding various additives. In order to improve the battery rechargeability, the textural evolution of the positive active material, life cycle and the electrical conductivity of gelled-electrolyte were optimized by using sodium sulfate, orthophosphoric acid, conducting polymers (polyaniline, polypyrrole and poly(1,4-phenylene sulfide)), mixtures of sodium sulfate and orthophosphoric acid, mixtures of sodium sulfate and conducting polymers and mixture of sodium sulfate, orthophosphoric acid and conducting polymers. Moreover, the gelling time and the oxygen recombination process of gelled-electrolytes with various types of additives were investigated. Finally, the discharge capacity was compared with the standard capacity (at 25°C) of VRLA battery containing a liquid electrolyte at a 1-hour rate.

From the results, it was found that fumed silica, sulfuric acid and additives affected the electrical conductivity and the gelling time of gelled electrolyte. The conductivity of the gelled electrolytes was related to the discharge capacity of VRLA batteries containing gelled-electrolytes. The high discharge capacities were obtained from gelled electrolytes containing only polypyrrole and a mixture of polypyrrole and sodium sulfate. These electrolytes provided the least water loss. In addition, the gelled electrolytes containing conducting polymers including polyaniline, polypyrrole and poly(1,4-phenylene sulfide) and/or sodium sulfate and without adding additives increased the capacity when compared to the standard VRLA battery containing liquid electrolyte. On the contrary, the gelled electrolytes containing phosphoric acid showed the lowest conductivity and discharge capacity.

Field of Study : Petrochemistry and Polymer Science Student's Signature

Academic Year : 2008 Advisor's Signature

ACKNOWLEDGEMENTS

Firstly, I would like to express my gratitude to my advisor, Associate Professor Dr. Orawon Chailapakul, for continuously providing important guidance and always giving the great opportunity throughout my three year of Master's Degree study at Chulalongkorn University. I truly appreciate and thank her for unwavering encouragement during the writing of this thesis. I also would like to thank members of the thesis examination committee, Associate Professor Dr. Supawan Tantayanon, Associate Professor Dr. Nuanphun Chantarasiri and Dr. Passapol Ngamukot, who give helpful comments and advice in this thesis. My sincere appreciation is also extended to the external committee member, Dr. Weena Siangproh, for her suggestions.

I truly thank the manager of N.V. Battery, Mr. Krisana Watakeyanon, who give helpful knowledge, place and batteries throughout this research. I also would like to thank Dr. Parichatr Vanalabhpatana, Dr. Charoenkwan Kraiya, Dr. Nisit Tantavichet, for their helpful knowledge and suggestions for this research. I also thank Ms. Worawon Siridetpan and Ms. Titiporn Tantichanakul, who provide their help in this research.

I especially want to thank the members of electrochemical groups at Chulalongkorn University, who provide their help throughout this research. Also I would like to thank Center of Excellence for Petroleum, Petrochemicals, and Advanced Materials and CU. Graduate School Thesis Grant for financial support. I also thank Chulalongkorn University for partial financial supports and giving the opportunity to study, laboratory facilities, chemical and equipments.

Finally, I am affectionately thankful to my family, Ms. Wanna Chaiyasit, Mr. Amornsak Chaiyasit and Mr. Sutanai Krintrakul for their helpful and heartfelt unlimited support, financial support, kindness, and encouragement throughout my education and my life.

CONTENTS

| | PAGE |
|--|-------------|
| ABSTRACT (Thai) | iv |
| ABSTRACT (English) | v |
| ACKNOWLEDGMENTS | vi |
| CONTENTS | vii |
| LIST OF TABLES | xi |
| LIST OF FIGURES | xiii |
| LIST OF ABBREVIATIONS | xvi |
| | |
| CHAPTER I INTRODUCTION | 1 |
| 1.1 Introduction..... | 1 |
| 1.2 Objectives of the research..... | 3 |
| 1.3 Scope of the research..... | 3 |
| | |
| CHAPTER II THEORY AND LITERATURE SURVEY | 4 |
| 2.1 History..... | 4 |
| 2.1.1 Lead-acid battery..... | 4 |
| 2.1.2 VRLA battery..... | 7 |
| 2.2 The lead-acid battery system..... | 8 |
| 2.2.1 Electrochemical reactions..... | 8 |
| 2.2.2 Equilibrium voltage..... | 11 |
| 2.2.3 Electrolyte stratification..... | 14 |
| 2.2.4 Conductivity of sulfuric acid..... | 16 |
| 2.2.5 Self-discharge..... | 17 |
| 2.2.6 Immobilized electrolyte..... | 18 |
| 2.3 Comparisons of vented (flooded) and valve-regulated technologies.... | 20 |
| 2.3.1 Reaction..... | 20 |
| 2.3.2 Construction materials..... | 20 |
| 2.3.3 Aging and failure mechanisms..... | 20 |
| 2.3.3.1 Dryout..... | 20 |
| 2.3.3.2 Thermal runaway..... | 21 |

| | PAGE |
|---|-------------|
| 2.3.3.3 Negative plate self-discharge..... | 22 |
| 2.3.3.4 Seal or valve failures..... | 22 |
| 2.3.3.5 Temperature effects..... | 23 |
| 2.3.3.6 Loss of absorbed glass mat compression..... | 23 |
| 2.3.3.7 Ripple current..... | 23 |
| 2.3.4 Electrolyte specific gravity..... | 24 |
| 2.3.5 Charging voltage..... | 24 |
| 2.3.5.1 Float voltage..... | 24 |
| 2.3.5.2 Temperature compensation of charging voltage..... | 24 |
| 2.3.6 Absence of free electrolyte..... | 25 |
| 2.3.7 Maintenance and testing..... | 25 |
| 2.3.8 Orientation in use..... | 25 |
| 2.3.9 Vented gas..... | 25 |
| 2.3.10 Historical service life..... | 26 |
| 2.3.11 VRLA advantages and disadvantages..... | 26 |
| 2.4 Gel electrolyte immobilization with fumed silica (pyrogenic silica).... | 28 |
| 2.5 Conducting polymer..... | 30 |
| 2.5.1 Polyaniline (PANI)..... | 30 |
| 2.5.2 Polypyrrole (PPy)..... | 31 |
| 2.5.3 Poly (p-phenylene sulfide) (PPS)..... | 34 |
| 2.6 Cyclic voltammetry..... | 35 |
| 2.7 Electrochemical cells..... | 37 |
| 2.8 Electrical Conductivity..... | 39 |
| 2.8.1 Definition of conductivity..... | 39 |
| 2.8.2 The measurement of conductivity..... | 39 |
| 2.8.3 Units of Measurement..... | 40 |
| 2.8.4 Conductive solution..... | 41 |
| 2.8.4.1 Strong electrolytes..... | 41 |
| 2.8.4.2 Weak electrolytes..... | 41 |
| 2.8.5 Definition of terms..... | 41 |
| 2.8.5.1 Resistance..... | 41 |

| | PAGE |
|--|-------------|
| 2.8.5.2 Conductance..... | 42 |
| 2.8.5.3 Cell constant..... | 42 |
| 2.8.5.4 Conductivity..... | 42 |
| 2.8.5.5 Resistivity..... | 42 |
| 2.9 Literature reviews of lead-acid batteries..... | 43 |
| CHAPTER III EXPERIMENTAL..... | 48 |
| 3.1 Gelled electrolyte preparations..... | 48 |
| 3.1.1 Instrument..... | 48 |
| 3.1.2 Chemicals..... | 48 |
| 3.1.3 Methodology..... | 49 |
| 3.2 Electrical conductivity test..... | 50 |
| 3.2.1 Instruments..... | 50 |
| 3.2.2 Gelled electrolytes for conductivity test..... | 51 |
| 3.2.3 Methodology..... | 53 |
| 3.3 Gelling time test..... | 53 |
| 3.3.1 Gelled electrolytes for gelling time test..... | 53 |
| 3.3.2 Methodology..... | 55 |
| 3.4 Performance of battery test..... | 55 |
| 3.4.1 Instruments..... | 55 |
| 3.4.2 Gelled electrolytes for performance of battery test | 55 |
| 3.4.3 Methodology..... | 57 |
| 3.5 Electrochemical test..... | 57 |
| 3.5.1 Instruments | 57 |
| 3.5.2 Gelled electrolytes and acid solution for electrochemical test..... | 58 |
| 3.5.3 Methodology..... | 59 |
| CHAPTER IV RESULTS AND DISCUSSION..... | 60 |
| 4.1 Characterization of gelled electrolytes..... | 60 |
| 4.2 Optimization of gelled electrolytes by measuring conductivity..... | 62 |

| | PAGE |
|--|-------------|
| 4.3 Gelling time of gelled electrolytes..... | 74 |
| 4.4 Performance of VRLA batteries..... | 74 |
| 4.4.1 Charge and discharge characteristic of VRLA batteries..... | 74 |
| 4.4.2 Initial discharge curves of VRLA batteries..... | 79 |
| 4.4.3 Discharge capacities of VRLA batteries..... | 80 |
| 4.5 Oxygen recombination reaction of gelled electrolyte..... | 81 |
| CHAPTER V CONCLUSIONS AND FUTURE PERSPECTIVE..... | 83 |
| 5.1 Conclusions..... | 83 |
| 5.2 Future perspective..... | 84 |
| REFERENCES..... | 85 |
| APPENDICES..... | 90 |
| APPENDIX A..... | 91 |
| APPENDIX B..... | 93 |
| APPENDIX C..... | 95 |
| APPENDIX D..... | 100 |
| VITA..... | 110 |

LIST OF TABLES

| TABLE | PAGE |
|--------------|---|
| 2.1 | Events in technical development of lead-acid battery..... 5 |
| 2.2 | Acid-concentration parameters: acid density (kg/L), H ₂ SO ₄ content and H ₂ SO ₄ concentration in mol/L, and molality. Cell voltage and electrode potentials referred to the standard hydrogen electrode, T=25°C..... 13 |
| 3.1 | List of chemicals for gelled electrolyte preparations..... 49 |
| 3.2 | List of gelled electrolytes without adding additives for electrical conductivity test..... 51 |
| 3.3 | List of gelled electrolytes with adding additives for electrical conductivity test..... 52 |
| 3.4 | List of gelled electrolytes for gelling time test..... 54 |
| 3.5 | List of instruments for performance of battery test..... 55 |
| 3.6 | List of VRLA batteries with different gelled electrolytes for performance of battery test..... 56 |
| 3.7 | List of instruments for electrochemical test..... 58 |
| 3.8 | List of different gelled electrolytes and acid solution for electrochemical test..... 58 |
| 4.1 | The characteristics of gelled electrolytes with different fumed silica and H ₂ SO ₄ concentration after stirring at room temperature (25±1°C)..... 61 |
| 4.2 | The conductivities of gelled electrolytes containing 1 %(w/v) of fumed silica and various concentration of H ₂ SO ₄ 63 |
| 4.3 | The conductivities of gelled electrolytes containing 2 %(w/v) of fumed silica and various concentration of H ₂ SO ₄ 63 |
| 4.4 | The conductivities of gelled electrolytes containing 3 %(w/v) of fumed silica and various concentration of H ₂ SO ₄ 64 |
| 4.5 | The conductivities of gelled electrolytes containing 4 %(w/v) of fumed silica and various concentration of H ₂ SO ₄ 64 |
| 4.6 | The conductivities of gelled electrolytes containing 5 %(w/v) of fumed silica and various concentration of H ₂ SO ₄ 65 |

| TABLE | PAGE |
|--|-------------|
| 4.7 The conductivities of gelled electrolytes containing 6 %(w/v) of fumed silica and various concentration of H ₂ SO ₄ | 65 |
| 4.8 The conductivities of gelled electrolytes containing 7 %(w/v) of fumed silica and various concentration of H ₂ SO ₄ | 66 |
| 4.9 The conductivities of gelled electrolytes containing 8 %(w/v) of fumed silica and various concentration of H ₂ SO ₄ | 66 |
| 4.10 The conductivities of gelled electrolytes containing 9 %(w/v) of fumed silica and 15 %(w/v) of H ₂ SO ₄ | 66 |
| 4.11 The highest conductivities of various gelled electrolytes..... | 67 |
| 4.12 Gelling time of various gelled electrolytes..... | 74 |

LIST FIGURES

| FIGURE | PAGE |
|--|------|
| 2.1 Discharge and charge reactions of the lead-acid cell. (a) Discharge reactions. (b) Charge reactions [12, 15]..... | 9 |
| 2.2 Typical voltage and specific gravity characteristics of lead-acid cell at constant rate discharge and charge [12]..... | 11 |
| 2.3 Acid-concentration parameters: acid density (kg/L), H ₂ SO ₄ content and density and acid concentration in weight% H ₂ SO ₄ . The dashed line represents the approximation of equation (2.10) [16]..... | 12 |
| 2.4 The origin of acid stratification, when the lead-acid battery is discharged and recharged without gassing or other means of mixing the electrolyte [13]..... | 15 |
| 2.5 Specific electric conductance of aqueous solution of sulfuric acid and its dependence on temperature. The dotted line denotes the maximum [16]..... | 16 |
| 2.6 (a) Capacity retention during standing or storage at 25°C. (b) Loss of specific gravity per day with temperature of a new fully charged lead-acid battery with 6% antimonial lead grids [12]..... | 18 |
| 2.7 (a) Powder of pyrogenic silica and (b) TEM of pyrogenic silica [19]..... | 28 |
| 2.8 Hydrogen bridge linkages between particles [19]..... | 29 |
| 2.9 The formation of the GEL structure is reversible at the beginning, by dispersing SOL and by setting GEL [19]..... | 29 |
| 2.10 The oxidative polymerization of aniline in an acidic solution. The synthesized PANI forms in its doped emeraldine salt state that then can be dedoped by a base to its emeraldine base form. The bottom left scheme illustrates a typical reaction for making PANI [22] | 31 |
| 2.11 Electronic structures of (a) neutral PPy, (b) polaron in partially doped PPy and (c) bipolaron in fully doped PPy [22]..... | 33 |

| FIGURE | PAGE |
|---|-------------|
| 2.12 Electronic energy diagrams for (a) neutral PPy, (b) polaron, (c) bipolaron and (d) fully doped PPy [22]..... | 34 |
| 2.13 The potential-time excitation signal in a cyclic voltammetric experiment [38] | 36 |
| 2.14 Typical cyclic voltammogram for a reversible $O + ne^- \rightleftharpoons R$ redox process [38]..... | 37 |
| 2.15 Schematic diagram of a cell for voltammetric measurements: WE-working electrodes; RE-reference electrode; CE-counter electrode. The electrodes are inserted through holes in the cell cover [38]..... | 38 |
| 2.16 The relationship between conductivity and ion concentration for two common solutions [39]..... | 39 |
| 2.17 Migration of ions in solution [40]..... | 40 |
| 3.1 The setting of instruments for the gelled electrolyte preparation..... | 48 |
| 3.2 The gelled electrolyte consisting of fumed silica, H ₂ SO ₄ and (a) without adding additives, (b) adding PANI, (c) adding PPy and (d) adding PPS... | 50 |
| 3.3 The conductivity meter and conductivity probe for electrical conductivity test..... | 50 |
| 3.4 The VRLA battery (12V)..... | 53 |
| 3.5 The setting of experimental for (a) battery charging and (b) battery discharging..... | 57 |
| 3.6 The electrochemical cell for electrochemical technique..... | 59 |
| 4.1 The conductivity of gelled electrolytes with various concentrations of fumed silica and H ₂ SO ₄ | 68 |
| 4.2 The conductivity of gelled electrolytes with various concentrations of H ₃ PO ₄ (2%w/v of fumed silica and 35%w/v of H ₂ SO ₄ were fixed)..... | 69 |
| 4.3 The conductivity of gelled electrolytes with various concentrations of Na ₂ SO ₄ (2%w/v of fumed silica and 35%w/v of H ₂ SO ₄ were fixed).... | 69 |
| 4.4 The conductivity of gelled electrolytes with various concentrations of H ₃ PO ₄ and Na ₂ SO ₄ (2%w/v of fumed silica and 35%w/v of H ₂ SO ₄ were fixed)..... | 70 |

| FIGURE | PAGE |
|---|-------------|
| 4.5 The conductivity of gelled electrolytes with various concentrations of PANI (2%w/v of fumed silica and 35%w/v of H ₂ SO ₄ were fixed)..... | 71 |
| 4.6 The conductivity of gelled electrolytes with various concentrations of PPy (2%w/v of fumed silica and 35%w/v of H ₂ SO ₄ were fixed)..... | 72 |
| 4.7 The conductivity of gelled electrolytes with various concentrations of PPS (2%w/v of fumed silica and 35%w/v of H ₂ SO ₄ were fixed)..... | 73 |
| 4.8 The charge characteristic of B1-B6 of (a) cycle 5 and (b) cycle 10 at 1-hour rate and 25°C±1, where a solid line is voltage of battery and a dot line is current of battery..... | 75 |
| 4.9 The charge characteristic of B7-B12 of (a) cycle 5 and (b) cycle 10 at 1-hour rate and 25°C±1, where a solid line is voltage of battery and a dot line is current of battery..... | 76 |
| 4.10 The discharge characteristic of B1-B6 of (a) cycle 5 and (b) cycle 10 at 1-hour rate and 25°C±1, where a solid line is voltage of battery and a dot line is current of battery..... | 77 |
| 4.11 The discharge characteristic of B7-B12 of (a) cycle 5 and (b) cycle 10 at 1-hour rate and 25°C±1, where a solid line is voltage of battery and a dot line is current of battery..... | 78 |
| 4.12 Initial discharge curves of B1-B12 with type I-III of gelled electrolytes; (a) without conducting polymer, (b) adding PANI, (c) adding PPy, and (d) adding PPS at 1-hour rate and 25°C±1..... | 79 |
| 4.13 Capacity test in each cycle number of B1-B12 with type I-III of gelled electrolytes; (a) without conducting polymer, (b) adding PANI, (c) adding PPy, and (d) adding PPS at 1-hour rate and 25°C±1..... | 80 |
| 4.14 Cyclic voltammogram of type I of gelled electrolytes containing only conducting polymer as additive and acid solution at scan rate of 20 mV s ⁻¹ | 81 |
| 4.15 Cyclic voltammogram of type II of gelled electrolytes containing Na ₂ SO ₄ and conducting polymer as additive and acid solution at scan rate of 20 mV s ⁻¹ | 82 |

LIST OF ABBREVIATIONS

| | |
|----------|---|
| VRLA | valve-regulated lead-acid |
| AGM | absorptive glass-mat |
| PANI | polyaniline |
| PPy | polypyrrole |
| PPS | poly(1,4-phenylene sulfide) |
| SLA | sealed lead-acid |
| UPS | uninterruptible power supply |
| DC | direct current |
| AC | alternating current |
| CFR | code of Federal regulation |
| DOT | department of transportation |
| IATA | international air transport association |
| TEM | transmission electron microscopy |
| BET | Brunauer, Emmett and Teller |
| THF | tetrahydrofuran |
| WE | working electrode |
| RE | reference electrode |
| CE | counter electrode |
| ABS | acrylonitrile butadiene styrene |
| PBGE | polysiloxane-based gelled electrolyte |
| CSGE | colloid silica gelled electrolyte |
| FSGE | fumed silica gelled electrolyte |
| CV | cyclic voltammetry |
| SD | standard deviation |
| σ | specific conductivity |

| | |
|-----------|---------------------------------|
| mS | milli Siemens |
| cm | centimeter |
| R | resistivity |
| S | Siemens |
| I | current |
| C | conductivity |
| L | length |
| A | area |
| R | resistance |
| G | conductance |
| d | distance |
| a | effective area |
| K | cell constant |
| V | voltage |
| mV | milli volt |
| W | Watts |
| Wh | Watts-hour |
| A | Ampere |
| h | hour |
| Ah | Ampere hour |
| Ω | Ohm |
| E | potential |
| E° | Nernst-potential |
| U° | equilibrium voltage of the cell |
| eV | electron volt |

| | |
|-----------------|--------------------------------------|
| T | temperature |
| T _g | glass transition temperature |
| T _m | melt temperature |
| °C | degree Celsius |
| °F | degree Fahrenheit |
| K | degree Kelvin |
| w/v | weight by volume |
| wt. % | weight-weight percentage |
| α | alpha |
| β | beta |
| M | molar |
| MW | molecular weight |
| M _w | weight average of molecular weight |
| M _n | number average of molecular weight |
| R | molar gas constant for an ideal gas |
| F | Faraday constant |
| a _i | activity of the reacting component i |
| J | Joule |
| mol | mole |
| cm ³ | cubic centimeter |
| dm ³ | cubic decimeter |
| cm ² | square centimeter |
| m ² | square meter |
| g | gram |
| kg | kilogram |
| L | liter |
| mL | milliliter |

| | |
|---------------|------------------|
| nm | nanometer |
| μm | micrometer |
| min | minute |
| s | second |
| rpm | round per minute |

CHAPTER I

INTRODUCTION

1.1 Introduction

During the last two decades, there have been increasing attention use of valve-regulated lead-acid (VRLA) batteries in various application such as hybrid electric vehicles, telecommunication and other backup power needs [1-2]. The VRLA batteries are usually called maintenance-free lead-acid batteries because the users do not need to add water to the battery as the maintenance step. They not only showed the great promise for electric vehicle but also provided the environmental benefit by replacing the gasoline-powered vehicles. In general, maintenance-free lead-acid batteries can be classified into three types: (i) flooded electrolyte type, using the low antimony spines in the positive plates and a large volume of reserve electrolyte to compensate for electrolyte loss; (ii) absorptive glass-mat (AGM) type, the electrolyte is completely absorbed in a glass-fiber separator, and maintenance-free operation is achieved using an internal oxygen cycle; (iii) gelled electrolyte type, the electrolyte is immobilized using organic or inorganic thixotropic agents, such as polymethyl methacrylate, colloidal silica and fumed silica [3-4].

In gelled electrolyte batteries, loss of water during overcharge either as hydrogen or oxygen is negligible. In addition, gelled electrolyte cells are virtually unaffected by acid stratification. More significantly, the immobilization of the electrolyte by gelling permitted the production of sealed batteries with highly improved cycle-life and high-charge acceptance [3]. In the AGM VRLA batteries, the immobilization of the electrolyte reduced the degree of electrolyte stratification, but at the same time, it also removes its possible remedy because violent gassing is impossible. Electrolyte stratification is common in the large and aged AGM VRLA cells and batteries [5].

The VRLA batteries used in telecommunication are required to be highly reliable and have a long service life. Accordingly, the design of tubular positive plates and gelled electrolytes is very suitable for telecom applications. In the gelled

electrolyte, the corrosion rate of the positive grids is lower than the AGM types. Moreover, its overpotential of hydrogen evolution on the negative plate is also higher. This is mainly due to the high performance and long life cycle of gelled electrolytes compared to VRLA batteries. Furthermore, there is no electrolyte stratification, which greatly contributes to the resistance against the sulfation of the active mass [6].

In the gel VRLA battery, sulfuric acid is mixed with finely divided silica and forms a gel. The recombination reaction of oxygen from the positive to the negative plate occurs through a network of micro-cracks in the gelled electrolyte. The batteries therefore can, operate in a fully sealed manner without any requirement for routine maintenance [7].

Much research and development has been done, during the 1990s to understand and improve the technological knowledge base for VRLA batteries [8]. By contrast, there has been comparatively little documented and published work on advancing the design, durability and performance characteristics of the gelled electrolyte battery system since its inception [4].

In order to obtain a high discharge capacity and power output, a novel gelled-electrolyte using conducting polymers has been developed in this work. It is well known that conducting polymers have been interesting in various fields of electronics, industry, agriculture and so on. Conducting polymers are generally composed of conjugated monomer units with π -electrons delocalized along the polymer back bone. The conducting polymers have many advantages over their metallic counterparts: low cost materials, simple fabrication techniques, easy deposition on various substrates, and flexible molecular architectures. Moreover, conducting polymers have good characteristics in rechargeable batteries [9-11].

1.2 Objective of the research

This research is devoted to develop a new gelled electrolyte for VRLA batteries using conducting polymers and the investigating the performance of gelled VRLA batteries. The PANI, PPy and PPS conducting polymers were chosen to improve the conductivity of the gelled electrolyte. In addition, several of the gelled electrolytes were optimized by conductometry, and the cycling of the batteries was investigated by measuring the capacities.

1.3 Scope of the research

To achieve the research objective, the following scope was set:

(i) Research and study the information of lead-acid batteries, VRLA batteries and gelled electrolytes.

(ii) Study the effect of fumed silica, sulfuric acid and additives on the performance of VRLA batteries.

(iii) Prepare the new gelled electrolyte using fumed silica, sulfuric acid, sodium sulfate and/or orthophosphoric acid and conducting polymers such as PANI, PPy and PPS.

(iv) Investigate the conductivity values, the gelling time, the discharge capacities and the oxygen recombination reaction of the gelled electrolytes.

(v) Finally, all the results are discussed.

CHAPTER II

THEORY AND LITERATURE SURVEY

2.1 History

2.1.1 Lead-acid battery [12]

Practical lead-acid batteries began with the research and inventions of Raymond Gaston Planté in 1860, although batteries containing sulfuric acid or lead components were discussed earlier. Table 2.1 lists the events in the technical development of the lead-acid battery. In Planté's fabrication method, two long strips of lead foil and intermediate layers of coarse cloth were spirally wound and immersed in a solution of about 10% sulfuric acid. The early Planté cells had little capacity, since the amount of stored energy depended on the corrosion of one of the pieces of lead foil to lead dioxide to form the positive active material, and similarly roughening of the other piece of foil (on cycling) to form an extended surface and create the negative electrode. Primary cells were used as the power sources for this formation. The capacity of Planté cells was increased on repeated cycling as corrosion of the substrate foil created more active material and increased the surface area. In the 1870s, magnetoelectric generators became available to Planté, and about this time the Siemens dynamo started appearing in central electric plants. Lead-acid batteries found an early market to provide load leveling and to average out the demand peaks. They were charged at night, similar to the procedure now planned for modern load-leveling energy-storage systems.

Table 2.1 Events in technical development of lead-acid battery

| Precursor systems | | |
|-------------------------------|----------------------|--|
| 1836 | Daniell | Two-fluid cell; copper/copper sulfate/sulfuric acid/zinc |
| 1840 | Grove | Two-fluid cell; carbon/fuming nitric acid/sulfuric acid/zinc |
| 1854 | Sindesten | Polarized lead electrodes with external source |
| Lead-acid battery development | | |
| 1860 | Planté | First practical lead-acid battery, corroded lead foils to form active material |
| 1881 | Faure | Pasted lead foils with lead oxide-sulfuric acid pastes for positive electrode, to increase capacity |
| 1881 | Sellon | Lead-antimony alloy grid |
| 1881 | Volckmar | Perforated lead plates to provide pockets for support of oxide |
| 1882 | Brush | Mechanically bonded lead oxide to lead plates |
| 1882 | Gladstone and Tribes | Double sulfate theory of reaction in lead-acid battery: $\text{PbO}_2 + \text{Pb} + 2\text{H}_2\text{SO}_4 \rightleftharpoons 2\text{PbSO}_4 + 2\text{H}_2\text{O}$ |
| 1883 | Tudor | Pasted mixture of lead oxides on grid pretreated by Planté method |
| 1886 | Lucas | Formed lead plates in solutions of chlorates and perchlorates |
| 1890 | Phillipart | Early tubular construction-individual rings |
| 1890 | Woodward | Early tubular construction |
| 1910 | Smith | Slotted rubber tube, Exide tubular construction |
| 1920 to present | | Materials and equipment research, especially expanders, oxides, and fabrication techniques |
| 1935 | Haring and Thomas | Lead-calcium alloy grid |
| 1935 | Hamer and Harned | Experimental proof of the double sulfate theory of reaction |

Table 2.1 Events in technical development of lead-acid battery (continued)

| Lead-acid battery development | | |
|-------------------------------|--|--|
| 1956- | Bobbe and Voss | Clarification of properties of two crystalline forms of |
| 1960 | Ruetschi and Cahan Burbank Feitknecht | PbO ₂ (alpha and beta) |
| 1970s | McClelland And Devit | Commercial spiral-wound sealed lead acid battery Expanded metal grid technology; composite plastic/metal grids; sealed and maintenance-free lead-acid batteries; glass fiber and improved separators; through-the-partition intercell connectors; heat-sealed plastic case-to-cover assemblies; high- energy-density batteries (above 40Wh/kg); conical grid (round) cell for long-life float service in telecommunications facilities |
| 1980s | | Sealed valve-regulated batteries; quasi-bipolar engine starter batteries; improved low-temp. performance; world's largest battery installed (Chino, Calif.); 40- MWh lead-acid load leveling |
| 1990s | | Electric-vehicle interest reemerges; bipolar battery designs for high power |

Subsequent to Planté's first developments, numerous experiments were done to accelerate the formation process by coating lead foil with oxides on a lead plate pretreated by the Planté method. Attention then turned to other methods for retaining active material, and two main technological paths evolved. One is the flat-plate design, in which the active material developed structural strength and retention properties by a cementation process (interlocked crystalline lattice) through the grid and active mass. The other is the tubular electrode design, in which a central conducting

wire or rod is surrounded by active material and the assembly is encased in an electrolyte that is porous and insulated.

Alongside the advances in developing and retaining active material was work in strengthening the grid by casting it from lead alloys, such as lead-antimony or lead-calcium. The technical knowledge for economically manufacturing reliable lead-acid batteries was in place by the end of the nineteenth century, leading to subsequent rapid growth of the industry. Improvements in design, manufacturing equipment and methods, recovery methods, active material utilization and production, supporting structures and components, and inactive components such as separators, cases, and seals continue to improve the economic and performance characteristics of lead-acid batteries. Recently more intensive developmental work has started for new applications, especially for energy storage and electric vehicles.

2.1.2 VRLA battery

Different names are in use for this kind of lead-acid battery. An earlier proposal was 'sealed valve-regulated lead-acid battery', but the term 'sealed' is redundant in this situation because a valve can operate only when the battery itself is sealed. The term now mostly accepted is 'valve-regulated lead-acid battery', and this name describes quite well the special feature of this design:

(i) The interior of the VRLA battery does not have a continuous connection with the surrounding atmosphere to exchange gases, as is characteristic of the vented lead-acid battery.

(ii) The VRLA battery cannot be sealed completely but has to be equipped with a valve that opens even in normal operation conditions from time to time for gas escape. This is basically different from 'sealed' batteries [13].

The sealed lead-acid (SLA) cells are made in two designs one with spirally wound plates (jelly-roll construction) in a cylindrical metal container and the other with flat plates in a prismatic (usually plastic) container. The venting characteristics of the cylindrical and prismatic designs are usually different. The prismatic cell is designed to vent at low pressures ($0.04-1 \times 10^5$ Pa), and these designs

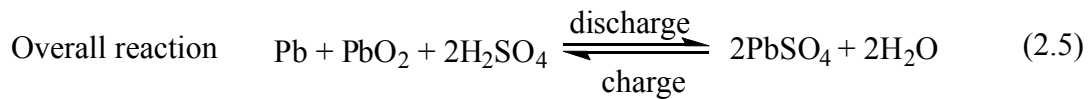
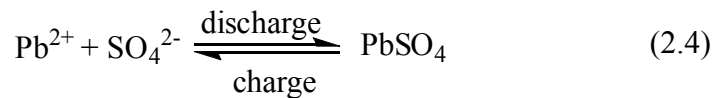
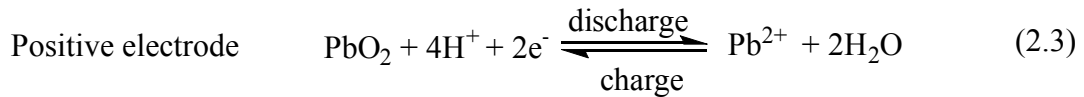
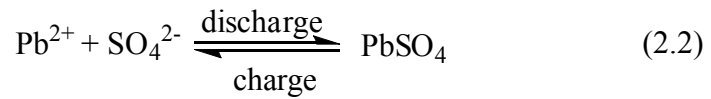
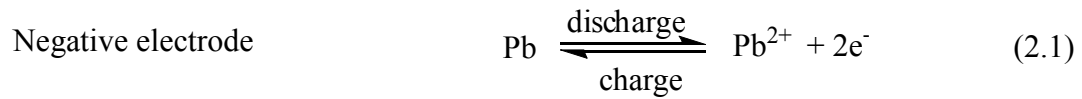
are commonly referred to as VRLA cells. The cylindrical cells have vents that operate at $2-4 \times 10^5$ Pa and are commonly referred to as SLA cells.

The use of SLA and VRLA designs is becoming more popular. VRLA batteries account for about 60% of the telecommunications batteries and in 85% of the uninterruptible power supply (UPS) applications (1992). Use of VRLA batteries in cycle service, such as forklift trucks where fast recharging may be required, will be dependent on the development of suitable charging techniques. A new market opportunity in portable electronics, power tools, and hybrid electric vehicles has stimulated the development of new types of lead-acid batteries with higher energy and power density and faster recharge [12].

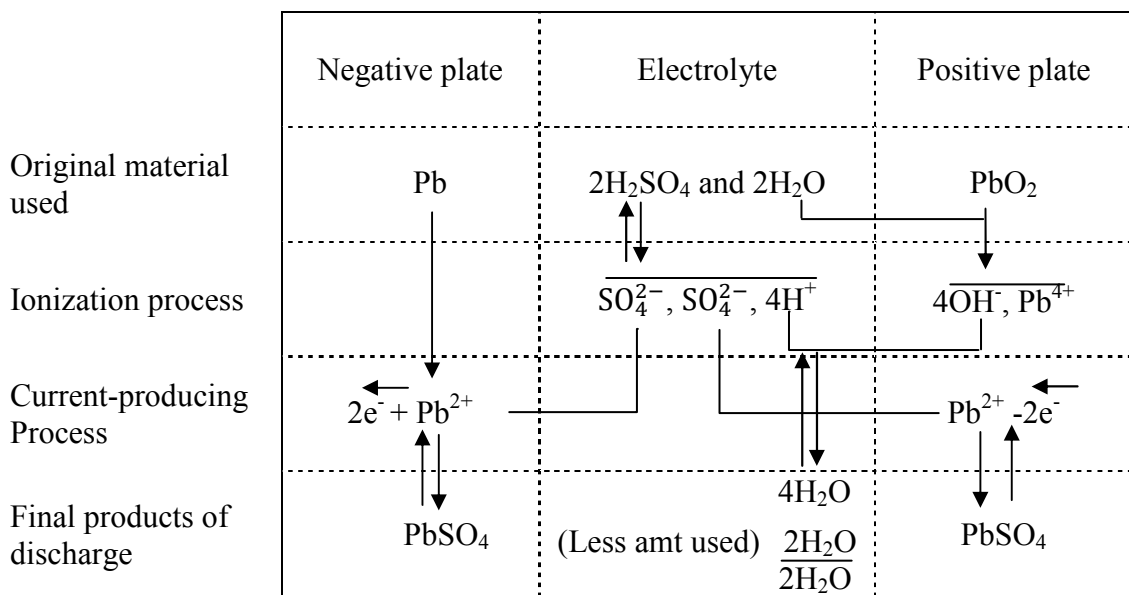
2.2 The lead-acid battery system

2.2.1 Electrochemical reactions [12, 14-15]

The lead-acid battery used lead dioxide as the active material of the positive electrode and metallic lead, in a high-surface-area porous structure, as the negative material. Typically, a charged positive electrode contains both α -PbO₂ (orthorhombic) and β -PbO₂ (tetragonal) variations. The equilibrium potential of the α -PbO₂ is more positive than that of β -PbO₂ by 0.01 V. The α form is also larger and has a more compact crystal morphology, which is less active electrochemically and slightly lower in capacity per unit weight but does, however, promote a longer cycle life. The preparation of the active material precursor consists of a series of mixing and curing operations using leady lead oxide (PbO + Pb), sulfuric acid, and water. The ratios of the reactants and curing conditions (temperature, humidity, and time) affect the development of crystallinity and pore structure. The cured plate consists of lead sulfate, lead oxide, and some residual lead (<5%). The electrolyte is a sulfuric acid solution, typically with a specific gravity of 1.28 or 37% acid by weight in a fully charged condition. As the cell discharges, both electrodes are converted to lead sulfate. The process reverses on charge:



As shown, the basic electrode processes in the positive and negative electrodes involves a dissolution-precipitation mechanism and not a solid-state ion transport or film formation mechanism. The discharge-charge mechanism, known as the double-sulfate reaction, is shown graphically in Fig. 2.1. As the sulfuric acid in the electrolyte is consumed during discharge and produces water, the electrolyte is an active material and in certain battery designs can be the capacity-limiting material.



(a)

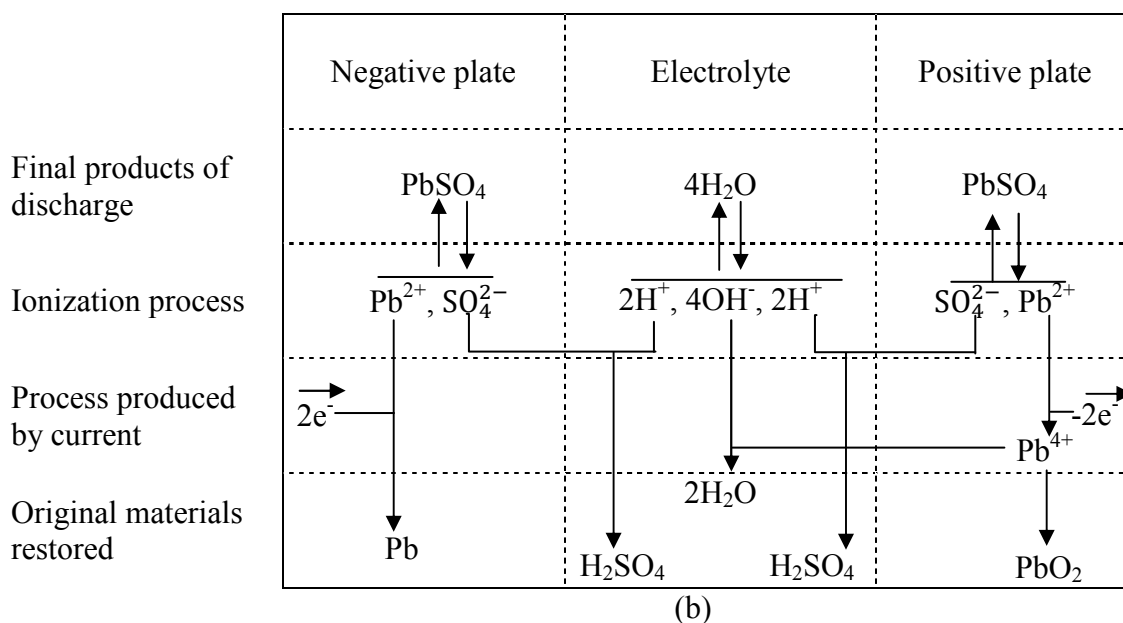
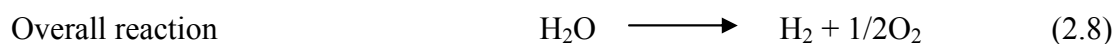
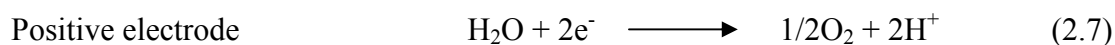
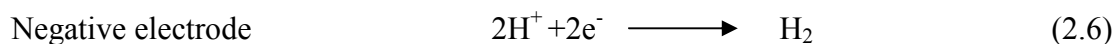


Figure 2.1 Discharge and charge reactions of the lead-acid cell. (a) Discharge reactions. (b) Charge reactions [12, 15].

As the cell approaches its full charge and the majority of the PbSO₄ has been converted to Pb or PbO₂, the cell voltage becomes greater than the gassing voltage (about 2.39V per cell) and the overcharge reaction begins, resulting in the production of hydrogen and oxygen (gassing) and the resultant loss of water. In SLA cells this reactions is controlled to minimize hydrogen evolution and the loss of water by recombination of the evolved oxygen with the negative plate.



The general performance characteristics of the lead-acid cell, during charge and discharge, are shown in Fig. 2.2. As the cell is discharged, the voltage decreases due to depletion of material, internal resistance losses, and polarization. If the discharge current is constant, the voltage under load decreases smoothly to the

cutoff voltage, and the specific gravity decreases in proportion to the ampere-hours discharged.

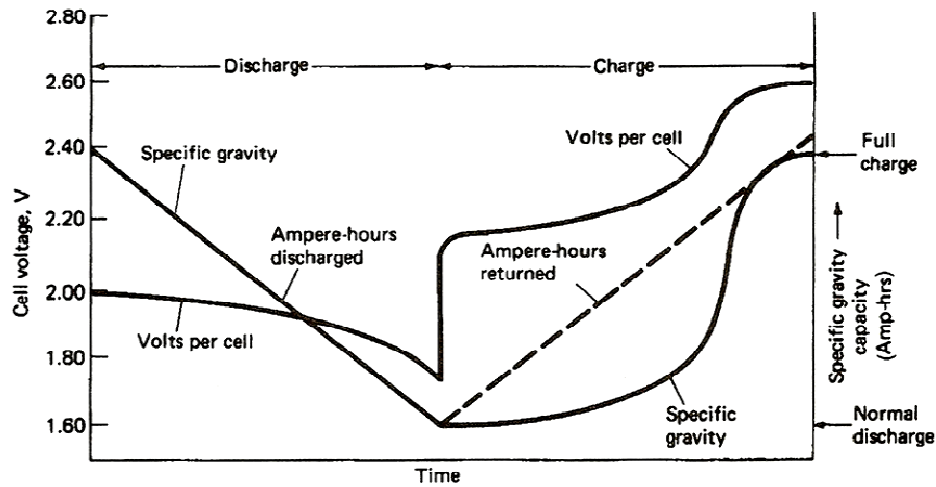


Figure 2.2 Typical voltage and specific gravity characteristics of lead-acid cell at constant rate discharge and charge [12].

2.2.2 Equilibrium voltage [16]

The dependence of the equilibrium voltage on concentration is given by the Nernst equation. The right hand side of the equation at $T = 298$ K and the conversion $\ln = 2.303 \cdot \log$ can be expressed for a lead-acid battery as:

$$U^{\circ} = 1.923 - \frac{R \cdot T}{2 \cdot F} \cdot \ln \frac{(a_{\text{H}_2\text{O}})^2}{(a_{\text{H}^+})^2 \cdot (a_{\text{HSO}_4^-})^2} = 1.923 + 0.0592 \cdot \log \frac{a_{\text{H}^+} \cdot a_{\text{HSO}_4^-}}{a_{\text{H}_2\text{O}}} \quad (2.9)$$

where; U° is the equilibrium voltage of the cell (V), R is the molar gas constant for an ideal gas ($8.3145 \text{ J} \cdot \text{K}^{-1} \cdot \text{mol}^{-1}$), T is the temperature (K), F is the Faraday constant ($96,485 \text{ coulombs/equivalent.}$), a_i is activity of the reacting component i ($\text{mol} \cdot \text{cm}^{-3}$) and the equilibrium voltage applies when the activities of the soluble components of the reaction, namely H^+ , HSO_4^- and H_2O amount to 1 mol/dm^3 , respectively.

According to this equation the equilibrium cell voltage depends only on the acid concentration and is independent of lead, lead dioxide and lead sulfate present in the battery as long as all three substances are available.

Results of equation (2.9) are plotted in Fig. 2.3 and also compiled in the column “Cell voltage” in Table 2.2 together with the single electrode potentials.

In battery practice, the approximation:

$$\text{Equilibrium cell voltage} = \text{acid density (in g/cm}^3 \text{ or kg/dm}^3) + 0.84 \quad (2.10)$$

Equation (2.10) is used instead of equation (2.9). Fig. 2.3 shows that the calculated curve and the approximate formula coincide quite well.

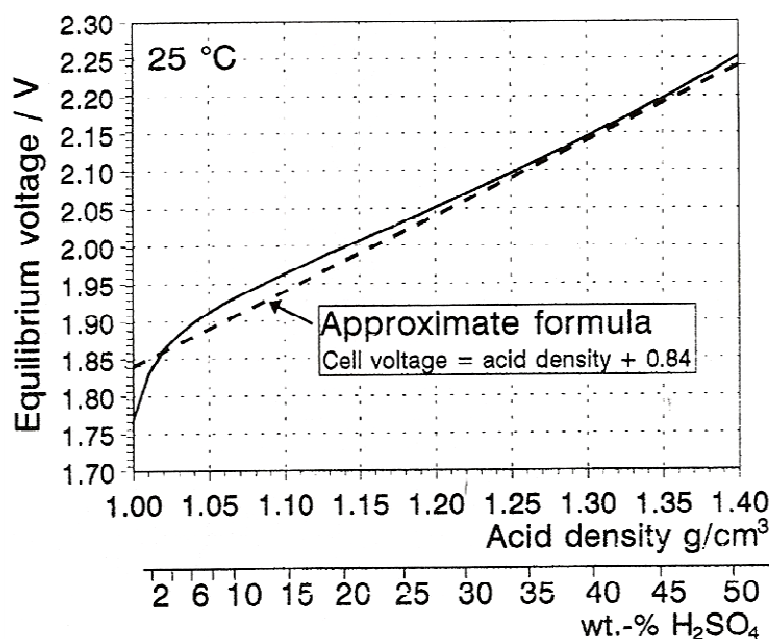


Figure 2.3 Equilibrium cell voltage of the lead-acid battery referred to acid density and acid concentration in weight% H₂SO₄. The dashed line represents the approximation of equation (2.10) [16].

The participation of H₂SO₄ in the cell reaction has considerable consequences. According to equation (2.9), the equilibrium potential depends on the acid concentration. On the other hand H₂SO₄ participates in the electrode reaction, and the electrolyte becomes more diluted during discharge and is re-concentrated during the charge. This means that the cell voltage does not remain constant even at low discharge rates, and the conductivity of the acid varies when the battery is charged or discharged. If the discharge occurs in cold climates, the acid may freeze. On the other hand, in flooded cells, acid dilution provides a tool to determine the state of charge.

Table 2.2 Acid-concentration parameters: acid density (kg/L), H₂SO₄ content and H₂SO₄ concentration in mol/L, and molality. Cell voltage and electrode potentials referred to the standard hydrogen electrode, T=25°C.

| Acid-concentration | | | | Cell Voltage U° Volts | Electrode potentials | |
|--------------------|--|-------------------|--|-----------------------------|-------------------------------|---|
| Dens. kg/L | H ₂ SO ₄ wt.% | Molarity mol/L | Molality mol/kg H ₂ O | | V ref. to std. Positive | H ₂ electrode Negative |
| 1.02 | 3.48 | 0.362 | 0.367 | 1.860 | 1.595 | -0.265 |
| 1.03 | 5.00 | 0.525 | 0.537 | 1.883 | 1.607 | -0.276 |
| 1.04 | 6.49 | 0.688 | 0.708 | 1.899 | 1.616 | -0.283 |
| 1.05 | 7.77 | 0.832 | 0.859 | 1.913 | 1.623 | -0.290 |
| 1.06 | 9.42 | 1.018 | 1.060 | 1.924 | 1.630 | -0.294 |
| 1.07 | 10.86 | 1.184 | 1.242 | 1.935 | 1.634 | -0.301 |
| 1.08 | 12.28 | 1.352 | 1.428 | 1.945 | 1.641 | -0.304 |
| 1.09 | 13.69 | 1.521 | 1.617 | 1.955 | 1.645 | -0.310 |
| 1.10 | 15.08 | 1.691 | 1.811 | 1.964 | 1.650 | -0.314 |
| 1.11 | 16.45 | 1.861 | 2.007 | 1.973 | 1.654 | -0.319 |
| 1.12 | 17.80 | 2.032 | 2.207 | 1.982 | 1.659 | -0.323 |
| 1.13 | 19.13 | 2.204 | 2.412 | 1.991 | 1.663 | -0.328 |
| 1.14 | 20.46 | 2.378 | 2.623 | 2.000 | 1.668 | -0.332 |
| 1.15 | 21.78 | 2.553 | 2.838 | 2.008 | 1.673 | -0.335 |
| 1.16 | 23.08 | 2.729 | 3.059 | 2.017 | 1.667 | -0.340 |
| 1.17 | 24.36 | 2.906 | 3.283 | 2.026 | 1.682 | -0.344 |
| 1.18 | 25.63 | 3.084 | 3.514 | 2.034 | 1.687 | -0.347 |
| 1.19 | 26.89 | 3.262 | 3.749 | 2.043 | 1.691 | -0.352 |
| 1.20 | 28.14 | 3.443 | 3.992 | 2.052 | 1.696 | -0.356 |
| 1.21 | 29.38 | 3.625 | 4.242 | 2.061 | 1.700 | -0.361 |
| 1.22 | 30.61 | 3.807 | 4.498 | 2.070 | 1.705 | -0.365 |
| 1.23 | 31.83 | 3.992 | 4.760 | 2.079 | 1.710 | -0.369 |
| 1.24 | 33.05 | 4.178 | 5.033 | 2.088 | 1.715 | -0.373 |
| 1.25 | 34.25 | 4.365 | 5.311 | 2.097 | 1.720 | -0.376 |
| 1.26 | 35.44 | 4.553 | 5.597 | 2.107 | 1.725 | -0.381 |
| 1.27 | 36.62 | 4.742 | 5.892 | 2.116 | 1.730 | -0.386 |
| 1.28 | 37.79 | 4.932 | 6.194 | 2.126 | 1.735 | -0.391 |
| 1.29 | 38.95 | 5.123 | 6.506 | 2.136 | 1.740 | -0.396 |
| 1.30 | 40.10 | 5.315 | 6.826 | 2.145 | 1.745 | -0.400 |
| 1.31 | 41.24 | 5.508 | 7.155 | 2.156 | 1.751 | -0.405 |
| 1.32 | 42.37 | 5.702 | 7.496 | 2.166 | 1.757 | -0.409 |
| 1.33 | 43.49 | 5.897 | 7.846 | 2.176 | 1.762 | -0.414 |
| 1.34 | 44.59 | 6.092 | 8.206 | 2.187 | 1.768 | -0.419 |
| 1.35 | 45.68 | 6.287 | 8.573 | 2.197 | 1.773 | -0.424 |
| 1.36 | 46.74 | 6.482 | 8.949 | 2.208 | 1.778 | -0.430 |

Table 2.2 Acid-concentration parameters: acid density (kg/L), H₂SO₄ content and H₂SO₄ concentration in mol/L, and molality. Cell voltage and electrode potentials referred to the standard hydrogen electrode, T=25°C (continued).

| Acid-concentration | | | | Cell Voltage U ^o Volts | Electrode potentials | |
|--------------------|--|-------------------|--|---|-------------------------------|---|
| Dens. kg/L | H ₂ SO ₄ wt.% | Molarity mol/L | Molality mol/kg H ₂ O | | V ref. to std. Positive | H ₂ electrode Negative |
| 1.37 | 47.80 | 6.677 | 9.336 | 2.219 | 1.783 | -0.436 |
| 1.38 | 48.85 | 6.873 | 9.738 | 2.230 | 1.788 | -0.442 |
| 1.39 | 49.89 | 7.070 | 10.149 | 2.241 | 1.794 | -0.447 |
| 1.40 | 50.91 | 7.267 | 10.573 | 2.252 | 1.800 | -0.452 |

2.2.3 Electrolyte stratification [13]

Electrolyte stratification is connected with the changes of the specific weight of the electrolyte associated with the concentration changes during charge and discharge. In flooded lead-acid batteries, acid stratification may cause severe problems. The immobilization of the electrolyte, as required for VRLA batteries, reduces stratification effects to a large extent, or practically eliminates them in a gelled electrolyte.

Fig. 2.4 illustrates the origin of acid stratification. On the left, the battery has been floated for an extended period, or the electrolyte has been mixed by other means. The acid concentration is uniform all over the battery. This will always be the final state when the battery is on float, because the diffusion process always equalizes the acid concentration. Stratification can only be caused by discharge/charge processes.

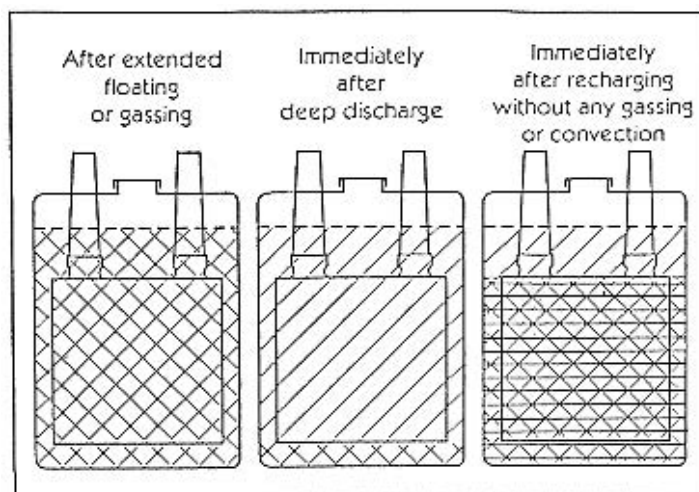


Figure 2.4 The origin of acid stratification, when the lead-acid battery is discharged and recharged without gassing or other means of mixing the electrolyte [13].

During charge, sulfuric acid is released from the active material in the plates and the concentration of the acid increases between the plates. Now the highest acid concentration is achieved between the plates, which initiate convection of this acid to the parts beside and underneath the plates. At the end of the charging process, the battery is filled with a slightly increased acid concentration to the upper edge of the plates. The acid above the plates remains diluted and there is no driving force for convection because of the low weight of this acid.

In the usual stationary application, acid stratification causes no problems, because the batteries are discharged only occasionally. There is enough time left for the diffusion to equalize the acid concentration. When the battery is running on a cycling schedule without electrolyte mixing, however, acid stratification causes uneven current distribution and reduces the efficiency of primarily the charging but also of the discharging process. Furthermore, acid stratification may become dangerous, because the concentration differences between the top and bottom parts of the cell are growing from cycle to cycle, especially in tall cells. In 55 cm tall cells of filled with 1.24 g/cm^3 , severe stratification effects were observed. After six full cycles the acid density decreased to 1.13 g/cm^3 at the top and 1.31 g/cm^3 at the bottom. The increasing acid concentration at the bottom may harm the negative plate, which is prone to sulfation when running in too high an acid concentration.

As a remedy against stratification, overcharging by 10 to 20% during each cycle is mostly applied for traction batteries. The gas evolution forms bubbles that mix the electrolyte. A more effective method is forced agitation of the electrolyte. Immobilization of the electrolyte, as required for VRLA batteries, eliminates stratification effects almost completely.

2.2.4 Conductivity of sulfuric acid [16]

Due to the concentration changes during the charge/discharge reactions, the conductivity of the sulfuric acid also varies, as shown in Fig. 2.5.

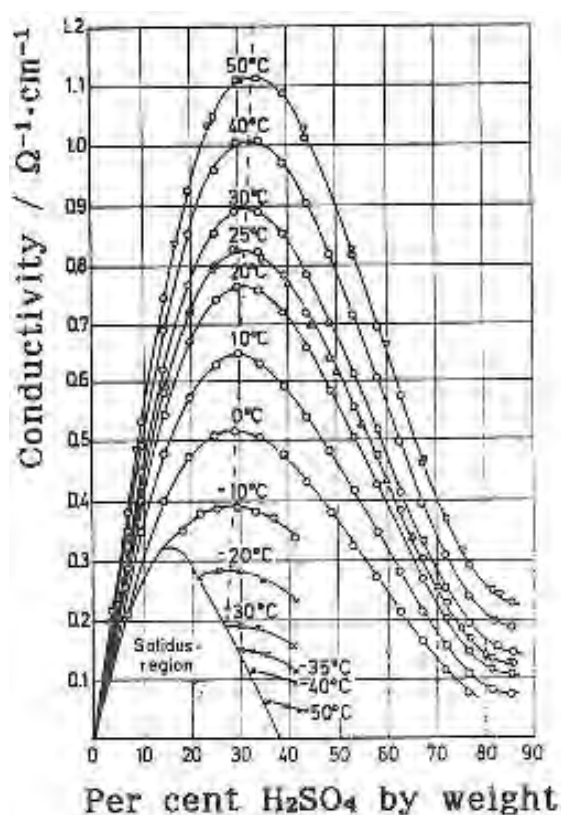


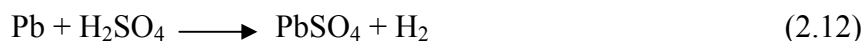
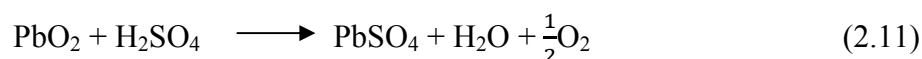
Figure 2.5 Specific electric conductance of aqueous solution of sulfuric acid and its dependence on temperature. The dotted line denotes the maximum [16].

The Figure shows that in charged batteries, the acid conductivity is close to its maximum. During deep discharge, however, the conductivity can reach fairly low values. Furthermore, the conductivity is considerably reduced at low temperatures.

2.2.5 Self-discharge [12]

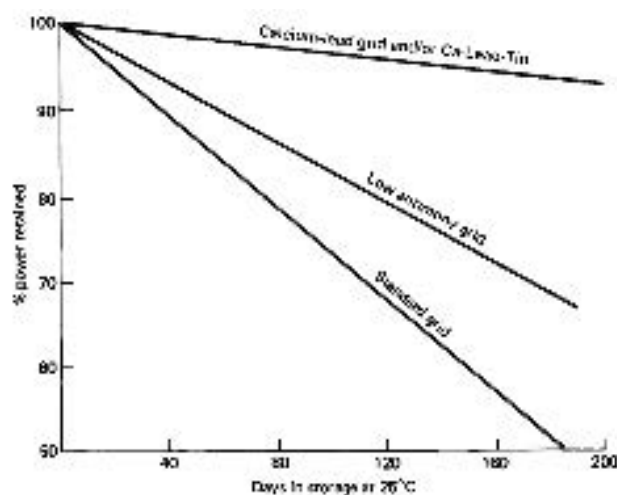
The equilibria of the electrode reactions are normally in the discharge direction, with the discharged state being the most thermodynamically stable. The rate of self-discharge [loss of capacity (charge) when no external load is applied] of the lead-acid cell is fairly rapid, but it can be reduced significantly by incorporating certain design features.

The rate of self-discharge depends on several factors. Lead and lead dioxide are thermodynamically unstable in sulfuric acid solutions, and in an open circuit, they react with the electrolyte. Oxygen is evolved at the positive electrode and hydrogen at the negative, at a rate dependent on the overvoltage, temperature, and acid concentration (the gassing rate increases with increasing acid concentration) as follows:

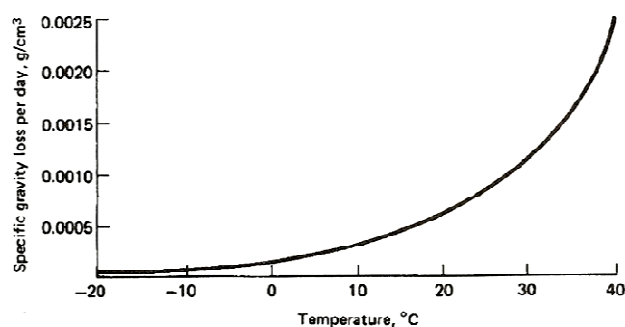


For most positive electrodes, the formation of PbSO_4 by self-discharge is slow, typically much less than 0.5%/day at 25°C. The self-discharge of the negative electrode is generally more rapid, especially if the cell is contaminated with various metallic ions. For example, antimony lost from the positive grids by corrosion can diffuse to the negative, where it is deposited resulting in a local action discharge cell which converts some lead active material to PbSO_4 . New batteries with lead-antimony grids lose about 1% of their charge per day at 25°C, but the charge loss increases by a factor of 2-5 as the battery ages. Batteries with nonantimonial lead grids lose less than 0.5% of charge per day regardless of age. This is illustrated in Fig. 2.6a. Maintenance-free and charge-retention-type batteries, where the self-discharge rate must be minimized, use low-antimony or antimony-free alloys (such as calcium-lead) grids. However, because of other beneficial effects of antimony, its complete elimination may not be desirable, and low-antimony-lead alloys are a useful compromise.

The self-discharge is temperature-dependent is shown in Fig. 2.6b. The graph shows the fall in specific gravity per day of a new fully charged battery with 6% antimonial lead grids. Self-discharge can be minimized by storing batteries in cool areas between 5 and 15°C.



(a)



(b)

Figure 2.6 (a) Capacity retention during standing or storage at 25°C. (b) Loss of specific gravity per day with temperature of a new fully charged lead-acid battery with 6% antimonial lead grids [12].

2.2.6 Immobilized electrolyte [16]

In VRLA batteries, immobilization of the electrolyte is required to provide open space for the fast transport of gaseous oxygen. Otherwise, the internal

oxygen cycle is hindered by the inadequate diffusion rate of the dissolved oxygen. In lead-acid batteries, two methods are used for electrolyte immobilization [4,16-17]:

(i) Application of AGM separators that are soaked in the acid so that liquid is not left within the cell.

(ii) Addition of about 6 wt.% of silica (SiO_2) that converts the acid into a stiff gel.

With both methods, after the first charge, a certain amount of electrolyte is observed above the separator or the gelled electrolyte that has been displaced by gas from larger pores in the felt or cracks of the gel. This liquid can be removed by suction to provide a void volume for fast oxygen transport in the separator. Otherwise, such space is automatically formed by the gradual loss of water due to electrochemical decomposition. In the latter case, the rate of the internal oxygen cycle at the beginning is limited, and the battery initially operates partly like a flooded one. A further advantage is that acid fumes do not escape from cells with immobilized electrolyte since they are hardly generated and there is no gas stream to carry them out of the cell.

In this research, the gelled electrolyte with added fumed silica was used. These electrolytes are environmentally safe, technically easy to handle, and have long term, even to the powerful oxidizing effects of the positive electrode. Fumed silica and sulfuric acid added to batteries forms a solid gel. It is a thixotropic gel that can be kept highly liquid by intensive agitation, which is taken advantage of when filling the battery. Real pores cannot be observed in the gelled electrolyte. The gelled sulfuric acid behaves in the same way as in a felt with a pore structure one order of magnitude finer than that of the usual micro glass-mat separator. Thus the acid is more strongly fixed and gravity effects that are observed in a 30 cm high AGM battery would be observed to a similar extent in a 3 m high battery with gelled electrolyte. Convection of the electrolyte, still possible to a small extent in glass mat separators, is almost repressed in the gelled electrolyte and ion movement is restricted to migration and diffusion. Accordingly, fill profiles caused by gravity are less pronounced, and stratification effects are not observed with gelled electrolyte.

2.3 Comparisons of vented (flooded) and valve-regulated technologies [18]

2.3.1 Reaction

Both technologies undergo the same chemical and electrochemical reactions. The rates of some of these reactions, however, are different.

2.3.2 Construction materials

Most of the materials used in vented and VRLA cells are the same. Notable exceptions are the absorbent separators used in absorbed electrolyte VRLA cells and the gelling agents used in gelled electrolyte VRLA cells. Also, vented-cell jars (containers) are typically transparent, whereas the containers for VRLA cells are opaque.

2.3.3 Aging and failure mechanisms

The common failure mechanisms of positive plate corrosion and growth, active material failure, post seal leakage, and container/cover seal leakage associated with vented cells also occur in VRLA cells. Some of these degradation mechanisms, however, are more significant in the VRLA cell design. Also VRLA cells are susceptible to additional failure modes that are normally not associated with vented cells. The aging effects and failure modes are described in 2.3.3.1 through 2.3.3.7.

2.3.3.1 Dryout

A vented battery is expected to require periodic watering to restore lost water. Any water loss from a VRLA battery, however, is usually irreversible in most designs because water cannot easily be added to the cell. As a VRLA cell loses water, it will eventually experience loss of capacity due to dryout.

The recombination process tends to be somewhat self-regulating in that recombination efficiency improves as water is lost. When first put into service, a VRLA cell can lose water until it reaches optimal recombination efficiency, with little water loss thereafter. However, other effects that occur during

normal and abnormal operation can also result in water loss and corresponding capacity loss. These effects are as follows:

(i) *Positive grid corrosion*: The grid corrosion process that occurs during normal aging of a lead-acid cell consumes part of the water in the electrolyte throughout its operational life. Small amounts of hydrogen gas are vented during normal float operation.

(ii) *Overcharging*: A higher than normal charge voltage results in increased oxygen generation from the positive plates. If the rate of oxygen generation exceeds the gas transport rate capability of the electrolyte and separator, both hydrogen and oxygen will be vented from the cell through the pressure relief valve. Therefore, the volume of the electrolyte solution declines over time.

(iii) *High temperature*: The gassing rate increases with temperature. At a high temperature, some gases may be vented rather than recombined inside the cell.

(iv) *Water vapor diffusion*: As the temperature increases or the humidity decreases, the water vapor diffusion rate through the cell container also increases. The diffusion rate varies with the type and thickness of container materials, operating temperature, and relative humidity around the cell. Manufacturers may select container materials that minimize water vapor diffusion, but they also consider other properties, such as dimensional stability and absorbed glass mat compression in AGM cells operated at high temperature.

2.3.3.2 Thermal runaway

When a VRLA cell is operating on float or overcharge in a fully recombinant mode, almost all of the overcharge energy results in heat generation. If the design of the system and its environment are such that the heat produced can be dissipated and thermal equilibrium can be reached, then there is no thermal runaway problem. However, if the recombination reaction gives rise to a rate of heat generation that exceeds the rate of heat dissipation, the battery temperature will rise and more current will be required to maintain the float voltage. The additional current results in still more recombination and heat generation that further

raises battery temperature, and so on. The net effect can be accelerated dryout and/or melting of the battery. This potential problem is further aggravated by elevated ambient temperatures or by cell or charging system malfunctions. The possibility of thermal runaway can be minimized by the use of appropriate ventilation/cooling between and around the cells and by limiting the charger output current and voltage such as by using temperature-compensated chargers. In the gelled electrolyte system, the gel provides better thermal conductivity than the absorbed electrolyte system, but is still inferior to a vented system.

2.3.3.3 Negative plate self-discharge

Although the basic principle of the recombination process might be relatively simple to understand, the actual implementation in a VRLA cell is quite complex. A delicate balance is maintained between oxygen recombination, positive grid corrosion and negative plate self-discharge (plate sulfation). If the balance is incorrect (due to cell design, operating temperature or other factors), the negative plate may slowly self-discharge. Research has determined that premature loss of capacity in VRLA cells is often due to a gradual discharge of the negative plates. Manufacturers may address this issue by modifying active materials to reduce the rate of negative self-discharge, or through the use of catalysts.

2.3.3.4 Seal or valve failures

In a vented cell, a post seal failure becomes a maintenance nuisance because of electrolyte leakage around the post. In a VRLA cell, post seal failure may allow a path for air ingress. If oxygen in the air enters the cell, it can discharge the negative plate. The recombination process limits the ability of the negative plates to be recharged. Seal or valve failures may also result in electrolyte leakage.

Air ingress through a pressure relief valve or container crack can also lead to eventual discharge of the negative plate. The cell will lose capacity as the negative plate discharges. For this reason, air ingress is a failure mode for VRLA cells.

2.3.3.5 Temperature effects

VRLA batteries tend to be more susceptible to degradation aging at higher temperatures than vented lead-acid batteries. The recombination process that allows these batteries to operate without the need for periodic water addition also generates heat. Some VRLA installations may have the cells tightly packed, limiting heat dissipation capability. All of these factors can combine to cause the battery to operate at a higher-than-ambient temperature, thereby decreasing battery life. Higher temperatures will also increase the possibility of dryout and susceptibility to thermal runaway.

2.3.3.6 Loss of absorbed glass mat compression

VRLA cells of the absorbed glass mat design can experience in the mat over time, which may result in a loss of mat compression. Contact between the mat and the plates are necessary to ensure that the active materials are in contact with the electrolyte. Over time, small voids can develop between the mat and the plates, thereby decreasing the available capacity. This effect is referred to as loss of compression and can be caused by manufacturing errors, improper design or design tolerances, and dryout.

Loss of compression can also be caused by relaxation of the container, due to container design and/or high-temperature environments. Battery manufacturers have used various methods and materials to limit container expansion.

2.3.3.7 Ripple current

The direct current (DC) is normally produced from the alternative current (AC), and the peaks of the ac signals in the rectifiers may appear as ripple on the output. Depending on the magnitude and frequency, this superimposed ripple can produce additional heating. VRLA cells appear to be more sensitive to this heating effect because of their lower heat transfer coefficient compared to vented cells. A higher cell internal temperature contributes to a decrease in expected service life, which is reduced by approximately 50% for every 8°C to 10°C increase in internal temperature.

2.3.4 Electrolyte specific gravity

By design, absorbed electrolyte VRLA cells have lower volumes of electrolyte than vented cells containing equivalent amounts of active materials. If AGM cells had the same electrolyte specific gravity as vented cells, they would exhibit lower long-duration capacities. In gelled electrolyte cells, the gel interferes with electrolyte diffusion and convection, which results in reduced high-rate capacities. In both cases, the expected reductions in capacity may be partially compensated for by increasing the electrolyte concentration (specific gravity).

Typical specific gravities of VRLA cells range from 1.280 to 1.340 (1.300 is most common), although some designs have specific gravities that are comparable to vented cells.

A higher specific gravity results in higher ampere-hour capacity per unit volume. It also increases chemical activity, thereby causing an increased positive plate corrosion rate. This increased corrosion reduces the service life of the cell.

2.3.5 Charging voltage

2.3.5.1. Float voltage

The electrolyte specific gravity that is typical of most VRLA cells results in a higher float voltage being required than for typical vented cells. The actual float voltage depends upon the specific gravity of the electrolyte being used. The recommended float voltage is provided by the battery manufacturer. This voltage is sufficient to keep the battery fully charged without causing excessive positive grid corrosion or forcing the battery to draw more current than is required to maintain a charge.

2.3.5.2 Temperature compensation of charging voltage

Temperature-compensated charging is any method of adjusting the output voltage of the battery charger to compensate for deviations in the battery operating temperature above or below a standard value, typically 25°C (77 °F). Because VRLA batteries are much more susceptible to thermal runaway than vented

cells, temperature-compensated charging is strongly recommended when they are used in a constant voltage float charge regime.

2.3.6 Absence of free electrolyte

Designs of VRLA cells are such that the electrolyte should be fully immobilized and thus little, if any, liquid electrolyte should leak from the cell in the event of a jar and/or cover break or crack. The absence of free electrolyte simplifies the handling of VRLA cells and also abates the need for spill containment.

2.3.7 Maintenance and testing

By the very nature of the designs of VRLA cells, specific gravity readings are impossible and routine water additions are either impossible or impractical. Consequently, the batteries have been referred to in the past as maintenance free. However, this is true only with respect to the electrolyte. Otherwise, VRLA battery maintenance is similar to that required for vented batteries, and will require special procedures to compensate for the inability to determine the amount and concentration of electrolyte.

2.3.8 Orientation in use

Unlike vented lead-acid cells where the only possible orientation is to stand the cell upright, certain VRLA cell designs allow for operation in other orientations, which may be advantageous when space considerations are an issue. Some AGM VRLA cells should be oriented in a particular way to minimize electrolyte stratification. Contact the VRLA manufacturer for preferable or required orientations of the batteries.

2.3.9 Vented gas

In a normally operating VRLA cell there will be a slow buildup of un-recombined gas, mostly hydrogen. When the internal pressure of the cell exceeds the valve release pressure, the gas will be vented into the atmosphere until the internal pressure returns to normal and the valve closes. Adequate ventilation should be

provided in order to prevent buildup of hydrogen gas in the area where the battery is located.

2.3.10 Historical service life

Many VRLA batteries are installed throughout the world and the experience to date indicates that a 20-year or 10-year VRLA battery design life is difficult to obtain in service.

The designed life of the cell is related to the intrinsic mechanical, electrical, and electrochemical characteristics of the cell. The designed life of the cell is rarely attained as a service life at the system level due to a variety of factors, including those mentioned in 2.3.3.

Industry experience shows that the actual VRLA battery system service life is often considerably less than its designed life. Also, the service life may be further reduced by environmental operating conditions in which the user places the battery. Although manufacturing practices continue to improve, and new techniques have been developed to address particular failure modes, the user should not plan for the batteries to last the entire designed life for a single cell or multicell unit. In summary, VRLA cells will not last as long as vented cells.

2.3.11 VRLA advantages and disadvantages

Much has been written about the drawbacks of VRLA batteries since they do have advantages over other battery types (most specifically, vented lead-acid cells). Some of the advantages and disadvantages include the followings:

(i) *Low initial cost:* Compared to many other technologies, VRLA batteries typically cost the least for equivalent energy-supply levels, especially in smaller size. However, the total life cycle cost of ownership (including maintenance, replacement, operating costs, etc.) should also be considered. Many applications (especially those in adverse operating conditions, like high temperature environments) should have a life-cost study performed in order to determine the appropriate battery type based on life cycle economics.

(ii) *Compact*: Compared to vented batteries, VRLA batteries are more compact and they can be placed in smaller spaces. Because of the way they are manufactured and packaged, VRLA cells can be made in sizes much smaller than those typically found for flooded vented lead-acid cells.

(iii) *No watering*: Because VRLA cells do not normally require watering, many users operate them on an install and forget basis. This, however does not excuse the user from maintenance. Those who do not perform maintenance open themselves up to an increased risk of battery failure.

(iv) *Easier installation*: VRLA batteries are typically less costly to install than vented batteries, and can typically be installed in less time than equivalently sized vented batteries.

(v) *Non-spillable (transport and placement)*: VRLA batteries that have passed the appropriate qualification tests set forth in the Code of Federal Regulation (CFR 49) can be classified by the U.S. Department of Transportation (DOT) as UN2800 – Batteries, Non-Spillable for road shipments (CFR 49). This classification allows these batteries to be transported with fewer restrictions than for vented batteries. VRLA batteries can also be air-shipped as non-spillable, non-dangerous, as long as they meet the non-spillable requirements mentioned above, in addition to a separate International Air Transport Association (IATA) requirement (A67) for a puncture test. Because they are essentially non-spillable, most VRLA cells can be placed in more convenient space-saving configurations, such as front terminal, or horizontal.

(vi) *Thermal issue*: VRLA batteries are more susceptible to potentially destructive and dangerous thermal runaway. They also have short lifetimes in high temperature environments.

(vii) *Short life*: VRLA batteries (even when kept in similar environments) have much shorter average lifetimes than vented lead-acid batteries, nickel-cadmium batteries, or other competing technologies.

(viii) *Lower reliability*: Due to the factors mentioned above (see also 2.3.10), use of VRLA batteries typically lowers the reliability of an application (in comparison to vented lead-acid batteries, for example). However, this loss of reliability can be mitigated by techniques such as using paralleled strings, etc.

2.4 Gelled electrolyte immobilization with fumed silica (pyrogenic silica) [19]

Pyrogenic silica is a very fine dispersed SiO_2 powder with an apparent density of 0.05 g/mL. It consists of primary compact particles with a diameter of 10 nm (0.01 μm) in average that can be seen with Transmission Electron Microscopy (TEM), as shown in Fig. 2.7 (a) and (b). Due to the small size of primary particles, the internal surface is very high, with measured as BET-surfaces of 200 m^2 per gram.

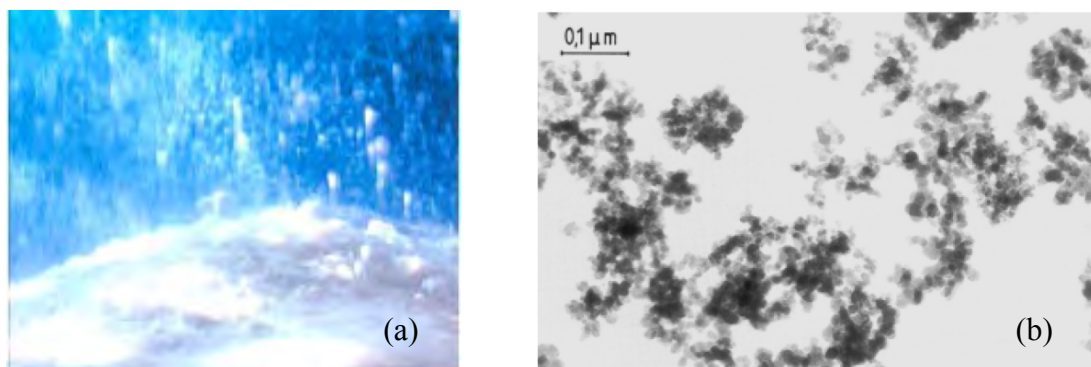


Figure 2.7 (a) Powder of pyrogenic silica and (b) TEM of pyrogenic silica [19].

The 10nm diameter primary spherical particles are bonded together in chainlike aggregates. These aggregates have a loose contact to each other and form agglomerates. This morphology is a direct consequence of the manufacturing process:

Evaporated silicon chloride is blown in an oxygen-hydrogen flame. At temperatures above 1500°C, SiO_2 molecules are formed. Around 10.000 SiO_2 molecules strongly bound in siloxane groups (Si-O-Si) bind together to spherical primary particles of 10 nm particles. As the particles move to colder areas, they bind together to form chain-like aggregates with lengths up to approximately 1 μm . After further cooling, they form agglomerates with a diameter of 10 to 250 μm . The binding

force between the primary particles is the hydrogen bridge linkage. The silanol groups (Si-O-H) of two particles come in contact and create the bridge linkage by the exchange of their hydrogen atoms (Fig. 2.8).

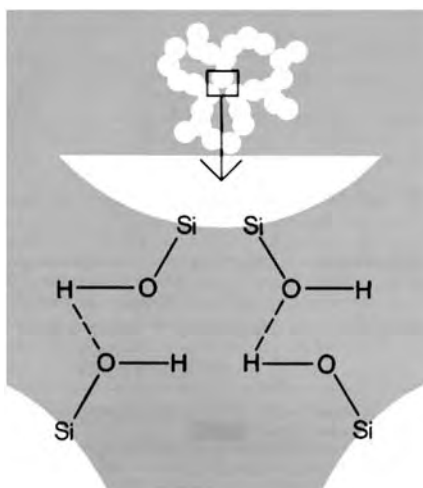


Figure 2.8 Hydrogen bridge linkages between particles [19].

These agglomerated aggregates of SiO_2 particles are mixed with acid and water, forming a liquid GEL (SOL) as seen in the left part of Fig. 2.9. After several hours of setting, the hydrogen bridge linkages form a three-dimensional structure. This is the GEL, seen in the right hand side of Fig. 2.9.

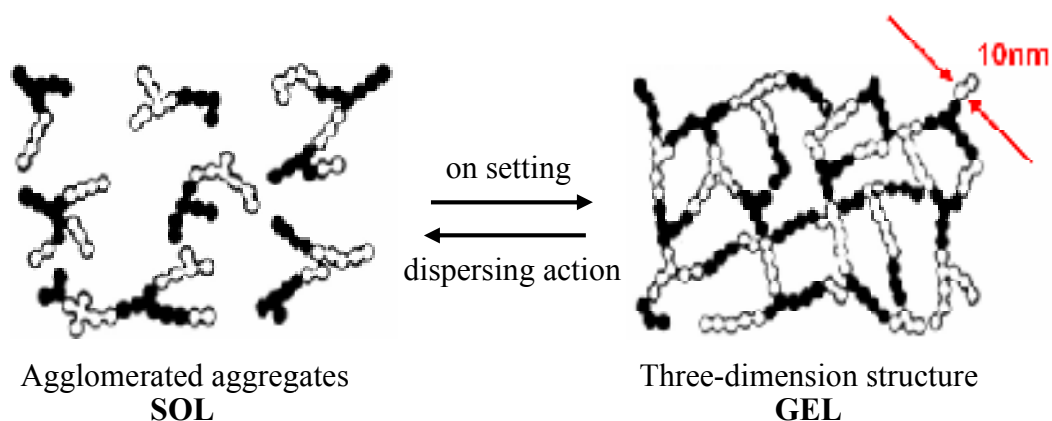


Figure 2.9 The formation of the GEL structure is reversible at the beginning, by dispersing SOL and by setting GEL [19].

The most important information is that water and sulfuric acid are trapped in a structure, which is formed by chains with a diameter of only 10nm or $0.01\mu\text{m}$.

2.5 Conducting polymer

Beginning in July 1988, conducting polymers were applied in various applications such as batteries, photovoltaic cells, chemical sensors, semiconductor devices and optical switches. Currently, the most active field of development is in batteries [20]. For example, Martha and co-workers [2] used PANI-coated negative plates in lead-acid batteries. They found that the cells with PANI-coated negative plates exhibited lower impedance in relation to conventional cells while sustaining higher discharge-rates with diminished capacity loss during prolonged charge-discharge cycling. Zhijiang [10] developed a polyindole-based aqueous polymer rechargeable battery. The batteries included poly(5-nitroindole) as the anode active material and PANI as the cathode active material. The results showed that the conducting polymer polyindole as the anode active material and PANI as the cathode active materials could be used to obtain a plastic battery with about a 1.3V electromotive force. Chew and co-workers [21] developed a novel nano-silicon/PPy composite, suitable for lithium-ion battery anodes, which was prepared by chemical polymerization. The results showed that the Si particles were uniformly distributed among the PPy particles. The PPy component in the composites effectively buffered the great volume changes during the cycling process.

2.5.1 Polyaniline (PANI) [22]

Since the discovery that conjugated polymers can be made to conduct electricity through doping, a tremendous amount of research has been carried out in the field of conducting polymers. PANI (Fig. 2.10) is an excellent example of a conjugated polymer that can be tailored for specific applications thorough the doping process. Since its conducting properties were rediscovered in the early 1980s, PANI has been studied for many other potential applications including lightweight battery electrodes, electromagnetic shielding devices, and anticorrosion coating [2, 9-10, 23-29]. Bulk PANI is now commercially available from several sources. PANI is electrically conductive in its emeraldine oxidation state when doped with a salt that protonates the imine nitrogens in the polymer backbone. Dopants can be added in any desired quantity until all of the imine nitrogens (half of the polymer total nitrogens) are doped, simply by controlling the pH of the dopant acid solution.

The conductivity of PANI increases with doping from the undoped insulating base form ($\sigma \leq 10^{-10}$ S/cm) to the fully doped, conducting acid form ($\sigma \geq 1$ S/cm). The doping and undoping processes are typically carried out chemically with common acids such as hydrochloric acid and bases such as ammonium hydroxide; electrochemical processes can also be used. In addition to affecting conductivity doping and undoping processes, dramatic effects on the morphology of the polymer films can also be observed.

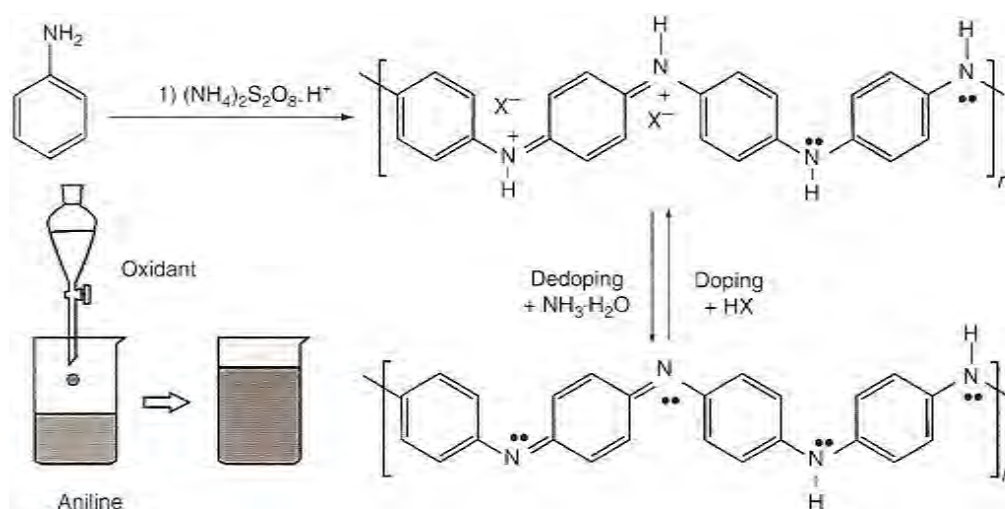


Figure 2.10 The oxidative polymerization of aniline in an acidic solution. The synthesized PANI forms in its doped emeraldine salt state that then can be dedoped by a base to its emeraldine base form. The bottom left scheme illustrates a typical reaction for making PANI [22].

2.5.2 Polypyrrole (PPy) [22]

Among the conducting polymers, PPy has attracted great attention because of its high electrical conductivity and good environmental stability. PPy has been considered as the key material to many potential applications such as electronic devices, electrodes for rechargeable batteries and supercapacitors, solid electrolytes for capacitors, electromagnetic shielding materials, sensors, corrosion-protecting materials, actuators, electrochromic devices, or membranes [11, 21, 28, 30-36]. The heteroaromatic and extended π -conjugated backbone structure of PPy provide it with chemical stability and electrical conductivity, respectively. The π -conjugated backbone structure, however, is not sufficient to produce appreciable conductivity on

its own. Partial charge extraction from PPy chain is also required, which is achieved by a chemical or an electrochemical process referred to as doping. The conductivity of the neutral PPy is remarkably changed from an insulating regime to a metallic one by doping. This is a very worthwhile feature for applications in which the electrical conductivity of a material must be controlled.

It was reported that the electronic and band structures of PPy were changed with the doping level of the PPy chain. Neutral PPy, with the benzenoid structure shown in Fig. 2.11a, is categorized as an insulator and its proposed electronic energy diagram is shown Fig. 2.12a. The band gap of neutral PPy is reported to be 3.16 eV, which is too wide for electrons to transfer from the valence to the conduction band at room temperature. The PPy chain is, however, simultaneously doped during polymerization. Counteranions in the reaction medium are incorporated into the growing PPy chain to maintain electrical neutrality of the polymer system. Upon extraction of a negative charge from a neutral segment of a PPy chain by the doping process, a local deformation to the energetically favored quinoid structure occurs (Fig. 2.11b). In combination with the quinoid structure, the positive charge and the unpaired spin are referred to as a polaron (Fig. 2.11b). Referring to Fig. 2.12b, the formation of a polaron induces two new intermediate states (bonding and antibonding) within the band gap while the unpaired electron occupies the bonding (low energy) state, thus giving the polaron a spin of $1/2$.

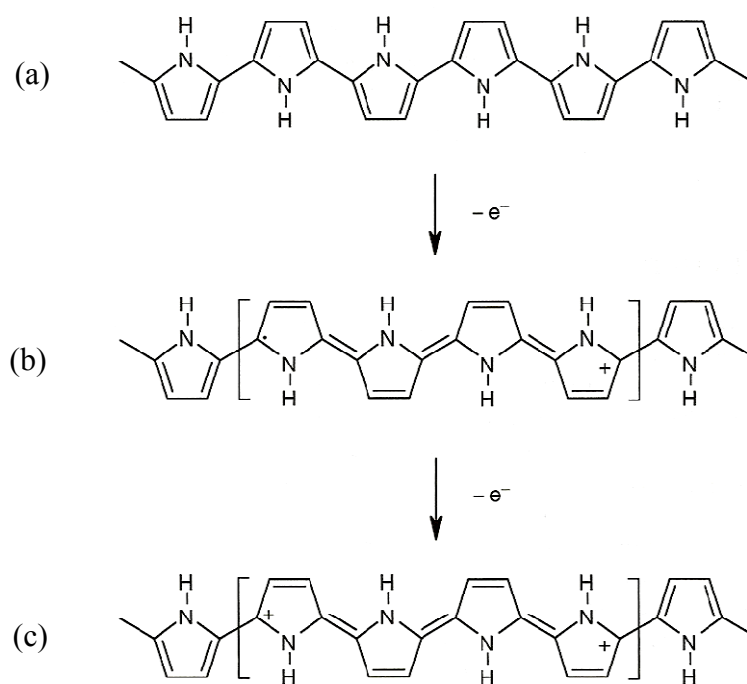


Figure 2.11 Electronic structures of (a) neutral PPy, (b) polaron in partially doped PPy and (c) bipolaron in fully doped PPy [22].

As oxidation continues further, another electron has to be removed from a PPy chain that already contains a polaron, resulting in the formation of a bipolaron which is energetically preferred to the formation of two polarons. A bipolaron is known to extend over about four pyrrole rings (Fig. 2.11c). The bipolaron states lie further from the band edges. (Fig. 2.12c). The lower energy state of the bipolaron is empty, thereby leading to a species with zero spin. As the degree of oxidation increases, the bipolaronic energy state overlaps, resulting in the formation of narrow intermediate band structures (Fig. 2.12d). The energy diagram shown in Fig. 2.12d corresponds to a doped state of about 33 mol%, which is close to the maximum value found in electrochemically oxidized PPy. The typical doping level of PPy is in the range of 20 to 40 mol%. At this doping level, bipolarons are predominant in PPy with few polarons, and thus the charge carriers in the conducting PPy have zero-spin number.

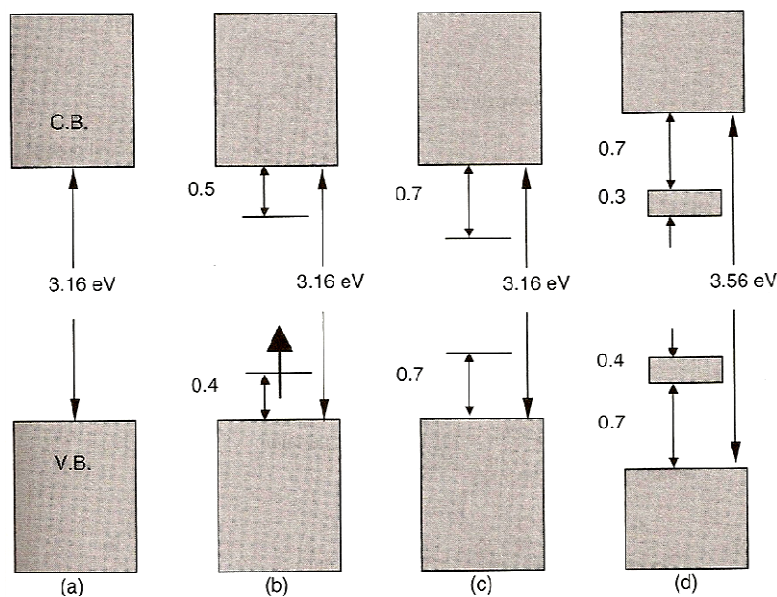
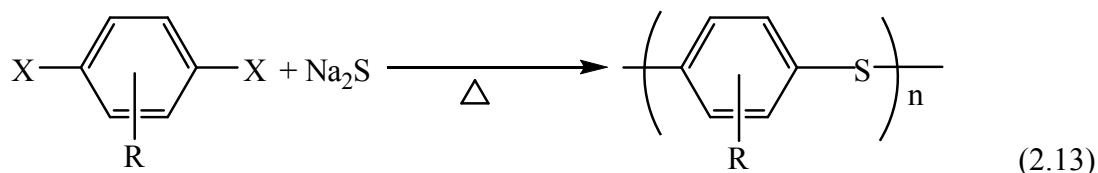


Figure 2.12 Electronic energy diagrams for (a) neutral PPy, (b) polaron, (c) bipolaron and (d) fully doped PPy [22].

2.5.3 Poly (p-phenylene sulfide) (PPS) [37]

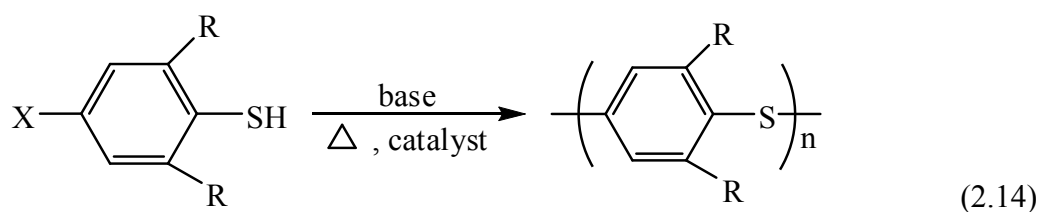
PPS was the first nonrigid, not fully carbon-backbone-linked polymer made highly conducting upon doping. This discovery was particularly exciting because the pristine polymer is a commercially available melt and solution-processible polymer that provided precedent for potentially obtaining commercially viable conducting plastics. Not only was PPS the first processible polymer to be made highly conducting, but as will be seen later on, it was the first system discovered to be processible in its conductive form. Furthermore, PPS is just one of what is now recognized as a general class of processible conducting polymers, namely, the polyphenylene chalcogenides.

Although PPS has been made by many processes, the Edmonds-Hill process and the Lenz process, stand out as being the most useful. The Edmonds-Hill process (equation 2.13) involves condensation of a dihalogenated aromatic with Na_2S in N-methylpyrrolidone at high temperature and to provide polymers with aromatic rings linked in known positions (regiospecificity):



X = Halogen; R = Substituents or H

The process is most useful in preparing symmetrical polymers. On the other hand, the Lenz process involves self-condensation of a halogenated thiophenol (equation 2.14), which results in “head-to-tail” polymerization:



The Lenz process is useful in preparing asymmetrically substituted polyarylene sulfides regiospecifically.

PPS displays a glass transition temperature (T_g) at 92°C and melt (T_m) at 280°C . The virgin polymer is a good insulator ($10^{-16} \Omega^{-1} \text{cm}^{-1}$). Although soluble in organic solvents, not much solubility is noted until temperature of $200\text{--}220^\circ\text{C}$ are reached. Common solvents are diphenyl ether, chloronaphthalene, and N-methylpyrrolidinone. Tetrahydrofuran (THF) and CH_2Cl_2 have been used to extract low molecular weight oligomers from the virgin polymer before processing and doping. In fact, from the THF extracts a cyclic hexamer of PPS (mp 349.7°C) was isolated, while a cyclic pentamer and tetramer were isolated from CH_2Cl_2 extracts.

2.6 Cyclic voltammetry [38]

Cyclic voltammetry is the most widely used technique for acquiring qualitative information about electrochemical reactions. The power of cyclic voltammetry results from its ability to rapidly provide considerable information on the thermodynamics of redox processes, the kinetics of heterogeneous electron transfer reactions and coupled chemical reactions or adsorption processes. Cyclic

voltammetry is often the first experiment performed in an electroanalytical study. In particular, it offers a rapid location of redox potentials of the electroactive species, and convenient evaluation of the effect of media on the redox process.

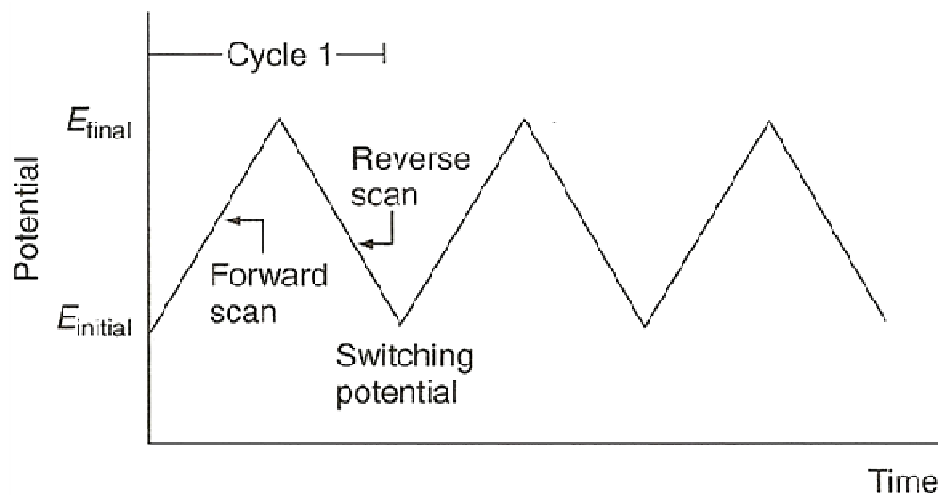


Figure 2.13 The potential-time excitation signal in a cyclic voltammetric experiment [38].

Cyclic voltammetry consists of linearly scanning the potential of a stationary working electrode (in an unstirred solution), using a triangular potential waveform (Fig. 2.13). Depending on the information sought, single or multiple cycles can be used. During the potential sweep, the potentiostat measures the current resulting from the applied potential. The resulting current-potential plot is termed a cyclic voltammogram. The cyclic voltammogram is a complicated, time-dependent function of a large number of physical and chemical parameters.

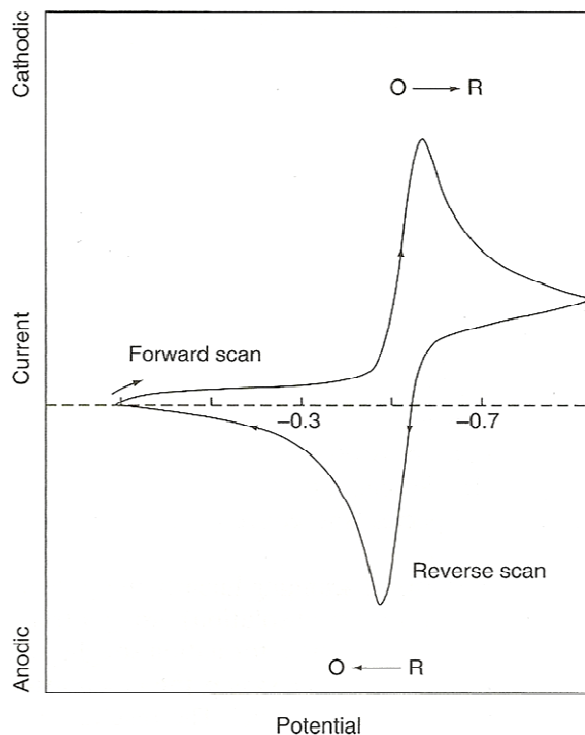


Figure 2.14 Typical cyclic voltammogram for a reversible $O + ne^- \rightleftharpoons R$ redox process [38].

Fig. 2.14 illustrates the expected response of a reversible redox couple during a single potential cycle. It is assumed that only the oxidized form of O is present initially. Thus, a negative potential scan is chosen for the first half-cycle, starting from a value where no reduction occurs. As the applied potential approaches the characteristic E^0 for the redox process, a cathodic current begins to increase, until a peak is reached. After traversing the potential region in which the reduction process takes place (at least $90/n$ mV beyond the peak), the direction of the potential sweep is reversed. During the reverse scan, R molecules (generated in the forward half-cycle, and accumulated near the surface) are reoxidized back to O, resulting in an anodic peak.

2.7 Electrochemical cells [38]

Three-electrode cells (see Fig. 2.15) are commonly used in controlled-potential experiments. The cell contains three electrodes (working, reference, and auxiliary), which are immersed in the sample solution. While the working electrode

is the electrode at which the reaction of interest occurs, the reference electrode provides a stable and reproducible potential, against which the potential of the working electrode is compared. Such buffering against potential changes is achieved by a constant composition of both forms of its redox couple, such as Ag/AgCl or Hg/Hg₂Cl₂, as common with the silver-silver chloride and the saturated calomel reference electrodes, respectively. To minimize contamination of the sample solution, the reference electrode may be insulated from the sample through an intermediate bridge. An inert conducting material, such as a platinum wire or graphite rod, is generally used as the current-carrying auxiliary electrode. The relative position of these electrodes and their proper connection to the electrochemical analyzer should be noted. The three electrodes, as well as the tube used for bubbling deoxygenating gas, are supported in five holes in the cell cover. are supported in five holes in the cell cover.

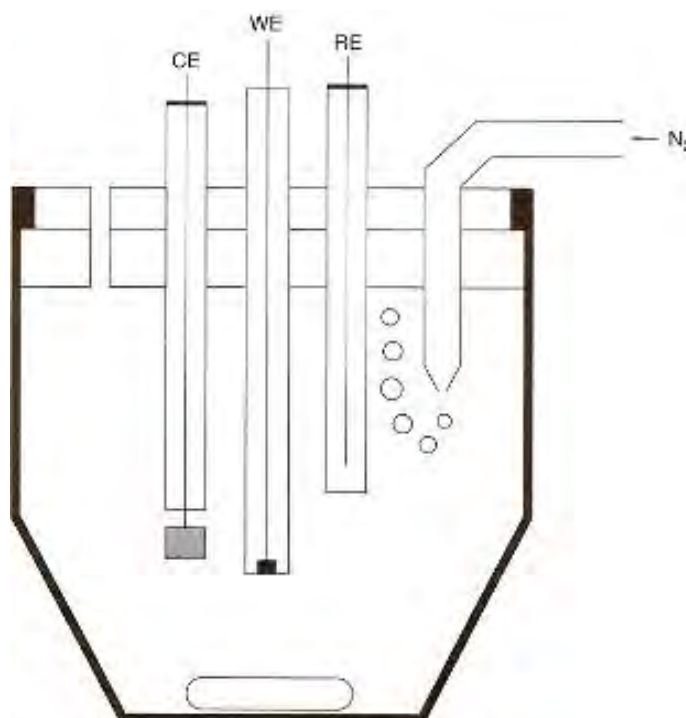


Figure 2.15 Schematic diagram of a cell for voltammetric measurements: WE-working electrodes; RE-reference electrode; CE-counter electrode. The electrodes are inserted through holes in the cell cover [38].

2.8 Electrical Conductivity [39-40]

2.8.1 Definition of conductivity

Conductivity is the ability of a material to conduct electric current. The principle by which instruments measure conductivity is simple. Two plates are placed in the sample, a potential is applied across the plates (normally a sine wave voltage), and the resultant current is measured. Conductivity (C), the inverse of resistivity (R), is determined from the voltage and current values according to Ohm's law.

$$C = 1/R = I \text{ (amps)} / E \text{ (volts)} \quad (2.15)$$

Since the charge on ions in solution facilitates the conductance of electrical current, the conductivity of a solution is proportional to its ion concentration. In some situations, however, conductivity may not correlate directly to concentration. Fig. 2.16 illustrates the relationship between conductivity and ion concentration for two common solutions. Notice that the graph is linear for the sodium chloride solution, but is not linear for highly concentrated sulfuric acid. Ionic interactions can alter the linear relationship between conductivity and concentration in some highly concentrated solutions.

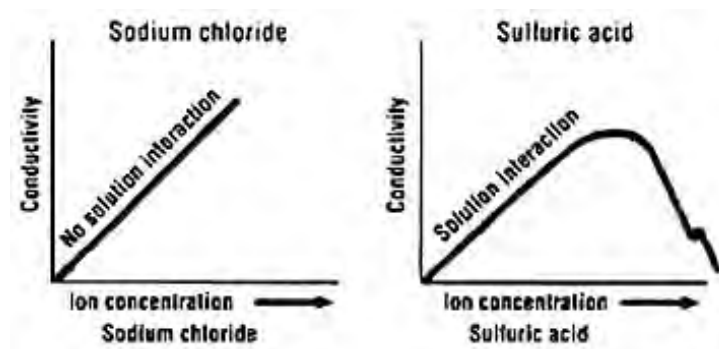


Figure 2.16 The relationship between conductivity and ion concentration for two common solutions [39].

2.8.2 The measurement of conductivity

Conductivity may be measured by applying an alternating electrical current (I) to two electrodes immersed in a solution and measuring the resulting voltage (V). During this process, the cations migrate to the negative electrode, the anions to the positive electrode and the solution acts as an electrical conductor as shown in Fig. 2.17.

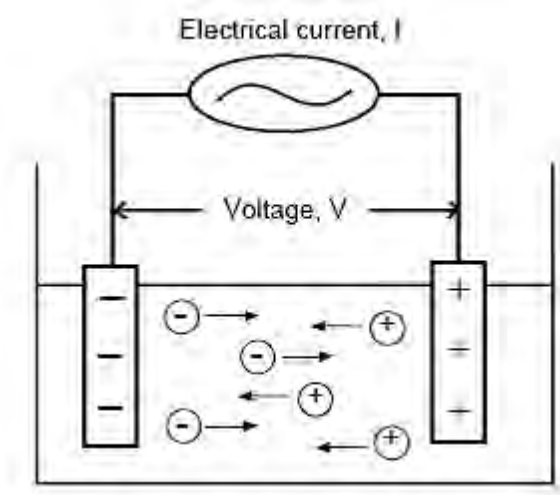


Figure 2.17 Migration of ions in solution [40].

2.8.3 Units of Measurement

The basic unit of conductivity is the siemens (S), formerly called the mho. Since cell geometry affects conductivity values, standardized measurements are expressed in specific conductivity units (S/cm) to compensate for variations in electrode dimensions. Specific conductivity (σ) is simply the product of measured conductivity (C) and the electrode cell constant (L/A), where L is the length of the column of liquid between the electrode and A is the area of the electrodes.

$$\sigma = C \times (L/A) \quad (2.16)$$

If the cell constant is 1 cm^{-1} then the specific conductivity is the same as the measured conductivity of the solution. Although electrode shape varies, an electrode can always be represented by an equivalent theoretical cell.

2.8.4 Conductive solution

Conductivity is typically measured in aqueous solutions of electrolytes. Electrolytes are substances containing ions, i.e., solutions of ionic salts or of compounds that ionize in solution. The ions formed in solution are responsible for carrying the electric current. Electrolytes include acids, bases and salts can be either strong or weak. Most conductive solutions measured are aqueous solutions, as water has the capability of stabilizing the ions formed by a process called solvation.

2.8.4.1 Strong electrolytes

Strong electrolytes are substances that are fully ionized in solution. As a result, the concentration of ions in solution is proportional to the concentration of the electrolyte added. They include ionic solids and strong acids, for example HCl. Solutions of strong electrolytes conduct electricity because the positive and negative ions can independently migrate under the influence of an electric field.

2.8.4.2 Weak electrolytes

Weak electrolytes are substances that are not fully ionized in solution. For example, acetic acid partially dissociates into acetate ions and hydrogen ions, so that an acetic acid solution contains both molecules and ions. A solution with a weak electrolyte can conduct electricity, but usually not as well as a strong electrolyte because there are fewer ions to carry the charge from one electrode to the other.

2.8.5 Definition of terms

2.8.5.1 Resistance

The resistance of the solution (R) can be calculated using Ohm's law ($V = R \times I$).

$$R = V/I \quad (2.17)$$

Where: V = voltage (volts) , I = current (amperes) and R = resistance of the solution (ohms).

2.8.5.2 Conductance

Conductance (G) is defined as the reciprocal of the electrical resistance (R) of a solution between two electrodes.

$$G = 1/R \text{ (S)} \quad (2.18)$$

The conductivity meter in fact measures the conductance, and displays the reading converted into conductivity.

2.8.5.3 Cell constant

This is the ratio of the distance (d) between the electrodes to the area (a) of the electrodes.

$$K = d/a \quad (2.19)$$

Where: K = cell constant (cm^{-1}), a = effective area of the electrodes (cm^2) and d = distance between the electrodes (cm).

2.8.5.4 Conductivity

Electricity is the flow of electrons. This indicates that ions in solution will conduct electricity. Conductivity is the ability of a solution to pass current. The conductivity reading of a sample will change with temperature.

$$C = G \cdot K \quad (2.20)$$

Where: C = conductivity (S/cm), G = conductance (S), where $G = 1/R$ and K = cell constant (cm^{-1}).

2.8.5.5 Resistivity

This is the reciprocal of the conductivity value and is measured in ohm·cm. It is generally limited to the measurement of ultrapure water, the conductivity of which is very low.

2.9 Literature reviews of lead-acid batteries

In 2001, Torcheux and Lailier [41] developed a new electrolyte formulation for cycling applications, especially for renewable energy markets in developing countries. The new acid formulation developed was a mixture of H_2SO_4 , liquid colloidal silica and other additives such as H_3PO_4 . The results showed that the battery life is significantly increased using this formulation due to, the prevention of acid stratification by the colloidal silica and the delay of positive active mass softening by H_3PO_4 .

In 2002, Wu et al. [42] studied the influence of the content of SiO_2 (in the form of soot) on the capacity and the self-discharge of lead-acid batteries. Moreover, the structure of the gelled electrolyte was investigated in detail by means of CV, electrochemical impedance spectroscopy and scanning electron microscopy. They found that the content of SiO_2 and the viscosity of the gelled electrolyte are important factors which affected the capacity of batteries. The colloidal particles become smaller with increasing the SiO_2 content because the three-dimensional web structure of the gelled electrolyte is more compact. Therefore, the SiO_2 contents of gelled electrolyte have to be carefully controlled.

In 2002, Lambert et al. [4] developed the gelled electrolyte technology for VRLA batteries. They focused on silica sols. The following four different commercially available, grades of silica sols were evaluated as potential gelling agents. Each sol was mixed with 100 g sulfuric acid (98 wt.%) in a total of 265 g of electrolyte to give a final relative density of 1.300 at 20°C.

(i) BINDZIL^{®3} AG4000 is a colloidal dispersion of discrete, spherical, silica particles (40 wt.%) in weakly alkaline water. This uniform, high surface area ($220 \text{ m}^2 \text{ g}^{-1}$), submicroscopic particles (diameter 12 nm) consist of pure amorphous silicon dioxide stabilized with a small amount of sodium hydroxide. The extremely low chloride content of this product allows a silica dosage of up to $\sim 15 \text{ wt.}\% \text{ SiO}_2$ in the total electrolyte weight without exceeding 5 mg L^{-1} of chloride in the filling acid, the limit according to the DIN 43 530 standard.

(ii) BINDZIL[®] AG3000 is a less concentrated (30 wt.% SiO_2) colloidal dispersion of much smaller (diameter 12 nm), very high surface area ($360 \text{ m}^2 \text{ g}^{-1}$), silica particles.

(iii) BINDZIL[®] AG2000 is a concentrated (40 wt.% SiO_2) dispersion of high surface area ($250 \text{ m}^2 \text{ g}^{-1}$), submicroscopic particles (diameter 11 nm).

(iv) BINDZIL[®] AG1000 is a less concentrated (30 wt.% SiO_2) dispersion of high surface area ($290 \text{ m}^2 \text{ g}^{-1}$), submicroscopic particles (diameter 9 nm).

The parameters including gelling time, gel strength and remaining gel strength were studied. The results showed that gelled electrolyte which are based on a mixture of silica sols and sulfuric acid (so-called, collision gels) had the following beneficial technological properties in VRLA batteries: simplified handling and mixing of the liquid silica sol; no liquid separation from the gelled electrolyte after setting; improved gel strength from a lower silica content; controlled gelling time; increased residual gel strength; high silica concentration in gelling additive; reduced levels of impurities detrimental to the life of a VRLA cell and lower cost.

In 2003, Martha et al. [43] reported the performance characteristics of gelled electrolyte VRLA batteries built in-house. The gelled electrolyte VRLA batteries were constructed by mixing 4.5 M aqueous H_2SO_4 and M-5 CAB-O-SIL[®] fumed silica to form thixotropic gel, which was filled into all the six cell containers up to the upper level of the plates. The performance of gelled electrolyte VRLA battery built in-house was compared with the AGM VRLA and flooded-lead-acid battery counterparts. It was found that the performance of gelled electrolyte VRLA batteries

was similar to both AGM VRLA and flooded-lead-acid batteries at temperature above 0°C. The performance of gelled electrolyte VRLA batteries, however, is better than both AGM VRLA and flooded-lead-acid batteries at temperature between 0°C and -40°C.

In 2005, Park et al. [7] investigated the rheological behavior of silica gel in H₂SO₄ by a small amplitude dynamic oscillation measurement method. In this method, the storage modulus was monitored with time. The gel strength and the gelation rate were measured from the time evolution of storage modulus during the gelation. The gelled electrolyte was prepared from 2-15 wt.% of fumed silica, 15 or 38 wt.% of H₂SO₄ and polyacrylamide (MW = 6 × 10⁶). The use of this gelled electrolyte can suppress the formation of micro-crack during battery operation. In addition, the gel strength and gelation rate were changed by changing the silica content, sulfuric acid concentration, gelation temperature and the amount of added polyacrylamide. The gel strength can be increased of 40% by decreasing the gelation temperature from 25 to 20°C and by adding 0.02 wt.% of polyacrylamide.

In 2006, Zhijiang [10] developed a polyindole-based aqueous polymer rechargeable battery which has a high electromotive force together with a high cycle property and fast charging and discharging. The batteries consisted of poly(5-nitroindole) as the anode active material and PANI as the cathode active material. H₂SO₄ (40%) was used as the electrolytic solution. It was reported that the conducting polymeric polyindoles and PANI could be used to obtain a plastic battery with about 1.3V electromotive force. The battery had excellent fast charge and discharge properties, probably due to movement of the proton, which is small. Moreover, the battery could achieve a 65 mA/g at charge and discharge current densities of 10³ A/m², which is about 77% of its theoretical capacity. The life cycle of the battery seems to be excellent although the experimental studies are still ongoing.

In 2006, Martha et al. [24] developed a new lead-acid battery with high specific-energy by improving the lightweight grids. The grids have been prepared from acrylonitrile butadiene styrene (ABS) copolymer followed by a coating of lead. Subsequently, the grids were electrochemically coated with a conductive and corrosion-resistant layer of PANI. They found that the lead-acid batteries with

specific energy value close to 50 Wh/kg were required in order to use a novel route to electrodeposit corrosion-resistant PANI layers onto the lead-coated lightweight grids.

In 2006, Guo and co-workers [6] studied the performance of self-discharged gel VRLA battery. In this work, the VRLA battery consisted of eight positive and nine negative plates and had 10 Ah capacity (2h rate). Analytical reagents and redistilled water were used. The H_2SO_4 solution (1.30 g/cm^3) and 5% fumed silica were mixed to prepare the gelled electrolyte. The gel VRLA batteries were shelved for nearly 3 years. In the shelved gel VRLA batteries, they found that there was not only stratification of the electrolyte, but also no sulfation on the positive plate. The positive grid also had a good corrosion layer structure meaning that the active mass structure of the positive plate and its polarization resistance were not substantially affected during the long shelving. On the negative plate, the potential of hydrogen evolution of the gel VRLA batteries was slightly more negative than that of AGM VRLA batteries. Its self-discharge rate was also slower.

In 2007, Tang et al. [44] prepared and investigated a polysiloxane-based gelled electrolyte (PBGE) as a new gelling agent for VRLA batteries. In addition, the initial cyclic properties of the absorptive glass mat (AGM)-PBGE and AGM-colloid silica gelled electrolyte (CSGE) hybrid batteries were investigated. They found that the comparison of AGM-PBGE batteries and AGM-CSGE, AGM-PBGE batteries display: (i) superior initial electrochemical performance, especially at higher discharge rate; (ii) improved low- and high-temperature properties; and (iii) better recharge and discharge performance under overcharging conditions. On the other hand, the AGM-CSGE batteries gave a poorer cycle performance at 10-h rate under the condition 100% of deep of discharge. In the same year, they compared the AGM-PBGE batteries with PVC-fumed silica gelled electrolyte (PVC-FSGE) tubular batteries [45]. The comparison showed that AGM-PBGE ones not only presented superior initial performance such as a high discharge rate, high-low temperature properties and oxygen-recombination rate, but also had a shorter manufacturing time and lower cost.

In 2008, Chen et al. [17] studied the effects of preparation conditions and particle size distribution on fumed silica gel VRLA battery performance. The fumed

silicas employed in this work were Aerosil 200, Aerosil 150 (produced by Degussa Co., Germany denoted as A200 and A150) and HL200 (produced by GBS Co., China). Mechanical dispersion of fumed silica nanoparticles was investigated as an important factor in the preparation of high performance gelled electrolytes. They found that optimal mechanical agitation time was the key factor in the preparation of gelled electrolytes with a high lead electrode redox peak current (capacity) and low internal resistance. Deviations of ± 10 min from the optimal agitation time caused a 40-70% decrease in lead electrode capacity. Using different producers, optimal agitation times varied because of different particle size distributions. Fumed silica with a diameter of 10 nm tended to aggregate easily; aggregation of 20 nm diameter silica was more difficult.

CHAPTER III

EXPERIMENTAL

3.1 Gelled electrolyte preparations

This chapter has given the information of instruments and equipments, apparatus, chemical and methodology used in this work.

3.1.1 Instrument

The instrument for gelled electrolyte preparations is rotating rod machine with speed between 500-3,000 rpm (supplied by Metrohm) as shown in Fig. 3.1.



Figure 3.1 The setting of instruments for the gelled electrolyte preparation.

3.1.2 Chemicals

The chemicals for gelled electrolyte preparations are listed in Table 3.1.

Table 3.1 List of chemicals for gelled electrolyte preparations

| Chemicals | Suppliers |
|--|---------------------|
| Fumed silica (Aerosil 200) | Degussa |
| Sulfuric acid 95-97% | Merck |
| Orthophosphoric acid, H ₃ PO ₄ | Carlo Erba Reagents |
| Sodium sulfate, Na ₂ SO ₄ | Univar |
| Polyaniline (emeraldine salt), average M _w > 15,000, particle size 3-100µm, 2-4 S cm ⁻¹ | Aldrich |
| Polypyrrole (dope) composite with carbon black, loading 20 wt.% carbon black, 30 S cm ⁻¹ | Aldrich |
| Poly (1,4-phenylene sulfide), average M _n ~10,000, 1 S cm ⁻¹ | Aldrich |
| Conductivity standard solution (100,000 µS cm ⁻¹) | Metter Toledo |

3.1.3 Methodology

The gelled electrolyte was prepared by mixing 1-15 %(w/v) of fumed silica with 15, 20, 25, 30, 35, 40, 45, 50, 55, 60, 65, 70 and 75 %(w/v) of H₂SO₄, de-ionized water and additives, respectively. There are two groups of additive. First group was 1.0, 1.5, 2.0, 2.5, 3.0, 3.5 and 4.0 g L⁻¹ of Na₂SO₄ and/or 1.0, 1.2, 1.4, 1.6, 1.8, 2.0, 2.2, 2.4, 2.6, 2.8 and 3.0 % of H₃PO₄. Second group was 0.01, 0.02, 0.03, 0.04, 0.05, 0.06, 0.07, 0.08, 0.09 and 0.10 %(w/v) of conducting polymer including PANI, PPy and PPS. The suspension was stirred at room temperature (25±1°C) by rotating rod machine with speed of 3,000 rpm for 10 min. Finally, a slurry of gelled electrolyte was generated as shown in Fig. 3.2 (a), (b), (c) and (d).

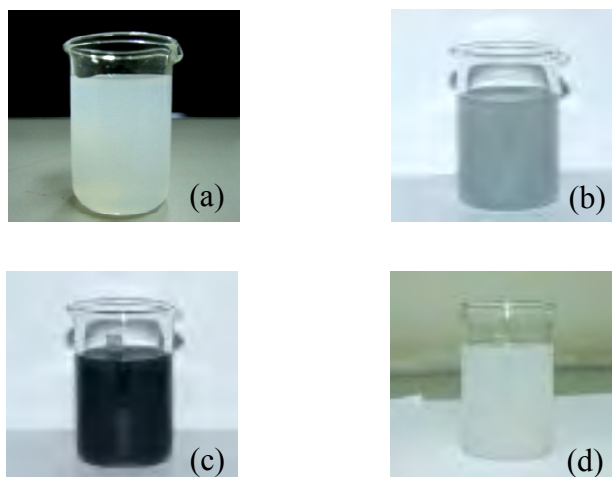


Figure 3.2 The gelled electrolyte consisting of fumed silica, H_2SO_4 and (a) without adding additives, (b) adding PANI, (c) adding PPy and (d) adding PPS.

3.2 Electrical conductivity test

3.2.1 Instruments

The instrument for electrical conductivity test is S70-K SevenMulti conductivity meter with inlab 730 conductivity probe 1-1000 mS cm^{-1} (supplied by Mettler Toledo) as shown in Fig. 3.3.



Figure 3.3 The conductivity meter and conductivity probe for electrical conductivity test.

3.2.2 Gelled electrolytes for conductivity test

The gelled electrolytes for conductivity test were prepared as same as the previous mentions (in section 3.1.3). These gelled electrolytes were classified into two types. First type was without adding additives as shown in Table 3.2 and second types was adding additives as shown in Table 3.3. In the second type, the best gelled electrolytes obtaining the highest conductivity were selected and classified into three types; (i) 2 %(w/v) of fumed silica and 35 %(w/v) of H₂SO₄ were fixed, (ii) 2 %(w/v) of fumed silica, 35 %(w/v) of H₂SO₄ and 3.5 g L⁻¹ of Na₂SO₄ were fixed and (iii) 2 %(w/v) of fumed silica, 35 %(w/v) of H₂SO₄, 2.5 g L⁻¹ of Na₂SO₄ and 1.2 % of H₃PO₄ were fixed.

Table 3.2 List of gelled electrolytes without adding additives for electrical conductivity test

| Fumed silica %(w/v) | H ₂ SO ₄ %(w/v) |
|---------------------|--|
| 1 | 15, 20, 25, 30, 35, 40, 45, 50, 55, 60, 65, 70, 75 |
| 2 | 15, 20, 25, 30, 35, 40, 45, 50, 55, 60, 65, 70, 75 |
| 3 | 15, 20, 25, 30, 35, 40, 45, 50, 55, 60, 65, 70, 75 |
| 4 | 15, 20, 25, 30, 35, 40, 45, 50, 55, 60, 65, 70 |
| 5 | 15, 20, 25, 30, 35, 40, 45, 50, 55 |
| 6 | 15, 20, 25, 30, 35, 40, 45 |
| 7 | 15, 20, 25, 30, 35, 40 |
| 8 | 15, 20, 25 |
| 9 | 15 |

Table 3.3 List of gelled electrolytes with adding additives for electrical conductivity test

| Gelled electrolytes | Additives |
|---|---|
| 2 %(w/v) of fumed silica and 35 %(w/v) of H ₂ SO ₄ | 1.0, 1.2, 1.4, 1.6, 1.8, 2.0, 2.2, 2.4, 2.6, 2.8, 3.0 of H ₃ PO ₄ |
| | 1.0, 1.5, 2.0, 2.5, 3.0, 3.5, 4.0 g L ⁻¹ of Na ₂ SO ₄ |
| | 2.0, 2.5, 3.0, 3.5 g L ⁻¹ of Na ₂ SO ₄ and 1.0, 1.2, 1.4, 1.6, 1.8, 2.0, 2.2, 2.4, 2.6, 2.8, 3.0 of H ₃ PO ₄ |
| | 0.01, 0.02, 0.03, 0.04, 0.05, 0.06, 0.07, 0.08, 0.09, 0.10 of PANI |
| | 0.01, 0.02, 0.03, 0.04, 0.05, 0.06, 0.07, 0.08, 0.09, 0.10 of PPy |
| 2 %(w/v) of fumed silica 35 %(w/v) of H ₂ SO ₄ and 3.5 g L ⁻¹ of Na ₂ SO ₄ | 0.01, 0.02, 0.03, 0.04, 0.05, 0.06, 0.07, 0.08, 0.09, 0.10 of PANI |
| | 0.01, 0.02, 0.03, 0.04, 0.05, 0.06, 0.07, 0.08, 0.09, 0.10 of PPy |
| | 0.01, 0.02, 0.03, 0.04, 0.05, 0.06, 0.07, 0.08, 0.09, 0.10 of PPS |
| 2 %(w/v) of fumed silica 35 %(w/v) of H ₂ SO ₄ 2.5 g L ⁻¹ of Na ₂ SO ₄ and 1.2 % of H ₃ PO ₄ | 0.01, 0.02, 0.03, 0.04, 0.05, 0.06, 0.07, 0.08, 0.09, 0.10 of PANI |
| | 0.01, 0.02, 0.03, 0.04, 0.05, 0.06, 0.07, 0.08, 0.09, 0.10 of PPy |
| | 0.01, 0.02, 0.03, 0.04, 0.05, 0.06, 0.07, 0.08, 0.09, 0.10 of PPS |

3.2.3 Methodology

To obtain the high performance of the batteries and investigate the effect of additives on the performance of battery, the study of conductivity of gelled electrolyte is necessary. The conductivity of gelled electrolyte was measured at $25\pm 1^\circ\text{C}$ by immersing the conductivity probe into the gelled electrolyte and press read after the gelled electrolyte covered the conductivity sensor. The conductivity sensor was calibrated with a conductivity standard solution ($100,000\ \mu\text{S cm}^{-1}$).

3.3 Gelling time test

3.3.1 Gelled electrolytes for gelling time test

The twelve of gelled electrolytes providing the highest conductivity were selected in order to study the effect of additives on the gelling time. The gelled electrolytes were filled into VRLA battery (12V) as seen in Fig.3.4. The twelve of gelled electrolytes (B1-B12) were classified into four types; (i) without adding conducting polymer, (ii) adding only conducting polymer, (iii) adding Na_2SO_4 and conducting polymer and (iv) adding Na_2SO_4 , H_3PO_4 and conducting polymer as shown in Table 3.4.



Figure 3.4 The VRLA battery (12V).

Table 3.4 List of gelled electrolytes for gelling time test

| Name of battery | Gelled electrolytes | Components |
|------------------------|--|--|
| B1 | Without adding conducting polymer | 2 %(w/v) of fumed silica and 35 %(w/v) of H ₂ SO ₄ |
| B2 | | 2 %(w/v) of fumed silica, 35 %(w/v) of H ₂ SO ₄ and 3.5 g L ⁻¹ of Na ₂ SO ₄ |
| B3 | | 2 %(w/v) of fumed silica, 35 %(w/v) of H ₂ SO ₄ , 2.5 g L ⁻¹ of Na ₂ SO ₄ and 1.2 % of H ₃ PO ₄ |
| B4 | Adding only conducting polymer | 2 %(w/v) of fumed silica, 35 %(w/v) of H ₂ SO ₄ and 0.02 % (w/v) of PANI |
| B5 | | 2 %(w/v) of fumed silica, 35 %(w/v) of H ₂ SO ₄ and 0.01 % (w/v) of PPy |
| B6 | | 2%(w/v) of fumed silica, 35 %(w/v) of H ₂ SO ₄ , and 0.05 % (w/v) of PPS |
| B7 | Adding Na ₂ SO ₄ and conducting polymer | 2 %(w/v) of fumed silica, 35 %(w/v) of H ₂ SO ₄ , 3.5 g L ⁻¹ of Na ₂ SO ₄ and 0.07 % (w/v) of PANI |
| B8 | | 2 %(w/v) of fumed silica, 35 %(w/v) of H ₂ SO ₄ , 3.5 g L ⁻¹ of Na ₂ SO ₄ and 0.08 % (w/v) of PPy |
| B9 | | 2%(w/v) of fumed silica, 35 %(w/v) of H ₂ SO ₄ , 3.5 g L ⁻¹ of Na ₂ SO ₄ and 0.05 % (w/v) of PPS |
| B10 | Adding Na ₂ SO ₄ , H ₃ PO ₄ and conducting polymer | 2 %(w/v) of fumed silica, 35 %(w/v) of H ₂ SO ₄ , 2.5 g L ⁻¹ of Na ₂ SO ₄ , 1.2 % of H ₃ PO ₄ and 0.02 %(w/v) of PANI |
| B11 | | 2 %(w/v) of fumed silica, 35 %(w/v) of H ₂ SO ₄ , 2.5 g L ⁻¹ of Na ₂ SO ₄ , 1.2 % of H ₃ PO ₄ and 0.08 %(w/v) of PPy |
| B12 | | 2 %(w/v) of fumed silica, 35 %(w/v) of H ₂ SO ₄ , 2.5 g L ⁻¹ of Na ₂ SO ₄ , 1.2 % of H ₃ PO ₄ and 0.07 %(w/v) of PPS |

3.3.2 Methodology

The different gelled electrolytes providing the highest conductivity were filled into VRLA batteries (12V) using a pasture pipette in order to investigate the gelling time at room temperature ($25\pm 1^\circ\text{C}$). Moreover, the effect of additives on the gelling time was also observed. After finishing the filling of gelled electrolyte the time was recorded. Then, the gelled electrolyte generated all over the battery, the recorded time is stopped.

3.4 Performance of battery test

3.4.1 Instruments

The instruments for performance of battery test are listed in Table 3.5.

Table 3.5 List of instruments for performance of battery test

| Instruments | Details |
|---------------------|-------------------------|
| Digital Multi Meter | Sunwa version CD770 |
| Clamp Meter | Ininipa version ET-3374 |
| Halogen lamp 35 W | Silvernia |
| Battery charger | Tiger star |
| Stop watch | Timer-5 |

3.4.2 Gelled electrolytes for performance of battery test

The twelve of gelled electrolytes providing the highest conductivity were selected and filled into VRLA batteries (12V) in order to study the performance of battery. The charge and discharge characteristic and discharge capacity of VRLA batteries were investigated. The twelve of gelled electrolytes (B1-B12) were classified into four types; (i) without adding conducting polymer, (ii) adding only conducting polymer, (iii) adding Na_2SO_4 and conducting polymer and (iv) adding Na_2SO_4 , H_3PO_4 and conducting polymer as shown in Table 3.6.

Table 3.6 List of VRLA batteries with different gelled electrolytes for performance of battery test

| Name of battery | Gelled electrolytes | Components |
|------------------------|--|--|
| B1 | Without adding conducting polymer | 2 %(w/v) of fumed silica and 35 %(w/v) of H ₂ SO ₄ |
| B2 | | 2 %(w/v) of fumed silica, 35 %(w/v) of H ₂ SO ₄ and 3.5 g L ⁻¹ of Na ₂ SO ₄ |
| B3 | | 2 %(w/v) of fumed silica, 35 %(w/v) of H ₂ SO ₄ , 2.5 g L ⁻¹ of Na ₂ SO ₄ and 1.2 % of H ₃ PO ₄ |
| B4 | Adding only conducting polymer | 2 %(w/v) of fumed silica, 35 %(w/v) of H ₂ SO ₄ and 0.02 % (w/v) of PANI |
| B5 | | 2 %(w/v) of fumed silica, 35 %(w/v) of H ₂ SO ₄ and 0.01 % (w/v) of PPy |
| B6 | | 2%(w/v) of fumed silica, 35 %(w/v) of H ₂ SO ₄ , and 0.05 % (w/v) of PPS |
| B7 | Adding Na ₂ SO ₄ and conducting polymer | 2 %(w/v) of fumed silica, 35 %(w/v) of H ₂ SO ₄ , 3.5 g L ⁻¹ of Na ₂ SO ₄ and 0.07 % (w/v) of PANI |
| B8 | | 2 %(w/v) of fumed silica, 35 %(w/v) of H ₂ SO ₄ , 3.5 g L ⁻¹ of Na ₂ SO ₄ and 0.08 % (w/v) of PPy |
| B9 | | 2%(w/v) of fumed silica, 35 %(w/v) of H ₂ SO ₄ , 3.5 g L ⁻¹ of Na ₂ SO ₄ and 0.05 % (w/v) of PPS |
| B10 | Adding Na ₂ SO ₄ , H ₃ PO ₄ and conducting polymer | 2 %(w/v) of fumed silica, 35 %(w/v) of H ₂ SO ₄ , 2.5 g L ⁻¹ of Na ₂ SO ₄ , 1.2 % of H ₃ PO ₄ and 0.02 %(w/v) of PANI |
| B11 | | 2 %(w/v) of fumed silica, 35 %(w/v) of H ₂ SO ₄ , 2.5 g L ⁻¹ of Na ₂ SO ₄ , 1.2 % of H ₃ PO ₄ and 0.08 %(w/v) of PPy |
| B12 | | 2 %(w/v) of fumed silica, 35 %(w/v) of H ₂ SO ₄ , 2.5 g L ⁻¹ of Na ₂ SO ₄ , 1.2 % of H ₃ PO ₄ and 0.07 %(w/v) of PPS |

3.4.3 Methodology

The different gelled electrolytes providing the highest conductivity were filled into VRLA batteries (12V) using a vacuum system in order to investigate the performance of cycling of batteries. Charge and discharge capacities were tested for 1-hour rate at room temperature ($25\pm 1^\circ\text{C}$). The experimental set up for charge and discharge were shown in Fig. 3.5 (a) and (b), respectively. The voltage and current were measured, throughout the experimental. For charge tests, the voltage and current were measured at every 30 min and cutoff point was 0.03 A. On the other hand, discharge tests, the voltage and current were measured at every 5 min and discharge cutoff point was 9.0 V. The performance of VRLA batteries was tested for 20 cycling.

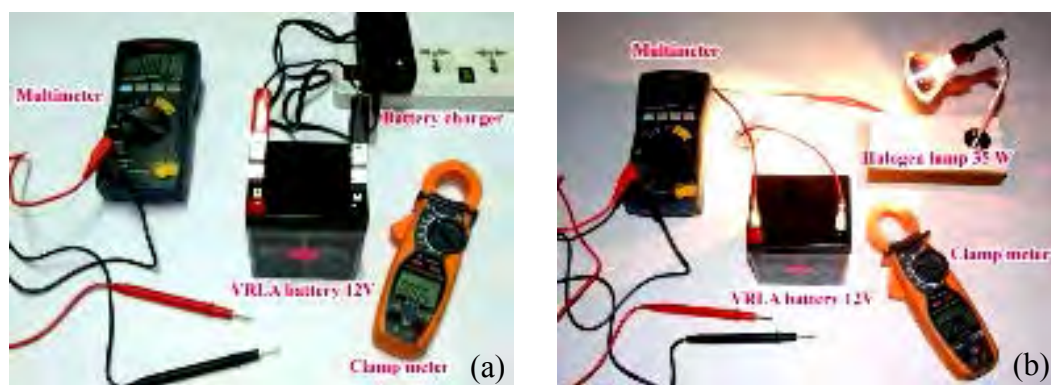


Figure 3.5 The setting of experimental for (a) battery charging and (b) battery discharging.

3.5 Electrochemical test

3.5.1 Instruments

The instruments for electrochemical test are listed in Table 3.7.

Table 3.7 List of instruments for electrochemical test

| Instruments | Details |
|---------------------------------|--|
| Potentiostat (PGSTAT30) | Auto lab |
| Planar Pb electrode (home made) | Use for WE and CE electrode with area of 0.5 x 1.0 cm ² |
| Ag/AgCl electrode (Metrohm) | Use for RE electrode |

3.5.2 Gelled electrolytes and acid solution for electrochemical test

In order to check the characteristic reaction and oxygen recombination reaction of gelled electrolyte, the electrochemical test was investigated. The gelled electrolytes providing the high discharge capacities of VRLA batteries were selected and compared with acid solution as shown in Table 3.8.

Table 3.8 List of different gelled electrolytes and acid solution for electrochemical test

| Electrolytes | Details |
|--|--|
| Acid solution | 35 %(w/v) of H ₂ SO ₄ |
| Adding only Na ₂ SO ₄ | 2 %(w/v) of fumed silica, 35 %(w/v) of H ₂ SO ₄ and 3.5 g L ⁻¹ of Na ₂ SO ₄ |
| Adding only conducting polymer | 2 %(w/v) of fumed silica, 35 %(w/v) of H ₂ SO ₄ and 0.02 % (w/v) of PANI 2 %(w/v) of fumed silica, 35 %(w/v) of H ₂ SO ₄ and 0.01 % (w/v) of PPy 2%(w/v) of fumed silica, 35 %(w/v) of H ₂ SO ₄ and 0.05 % (w/v) of PPS |
| Adding only Na ₂ SO ₄ and conducting polymer | 2 %(w/v) of fumed silica, 35 %(w/v) of H ₂ SO ₄ , 3.5 g L ⁻¹ of Na ₂ SO ₄ and 0.07 % (w/v) of PANI 2 %(w/v) of fumed silica, 35 %(w/v) of H ₂ SO ₄ , 3.5 g L ⁻¹ of Na ₂ SO ₄ and 0.08 % (w/v) of PPy 2%(w/v) of fumed silica, 35 %(w/v) of H ₂ SO ₄ , 3.5 g L ⁻¹ of Na ₂ SO ₄ and 0.05 % (w/v) of PPS |

3.4.3 Methodology

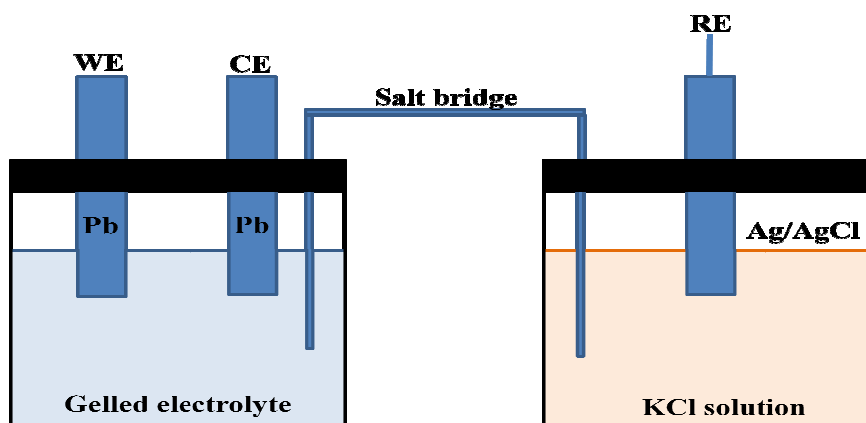


Figure 3.6 The electrochemical cell for electrochemical technique.

The characteristic reaction and oxygen recombination reaction of gelled electrolyte were tested by using the three electrode system of cyclic voltammetry (CV). The experimental set up is demonstrated in Fig. 3.6. The experiments were carried out using gelled electrolyte and H_2SO_4 solution by Potentiostat/Galvanostat method with a scan rate of 20 mV s^{-1} at $25 \pm 1^\circ\text{C}$.

CHAPTER IV

RESULTS AND DISCUSSION

4.1 Characterization of gelled electrolytes

A gelled electrolyte suspension is monitored by visualization before filling into the batteries. Table 4.1 shows the characteristics of gelled electrolytes with different concentrations of fumed silica and H₂SO₄ after stirring at room temperature (25±1°C). The results show that 1-3 %(w/v) of fumed silica and 15-75 %(w/v) of H₂SO₄ provide a characteristic suspension. The first characteristic of a gel were observed at 4 %(w/v) of fumed silica and 75 %(w/v) of H₂SO₄. Characteristic suspensions were also observed at the following concentrations: 5 %(w/v) of fumed silica and 15-55 %(w/v) of H₂SO₄, 6 %(w/v) of fumed silica and 15-45 %(w/v) of H₂SO₄, 7 %(w/v) of fumed silica and 15-40 %(w/v) of H₂SO₄, 8 %(w/v) of fumed silica and 15-25 %(w/v) of H₂SO₄, 9 %(w/v) of fumed silica and 15 %(w/v) of H₂SO₄. Concentrations of fumed silica more than or equal 10 %(w/v) provide a gel. This implies that increasing the fumed silica concentration and the H₂SO₄ concentration lead to gels. The electrical conductivity was measured in order to optimize the suspension characteristic.

Table 4.1 The characteristics of gelled electrolytes with different fumed silica and H₂SO₄ concentration after stirring at room temperature (25±1°C)

| | Concentration of H ₂ SO ₄ (%w/v) | | | | | | | | | | | | | | |
|--------------------------------------|--|----|----|----|----|----|----|----|----|----|----|----|----|---|--|
| | 15 | 20 | 25 | 30 | 35 | 40 | 45 | 50 | 55 | 60 | 65 | 70 | 75 | | |
| Concentration of fumed silica (%w/v) | | | | | | | | | | | | | | | |
| 1 | S | S | S | S | S | S | S | S | S | S | S | S | S | S | |
| 2 | S | S | S | S | S | S | S | S | S | S | S | S | S | S | |
| 3 | S | S | S | S | S | S | S | S | S | S | S | S | S | S | |
| 4 | S | S | S | S | S | S | S | S | S | S | S | S | S | G | |
| 5 | S | S | S | S | S | S | S | S | S | G | G | G | G | G | |
| 6 | S | S | S | S | S | S | S | G | G | G | G | G | G | G | |
| 7 | S | S | S | S | S | S | G | G | G | G | G | G | G | G | |
| 8 | S | S | S | G | G | G | G | G | G | G | G | G | G | G | |
| 9 | S | G | G | G | G | G | G | G | G | G | G | G | G | G | |
| 10 | G | G | G | G | G | G | G | G | G | G | G | G | G | G | |
| 11 | G | G | G | G | G | G | G | G | G | G | G | G | G | G | |
| 12 | G | G | G | G | G | G | G | G | G | G | G | G | G | G | |
| 13 | G | G | G | G | G | G | G | G | G | G | G | G | G | G | |
| 14 | G | G | G | G | G | G | G | G | G | G | G | G | G | G | |
| 15 | G | G | G | G | G | G | G | G | G | G | G | G | G | G | |

Where; S is the suspension characteristic and G is the gel characteristic.

4.2 Optimization of gelled electrolytes by measuring conductivity

The various gelled electrolytes were optimized by measuring the conductivity at 25°C as shown in Tables 4.2-4.10. In Table 4.2, the gelled electrolyte containing 1 %(w/v) of fumed silica and 35 %(w/v) of H₂SO₄ shows the highest conductivity of 815 mS/cm with a standard deviation of 2 mS/cm. In Table 4.3, the gelled electrolyte containing 2 %(w/v) of fumed silica and 35 %(w/v) of H₂SO₄ shows the highest conductivity of 838 mS/cm with standard deviation of 2 mS/cm. In Table 4.4, the gelled electrolyte containing 3 %(w/v) of fumed silica and 35 %(w/v) of H₂SO₄ shows the highest conductivity of 819 mS/cm with standard deviation of 3 mS/cm. In Table 4.5, the gelled electrolyte containing 4 %(w/v) of fumed silica and 35 %(w/v) of H₂SO₄ shows the highest conductivity of 807 mS/cm with standard deviation of 2 mS/cm. In Table 4.6, the gelled electrolyte containing 5 %(w/v) of fumed silica and 30 %(w/v) of H₂SO₄ shows the highest conductivity of 794 mS/cm with standard deviation of 2 mS/cm. In Table 4.7, the gelled electrolyte containing 6 %(w/v) of fumed silica and 30 %(w/v) of H₂SO₄ shows the highest conductivity of 802 mS/cm with standard deviation of 4 mS/cm. In Table 4.8, the gelled electrolyte containing 7 %(w/v) of fumed silica and 40 %(w/v) of H₂SO₄ shows the highest conductivity of 802 mS/cm with standard deviation of 4 mS/cm. In Table 4.9, the gelled electrolyte containing 8 %(w/v) of fumed silica and 25 %(w/v) of H₂SO₄ shows the highest conductivity of 757 mS/cm with standard deviation of 3 mS/cm. In Table 4.10, the gelled electrolyte containing 9 %(w/v) of fumed silica and 15 %(w/v) of H₂SO₄ shows the highest conductivity of 627 mS/cm with standard deviation of 1 mS/cm. The highest conductivities are shown and compared in Table 4.11. The results show that the maximum conductivity is obtained from 2 %(w/v) of fumed silica and 35 %(w/v) of H₂SO₄. For the sample with at 35 %(w/v) of H₂SO₄, the conductivities decrease if more than or equal 3 %(w/v) of fumed silica is added.

Table 4.2 The conductivities of gelled electrolytes containing 1 %(w/v) of fumed silica and various concentration of H₂SO₄

| Fumed silica (%w/v) | H ₂ SO ₄ (%w/v) | σ_1 mS/cm | σ_2 mS/cm | σ_3 mS/cm | σ_{avg} mS/cm | SD mS/cm | $\sigma_{avg} \pm SD$ mS/cm |
|---------------------|---------------------------------------|------------------|------------------|------------------|----------------------|----------|-----------------------------|
| 1 | 15 | 664 | 659 | 662 | 662 | 3 | 662 ± 3 |
| 1 | 20 | 725 | 719 | 726 | 723 | 4 | 723 ± 4 |
| 1 | 25 | 793 | 791 | 790 | 791 | 2 | 791 ± 2 |
| 1 | 30 | 815 | 813 | 814 | 814 | 1 | 814 ± 1 |
| 1 | 35 | 817 | 815 | 814 | 815 | 2 | 815 ± 2 |
| 1 | 40 | 737 | 734 | 733 | 735 | 2 | 735 ± 2 |
| 1 | 45 | 799 | 796 | 794 | 796 | 3 | 796 ± 3 |
| 1 | 50 | 765 | 761 | 760 | 762 | 3 | 762 ± 3 |
| 1 | 55 | 709 | 706 | 705 | 707 | 2 | 707 ± 2 |
| 1 | 60 | 717 | 716 | 713 | 715 | 2 | 715 ± 2 |
| 1 | 65 | 600 | 596 | 597 | 598 | 2 | 598 ± 2 |
| 1 | 70 | 561 | 557 | 556 | 558 | 3 | 558 ± 3 |
| 1 | 75 | 543 | 538 | 536 | 539 | 4 | 539 ± 4 |

Table 4.3 The conductivities of gelled electrolytes containing 2 %(w/v) of fumed silica and various concentration of H₂SO₄

| Fumed silica (%w/v) | H ₂ SO ₄ (%w/v) | σ_1 mS/cm | σ_2 mS/cm | σ_3 mS/cm | σ_{avg} mS/cm | SD mS/cm | $\sigma_{avg} \pm SD$ mS/cm |
|---------------------|---------------------------------------|------------------|------------------|------------------|----------------------|----------|-----------------------------|
| 2 | 15 | 657 | 654 | 654 | 655 | 2 | 655 ± 2 |
| 2 | 20 | 707 | 706 | 703 | 705 | 2 | 705 ± 2 |
| 2 | 25 | 768 | 763 | 765 | 765 | 3 | 765 ± 3 |
| 2 | 30 | 807 | 805 | 804 | 805 | 2 | 805 ± 2 |
| 2 | 35 | 840 | 836 | 838 | 838 | 2 | 838 ± 2 |
| 2 | 40 | 806 | 805 | 807 | 806 | 1 | 806 ± 1 |
| 2 | 45 | 790 | 787 | 785 | 787 | 3 | 787 ± 3 |
| 2 | 50 | 776 | 773 | 771 | 773 | 3 | 773 ± 3 |
| 2 | 55 | 720 | 717 | 717 | 718 | 2 | 718 ± 2 |
| 2 | 60 | 722 | 719 | 717 | 719 | 3 | 719 ± 3 |
| 2 | 65 | 772 | 771 | 769 | 771 | 2 | 771 ± 2 |
| 2 | 70 | 612 | 608 | 606 | 609 | 3 | 609 ± 3 |
| 2 | 75 | 493 | 489 | 488 | 490 | 3 | 490 ± 3 |

Table 4.4 The conductivities of gelled electrolytes containing 3 %(w/v) of fumed silica and various concentration of H₂SO₄

| Fumed silica (%w/v) | H ₂ SO ₄ (%w/v) | σ_1 mS/cm | σ_2 mS/cm | σ_3 mS/cm | σ_{avg} mS/cm | SD mS/cm | $\sigma_{avg} \pm SD$ mS/cm |
|---------------------|---------------------------------------|------------------|------------------|------------------|----------------------|----------|-----------------------------|
| 3 | 15 | 574 | 570 | 569 | 571 | 3 | 571 ± 3 |
| 3 | 20 | 717 | 714 | 713 | 715 | 2 | 715 ± 2 |
| 3 | 25 | 802 | 799 | 799 | 800 | 2 | 800 ± 2 |
| 3 | 30 | 819 | 817 | 818 | 818 | 1 | 818 ± 1 |
| 3 | 35 | 822 | 819 | 817 | 819 | 3 | 819 ± 3 |
| 3 | 40 | 794 | 793 | 789 | 792 | 3 | 792 ± 3 |
| 3 | 45 | 787 | 784 | 780 | 784 | 4 | 784 ± 4 |
| 3 | 50 | 745 | 741 | 741 | 742 | 2 | 742 ± 2 |
| 3 | 55 | 717 | 714 | 710 | 714 | 4 | 714 ± 4 |
| 3 | 60 | 724 | 723 | 721 | 723 | 2 | 723 ± 2 |
| 3 | 65 | 635 | 630 | 628 | 631 | 4 | 631 ± 4 |
| 3 | 70 | 628 | 625 | 623 | 625 | 3 | 625 ± 3 |
| 3 | 75 | 555 | 548 | 547 | 550 | 4 | 550 ± 4 |

Table 4.5 The conductivities of gelled electrolytes containing 4 %(w/v) of fumed silica and various concentration of H₂SO₄

| Fumed silica (%w/v) | H ₂ SO ₄ (%w/v) | σ_1 mS/cm | σ_2 mS/cm | σ_3 mS/cm | σ_{avg} mS/cm | SD mS/cm | $\sigma_{avg} \pm SD$ mS/cm |
|---------------------|---------------------------------------|------------------|------------------|------------------|----------------------|----------|-----------------------------|
| 4 | 15 | 675 | 674 | 674 | 674 | 1 | 674 ± 1 |
| 4 | 20 | 727 | 726 | 727 | 727 | 1 | 727 ± 1 |
| 4 | 25 | 781 | 782 | 780 | 781 | 1 | 781 ± 1 |
| 4 | 30 | 788 | 784 | 782 | 785 | 3 | 785 ± 3 |
| 4 | 35 | 808 | 805 | 808 | 807 | 2 | 807 ± 2 |
| 4 | 40 | 785 | 789 | 787 | 787 | 2 | 787 ± 2 |
| 4 | 45 | 773 | 773 | 768 | 771 | 3 | 771 ± 3 |
| 4 | 50 | 762 | 760 | 756 | 759 | 3 | 759 ± 3 |
| 4 | 55 | 691 | 689 | 685 | 688 | 3 | 688 ± 3 |
| 4 | 60 | 718 | 715 | 712 | 715 | 3 | 715 ± 3 |
| 4 | 65 | 646 | 642 | 637 | 642 | 5 | 642 ± 5 |
| 4 | 70 | 603 | 598 | 596 | 599 | 4 | 599 ± 4 |

Table 4.6 The conductivities of gelled electrolytes containing 5 %(w/v) of fumed silica and various concentration of H₂SO₄

| Fumed silica (%w/v) | H₂SO₄ (%w/v) | σ₁ mS/cm | σ₂ mS/cm | σ₃ mS/cm | σ_{avg} mS/cm | SD mS/cm | σ_{avg} ± SD mS/cm |
|----------------------------|---|----------------------------|----------------------------|----------------------------|------------------------------|-----------------|-----------------------------------|
| 5 | 15 | 634 | 631 | 631 | 632 | 2 | 632 ± 2 |
| 5 | 20 | 778 | 778 | 775 | 777 | 2 | 777 ± 2 |
| 5 | 25 | 781 | 778 | 777 | 779 | 2 | 779 ± 2 |
| 5 | 30 | 795 | 792 | 794 | 794 | 2 | 794 ± 2 |
| 5 | 35 | 621 | 619 | 619 | 620 | 1 | 620 ± 1 |
| 5 | 40 | 787 | 783 | 783 | 784 | 2 | 784 ± 2 |
| 5 | 45 | 773 | 771 | 770 | 771 | 2 | 771 ± 2 |
| 5 | 50 | 763 | 762 | 761 | 762 | 1 | 762 ± 1 |
| 5 | 55 | 704 | 701 | 698 | 701 | 3 | 701 ± 3 |

Table 4.7 The conductivities of gelled electrolytes containing 6 %(w/v) of fumed silica and various concentration of H₂SO₄

| Fumed silica (%w/v) | H₂SO₄ (%w/v) | σ₁ mS/cm | σ₂ mS/cm | σ₃ mS/cm | σ_{avg} mS/cm | SD mS/cm | σ_{avg} ± SD mS/cm |
|----------------------------|---|----------------------------|----------------------------|----------------------------|------------------------------|-----------------|-----------------------------------|
| 6 | 15 | 628 | 629 | 629 | 629 | 1 | 629 ± 1 |
| 6 | 20 | 744 | 745 | 744 | 744 | 1 | 744 ± 1 |
| 6 | 25 | 771 | 777 | 773 | 774 | 3 | 774 ± 3 |
| 6 | 30 | 807 | 800 | 799 | 802 | 4 | 802 ± 4 |
| 6 | 35 | 774 | 776 | 774 | 775 | 1 | 775 ± 1 |
| 6 | 40 | 798 | 795 | 793 | 795 | 3 | 795 ± 3 |
| 6 | 45 | 768 | 765 | 764 | 766 | 2 | 766 ± 2 |

Table 4.8 The conductivities of gelled electrolytes containing 7 %(w/v) of fumed silica and various concentration of H₂SO₄

| Fumed silica (%w/v) | H ₂ SO ₄ (%w/v) | σ_1 mS/cm | σ_2 mS/cm | σ_3 mS/cm | σ_{avg} mS/cm | SD mS/cm | $\sigma_{avg} \pm SD$ mS/cm |
|---------------------|---------------------------------------|------------------|------------------|------------------|----------------------|----------|-----------------------------|
| 7 | 15 | 577 | 574 | 575 | 575 | 2 | 575 \pm 2 |
| 7 | 20 | 728 | 726 | 725 | 726 | 2 | 726 \pm 2 |
| 7 | 25 | 770 | 764 | 762 | 765 | 4 | 765 \pm 4 |
| 7 | 30 | 767 | 763 | 761 | 764 | 3 | 764 \pm 3 |
| 7 | 35 | 799 | 793 | 790 | 794 | 5 | 794 \pm 5 |
| 7 | 40 | 802 | 806 | 799 | 802 | 4 | 802 \pm 4 |

Table 4.9 The conductivities of gelled electrolytes containing 8 %(w/v) of fumed silica and various concentration of H₂SO₄

| Fumed silica (%w/v) | H ₂ SO ₄ (%w/v) | σ_1 mS/cm | σ_2 mS/cm | σ_3 mS/cm | σ_{avg} mS/cm | SD mS/cm | $\sigma_{avg} \pm SD$ mS/cm |
|---------------------|---------------------------------------|------------------|------------------|------------------|----------------------|----------|-----------------------------|
| 8 | 15 | 642 | 644 | 637 | 641 | 4 | 641 \pm 4 |
| 8 | 20 | 758 | 756 | 754 | 756 | 2 | 756 \pm 2 |
| 8 | 25 | 760 | 757 | 754 | 757 | 3 | 757 \pm 3 |

Table 4.10 The conductivities of gelled electrolytes containing 9 %(w/v) of fumed silica and 15 %(w/v) of H₂SO₄

| Fumed silica (%w/v) | H ₂ SO ₄ (%w/v) | σ_1 mS/cm | σ_2 mS/cm | σ_3 mS/cm | σ_{avg} mS/cm | SD mS/cm | $\sigma_{avg} \pm SD$ mS/cm |
|---------------------|---------------------------------------|------------------|------------------|------------------|----------------------|----------|-----------------------------|
| 9 | 15 | 628 | 627 | 626 | 627 | 1 | 627 \pm 1 |

Table 4.11 The highest conductivities of various gelled electrolytes

| Fumed silica (%w/v) | H ₂ SO ₄ (%w/v) | σ_1 mS/cm | σ_2 mS/cm | σ_3 mS/cm | σ_{avg} mS/cm | SD mS/cm | $\sigma_{avg} \pm SD$ mS/cm |
|---------------------|---------------------------------------|------------------|------------------|------------------|----------------------|----------|-----------------------------|
| 1 | 35 | 817 | 815 | 814 | 815 | 2 | 815 \pm 2 |
| 2 | 35 | 840 | 836 | 838 | 838 | 2 | 838 \pm 2 |
| 3 | 35 | 822 | 819 | 817 | 819 | 3 | 819 \pm 3 |
| 4 | 35 | 808 | 805 | 808 | 807 | 2 | 807 \pm 2 |
| 5 | 30 | 795 | 792 | 794 | 794 | 2 | 794 \pm 2 |
| 6 | 30 | 807 | 800 | 799 | 802 | 4 | 802 \pm 4 |
| 7 | 40 | 802 | 806 | 799 | 802 | 4 | 802 \pm 4 |
| 8 | 25 | 760 | 757 | 754 | 757 | 3 | 757 \pm 3 |
| 9 | 15 | 628 | 627 | 626 | 627 | 1 | 627 \pm 1 |

In order to investigate the effect of the concentration of fumed silica and H₂SO₄ on the measured conductivity, the concentrations of fumed silica at 1-4 %(w/v) were plotted as shown in Fig. 4.1. The plot shows similar conductivity behavior of the gelled electrolytes with a maximum conductivity at approximately 35 %(w/v) of H₂SO₄, after which the conductivity decreases. Furthermore, these curves are similar to the conductivity curves of the H₂SO₄ solution as seen in Fig. 2.5 [16]. The conductivities decreases when the ionic conductivity is excess, which can make the exchanges of ionic conductivities are difficult. This demonstrates that the H₂SO₄ concentrations affect the electrical conductivity, although fumed silica had little effect on the conductivities.

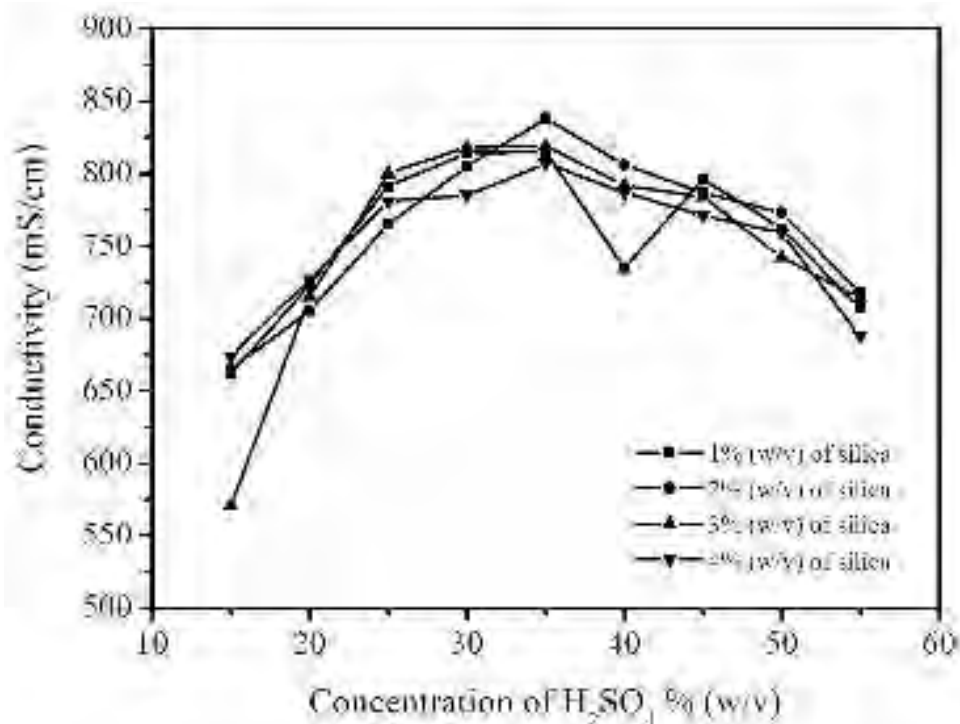


Figure 4.1 The conductivity of gelled electrolytes with various concentrations of fumed silica and H₂SO₄.

The maximum conductivity of the gelled electrolyte containing 2% (w/v) of fumed silica and 35 % (w/v) of H₂SO₄ was used to screen other additives. Fig. 4.2 and 4.3 show the electrical conductivity of the gelled electrolytes when H₃PO₄ and Na₂SO₄ were added. It was found that the addition of H₃PO₄ decreased the conductivity values from a maximum of 841 mS/cm at 1.2 % of H₃PO₄. The reason for this decrease is probably due to the interactions between H₃PO₄ and the silanol group (Si-O-H) on the surface of fumed silica. Hence, the exchanges of the ionic conductivities were difficult. Moreover, the H₃PO₄ is a weak acid providing small dissociation. Therefore, the conductivity of gelled electrolyte does not increase abundantly [17, 19]. On the contrary, the addition of Na₂SO₄ increased the conductivity leading to the highest conductivity of 860 mS/cm at 3.5 g L⁻¹ of Na₂SO₄, likely due to the strong dissociation of Na₂SO₄ [46].

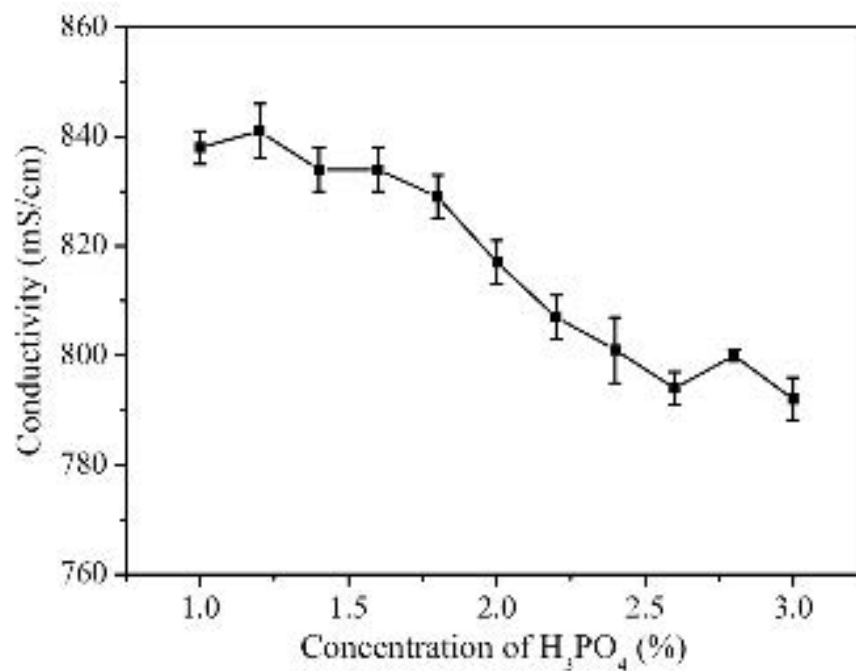


Figure 4.2 The conductivity of gelled electrolytes with various concentrations of H_3PO_4 (2%w/v of fumed silica and 35%w/v of H_2SO_4 were fixed).

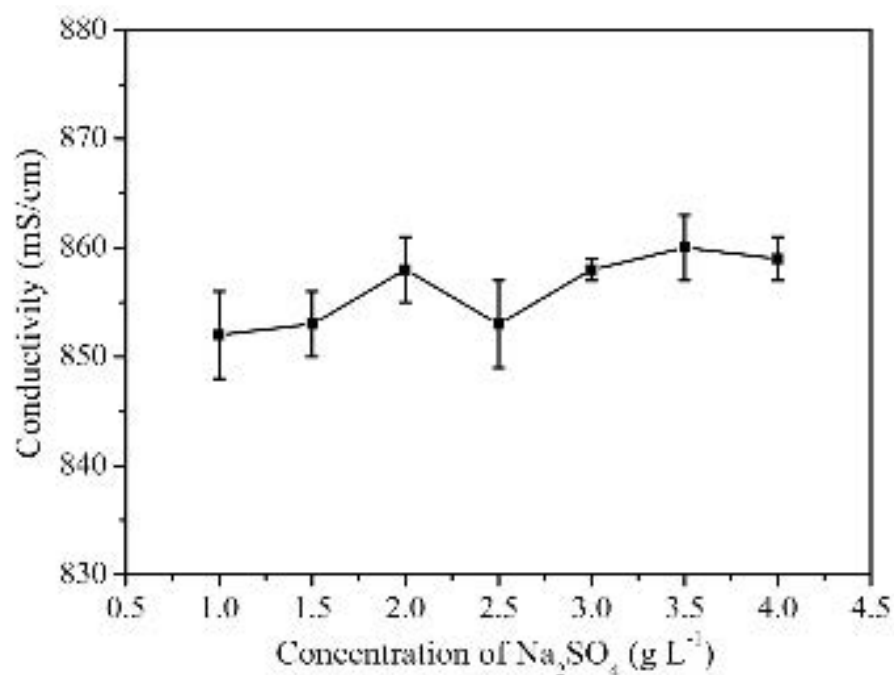


Figure 4.3 The conductivity of gelled electrolytes with various concentrations of Na_2SO_4 (2%w/v of fumed silica and 35%w/v of H_2SO_4 were fixed).

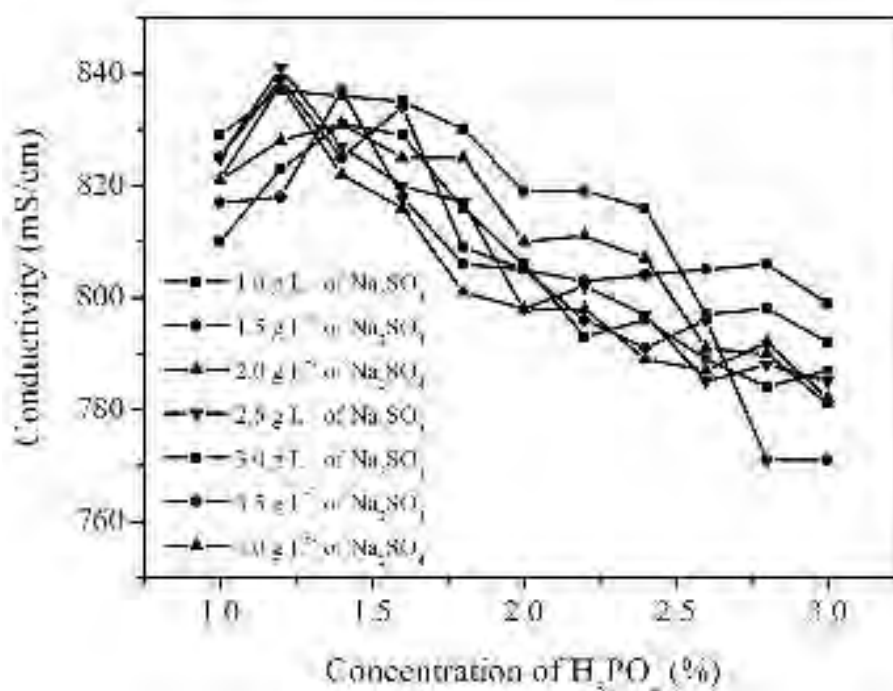


Figure 4.4 The conductivity of gelled electrolytes with various concentrations of H_3PO_4 and Na_2SO_4 (2%w/v of fumed silica and 35%w/v of H_2SO_4 were fixed).

The gelled electrolyte with both H_3PO_4 and Na_2SO_4 shows similar conductivity behavior to the gelled electrolytes containing only H_3PO_4 , as shown in Fig. 4.4. The conductivity decreased at concentrations greater than 1.2-1.4 % of H_3PO_4 and for all concentrations of Na_2SO_4 . This behavior is consistent with the results discussed above (Fig. 4.2). The more significant decreases were observed from the gelled electrolyte containing H_3PO_4 as an additive. The highest conductivity of 840 mS/cm was obtained from the gelled electrolyte containing 1.2 % of H_3PO_4 and 2.5 g L⁻¹ of Na_2SO_4 concentration. Subsequently, the gelled electrolytes with the highest conductivity were chosen for further development by adding conducting polymers (PANI, PPy and PPS). The gelled electrolytes were classified into three types based on additives: type I (without H_3PO_4 or Na_2SO_4), type II (containing only Na_2SO_4), and type III (containing both H_3PO_4 and Na_2SO_4).

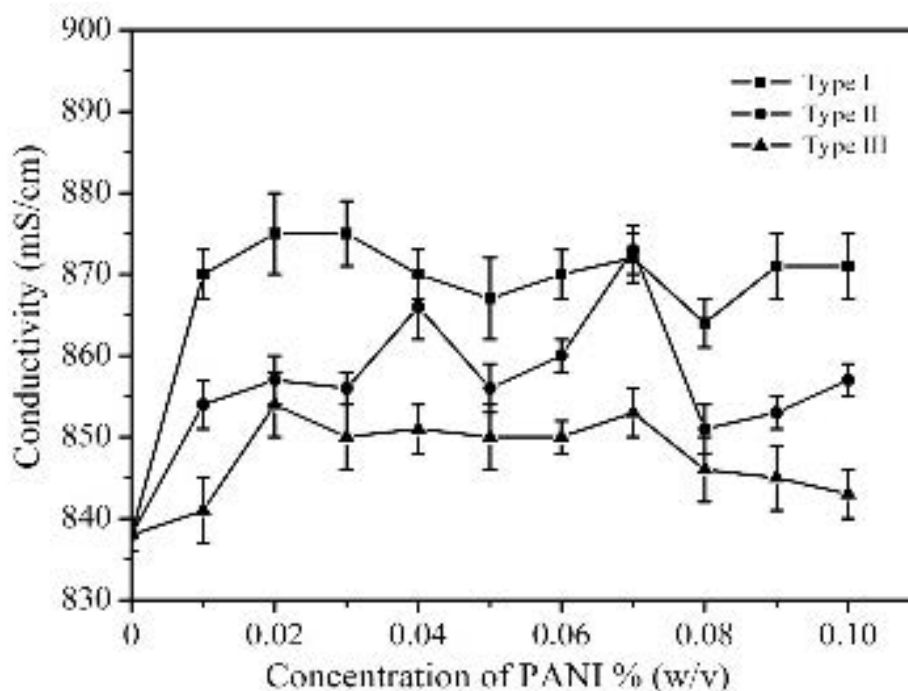


Figure 4.5 The conductivity of gelled electrolytes with various concentrations of PANI (2%w/v of fumed silica and 35%w/v of H₂SO₄ were fixed).

Fig. 4.5 shows the electrical conductivity of gelled electrolytes with various PANI concentrations. It was found that at all concentrations of PANI, the conductivity increased for the three types of gelled electrolytes. As previously discussed, the structural characteristics of the PANI come from the inclusion of conjugated double bonds [9-11, 22], which can lead to a high conductivity of the suspension. The type I/PANI resulted in a higher conductivity than the type II/PANI and type III/PANI. The highest conductivity of type I/PANI (875 mS/cm) and type II/PANI (873 mS/cm) show similar results and are higher than type III/PANI (854 mS/cm). The conductivity of type III/PANI is lower than the others, likely due to the addition of H₃PO₄. The highest conductivities of type I/PANI, type II/PANI and type III/PANI were observed with 0.02 %(w/v), 0.07 %(w/v) and 0.02 %(w/v) of PANI concentration, respectively.

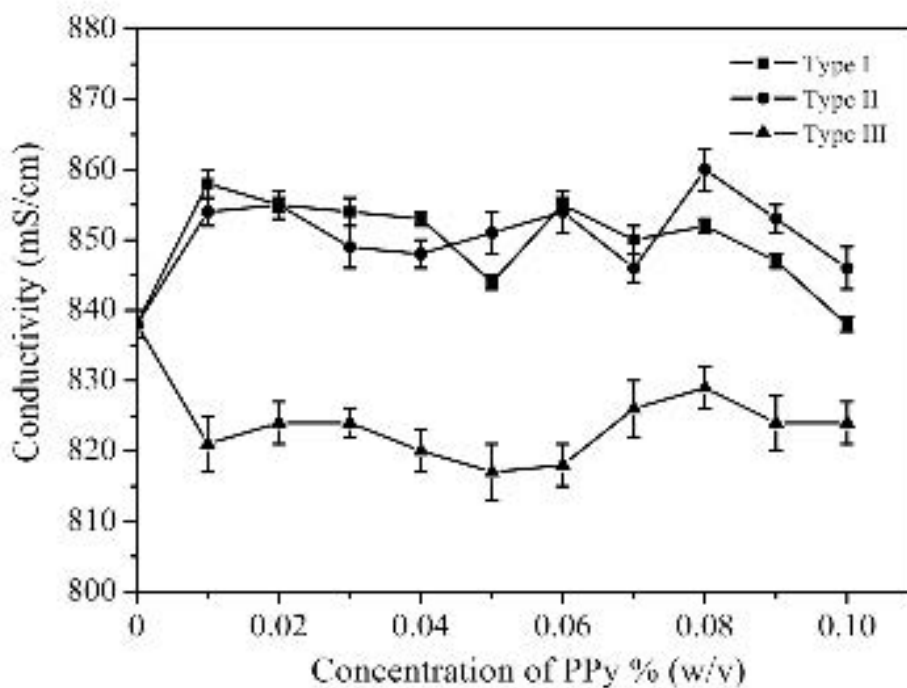


Figure 4.6 The conductivity of gelled electrolytes with various concentrations of PPy (2%w/v of fumed silica and 35%w/v of H_2SO_4 were fixed).

Fig. 4.6 shows the electrical conductivity of gelled electrolytes with various PPy concentrations. Type I/PPy and type II/PPy have similar conductivity values that increase at all concentration of PPy. As previously mentioned, the structural characteristics of the conjugated polymers are due to the conjugated double bonds [9-11, 22], which often lead to a high conductivity of the suspension. In contrast, type III/PPy presents a lower conductivity than the others as was observed in the conductivity results of type III/PAN after the addition of H_3PO_4 . The highest conductivities of type I/PPy (858 mS/cm), type II/PPy (860 mS/cm) and type III/PPy (829 mS/cm) were from PPy concentrations of 0.01 %(w/v), 0.08 %(w/v) and 0.08 %(w/v), respectively.

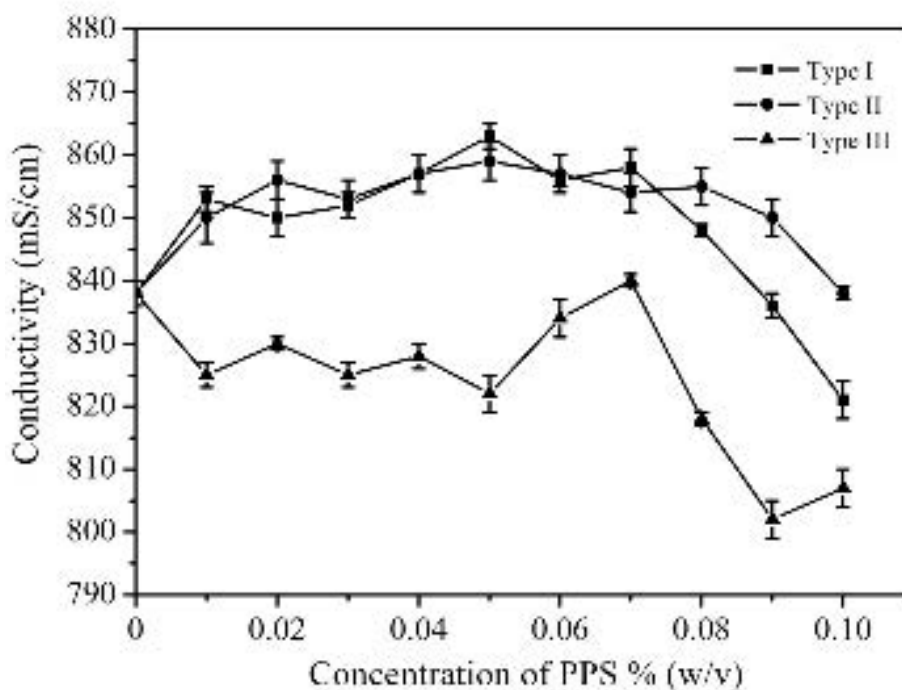


Figure 4.7 The conductivity of gelled electrolytes with various concentrations of PPS (2%w/v of fumed silica and 35%w/v of H_2SO_4 were fixed).

Fig. 4.7 shows the electrical conductivity of gelled electrolytes with various PPS concentrations. The data shows the similar characteristic curves to the gelled electrolyte with added PPy (Fig. 4.6), which is consistent with the previous explanations [9-11, 37]. The highest conductivities of type I/PPS (863 mS/cm), type II/PPS (859 mS/cm) and type III/PPS (840 mS/cm) were from PPS concentrations of 0.05 % (w/v), 0.05 % (w/v) and 0.07 % (w/v) of PPS concentration, respectively.

The high conductivity of the gelled electrolyte containing conducting polymers is generally explained by the increased free ion concentration as well as structural characteristics. The mechanism, however, is still not clearly understood.

4.3 Gelling time of gelled electrolytes

Table 4.12 Gelling time of various gelled electrolytes

| Name of battery | B1 | B2 | B3 | B4 | B5 | B6 | B7 | B8 | B9 | B10 | B11 | B12 |
|-----------------|----|----|----|----|----|----|----|----|----|-----|-----|-----|
| Time(min) | 10 | 19 | 12 | 17 | 10 | 9 | 17 | 8 | 7 | 16 | 8 | 6 |

The various gelled electrolytes were filled into a VRLA battery (B1-B12) to observe the gelling time as shown in Table 4.12. It was found that all gelled electrolytes had a good gelling time of less than 20 min at room temperature ($25^{\circ}\text{C} \pm 1$). Notably, the inclusion of additives, including PANI, in B4, B7 and B10 led to longer gelling times. This implies that the PANI structure affects the gelling time. In comparing B1, B5 and B6 after the addition of PPy and PPS, the gelling time was not affected. In contrast, not only B8 and B11, which included PPy and Na_2SO_4 and/or H_3PO_4 but also B9 and B12 decreased the gelling time. In summary, the gelled electrolytes containing PPy or PPS together with Na_2SO_4 and/or H_3PO_4 as additives (B5, B6, B8, B9, B11 and B12) provided the fast gelling times. The reason is probably due to the steric hindrance of conducting polymers. The structure of PPy has less the steric hindrance than PPS and PANI, respectively.

4.4 Performance of VRLA batteries

4.4.1 Charge and discharge characteristic of VRLA batteries

The similar charge characteristic curves of B1-B12 at cycle 5 and 10 are shown in Fig. 4.8 (a-b) and Fig. 4.9 (a-b). Notably, the voltage of the cell increases sharply as the full charge state is approached. This increase in voltage is caused by the plates going into overcharge when most of the active material on the plates has been converted from lead sulfate to lead on the negative plate and to lead dioxide on the positive plate as equations 2.1-2.5. The current of the cell is constant when the full charge state is approached and decreases smoothly to the cutoff current ($\sim 0.03\text{-}0.00\text{ A}$).

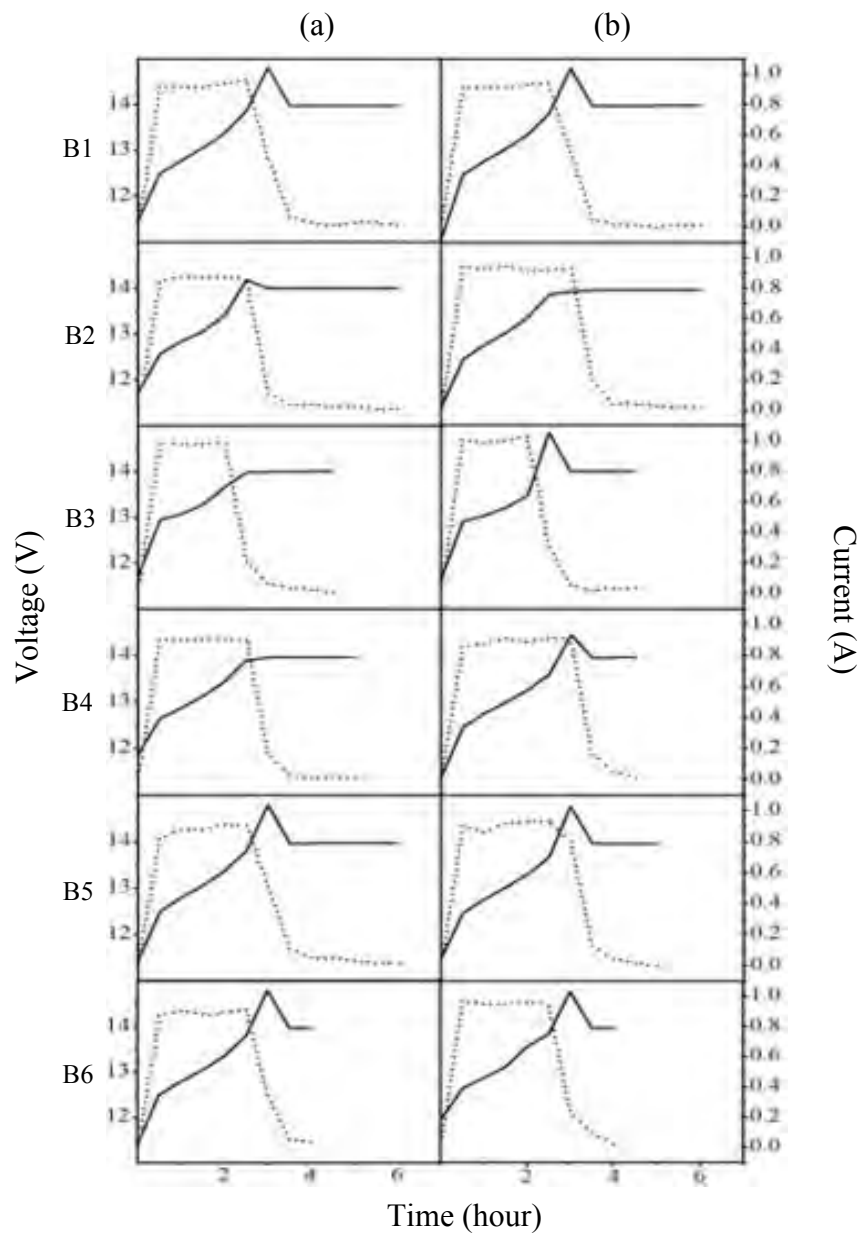


Figure 4.8 The charge characteristic of B1-B6 of (a) cycle 5 and (b) cycle 10 at 1-hour rate and $25^{\circ}\text{C}\pm 1$, where a solid line is voltage of battery and a dot line is current of battery.

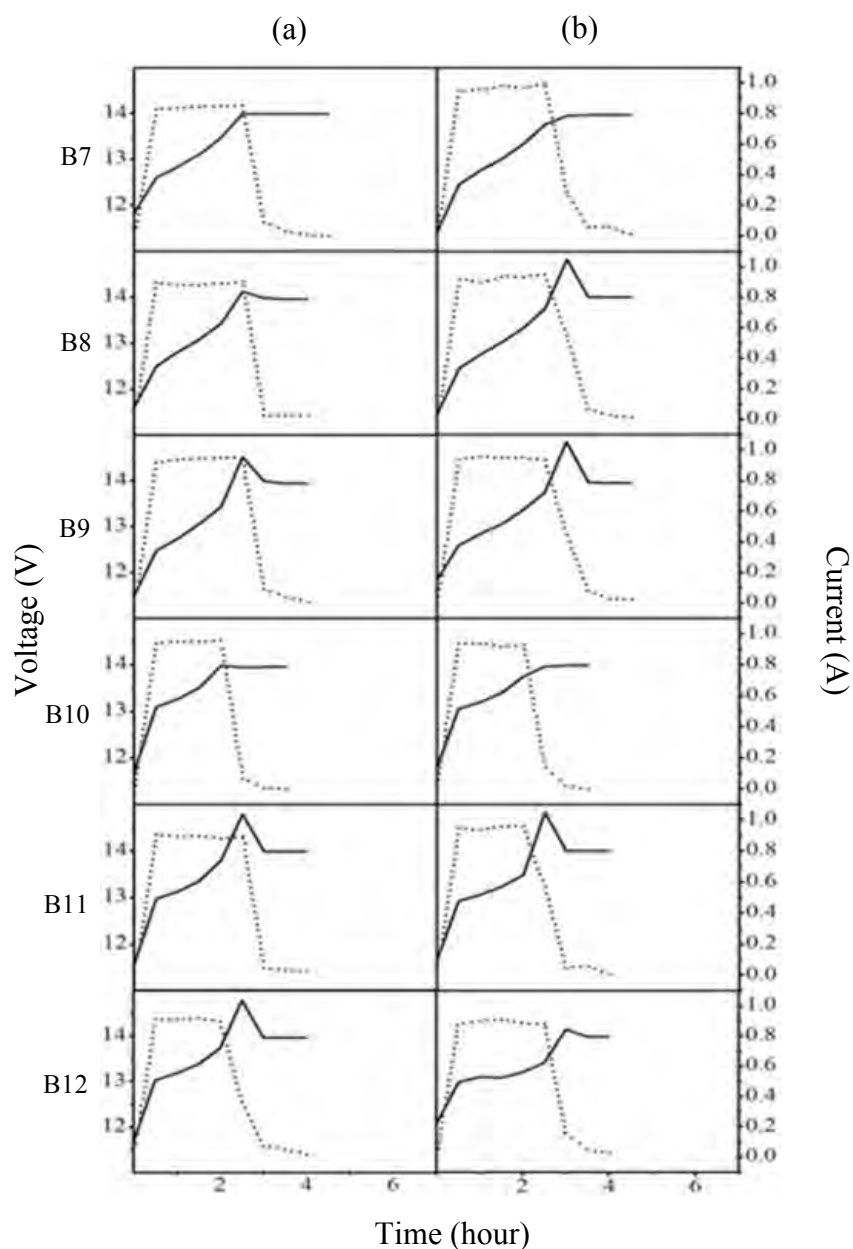


Figure 4.9 The charge characteristic of B7-B12 of (a) cycle 5 and (b) cycle 10 at 1-hour rate and $25^{\circ}\text{C}\pm 1$, where a solid line is voltage of battery and a dot line is current of battery.

The similar discharge characteristic curves of B1-B12 at cycle 5 and 10 are shown in Fig. 4.10 (a-b) and Fig 4.11 (a-b). As the cell is discharged, the voltage decreases due to depletion of material, as shown in equations 2.1-2.5, results in internal resistance losses and polarization. Although, the discharge current is constant, the voltage under load decreases smoothly to the cutoff voltage (9 V).

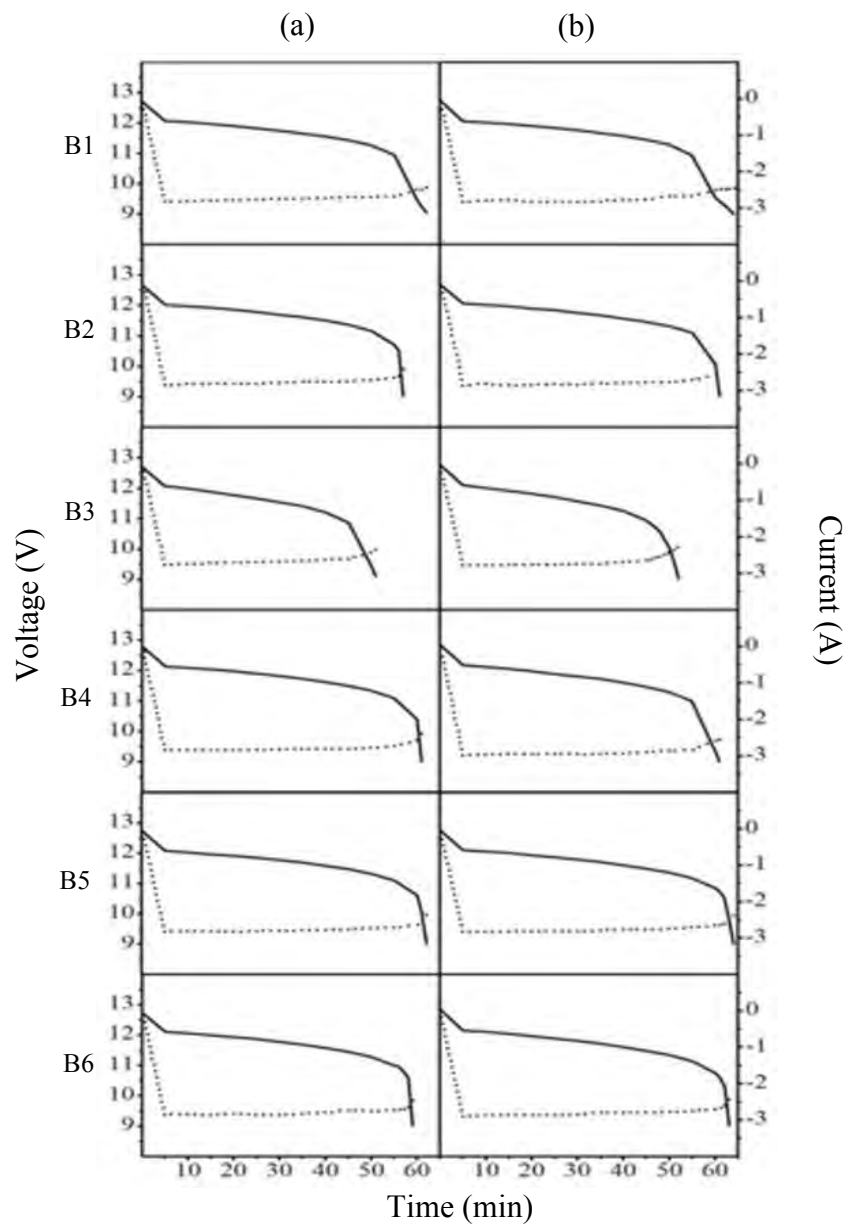


Figure 4.10 The discharge characteristic of B1-B6 of (a) cycle 5 and (b) cycle 10 at 1-hour rate and $25^{\circ}\text{C}\pm 1$, where a solid line is voltage of battery and a dot line is current of battery.

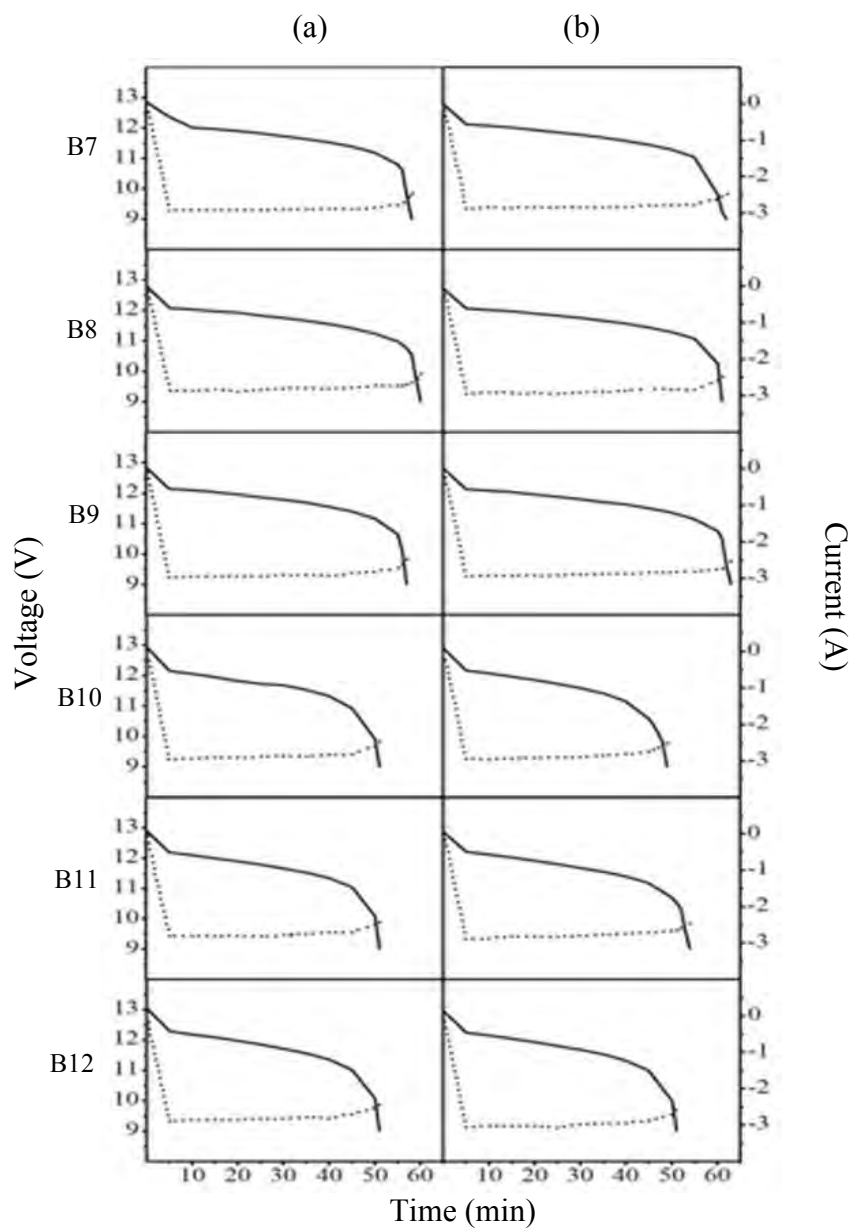


Figure 4.11 The discharge characteristic of B7-B12 of (a) cycle 5 and (b) cycle 10 at 1-hour rate and $25^{\circ}\text{C}\pm 1$, where a solid line is voltage of battery and a dot line is current of battery.

4.4.2 Initial discharge curves of VRLA batteries

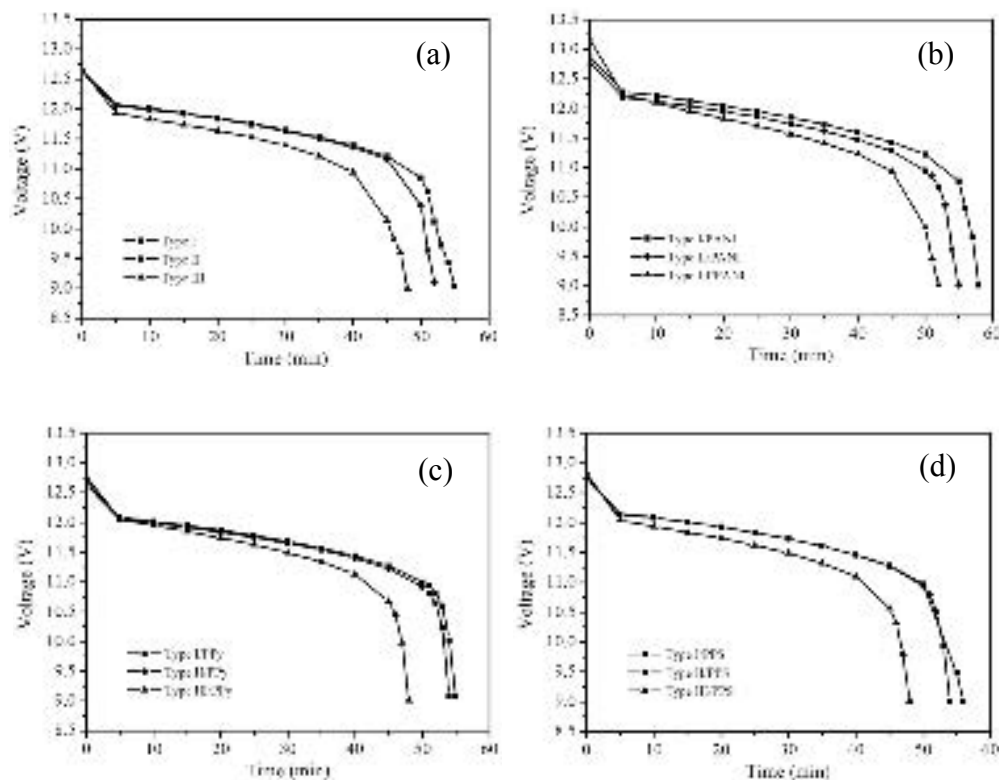


Figure 4.12 Initial discharge curves of B1-B12 with type I-III of gelled electrolytes; (a) without conducting polymer, (b) adding PANI, (c) adding PPy, and (d) adding PPS at 1-hour rate and $25^{\circ}\text{C}\pm 1$.

The gelled electrolytes with the highest conductivities were transferred into VRLA batteries (B1-B12), and the capacity was investigated at 1-hour rate in order to check the cycling performance. Fig. 4.12 (a-d) shows the similar initial discharge curves of the gelled electrolytes in VRLA batteries. The data suggest that the battery performance is directly affected by the conductivity. As expected from the conductivity results, the gelled electrolyte containing H_3PO_4 had the lowest initial discharge capacity. The gelled electrolyte containing PANI showed a higher discharge voltage and longer discharge capacity than the other electrolytes.

4.4.3 Discharge capacities of VRLA batteries

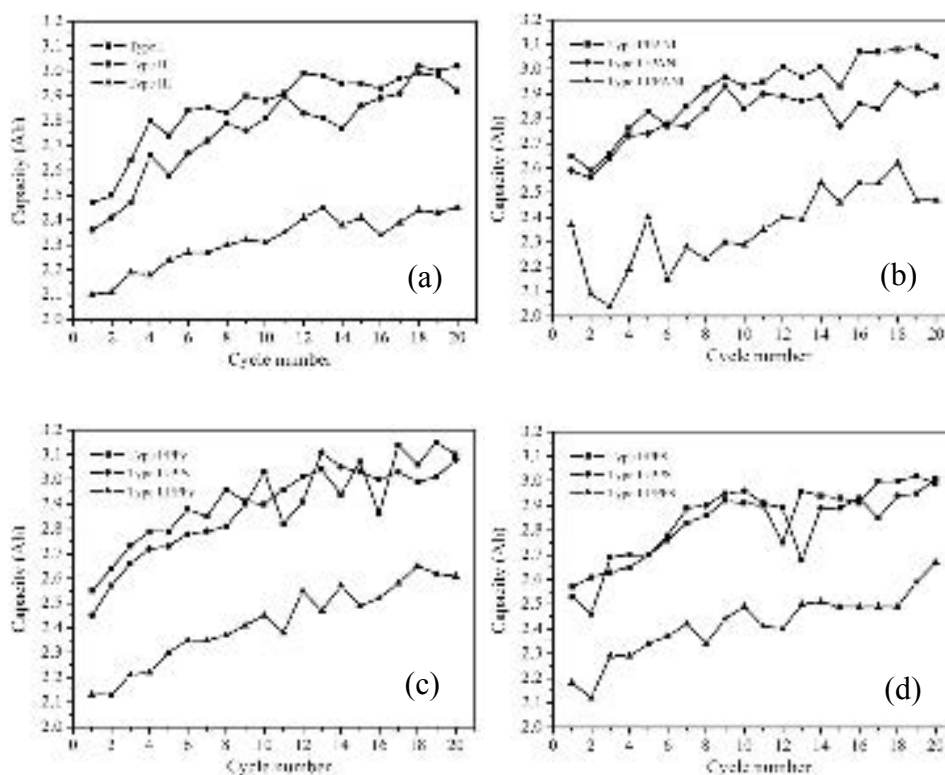


Figure 4.13 Capacity test in each cycle number of B1-B12 with type I-III of gelled electrolytes; (a) without conducting polymer, (b) adding PANI, (c) adding PPy, and (d) adding PPS at 1-hour rate and $25^{\circ}\text{C}\pm 1$.

The novel gelled electrolytes present surprising capacity results when compared to the standard capacity of 2.3 Ah at 1-hour rate (at 25°C) (supplied by N.V. Battery) [47] as shown in Fig. 4.13 (a-d). It is shown that the type I and type II gelled electrolytes had the best capacities and had increased capacities at all cycle numbers. In particular, type I/PPy and type II/PPy exhibited higher capacities than the others, whereas the type III exhibited lower capacity in the initial discharge curves (Fig. 4.12). The addition of H_3PO_4 , although known to slightly reduce the capacity, was previously reported to have a beneficial effect on cycle stability and had been used as an additive in flooded lead-acid batteries for many years [13]. The capacity results demonstrated that the type I/PPy and type II/PPy gave the highest performance under the cycling of VRLA batteries. The results of conductivity and capacity tests show that the proposed gelled electrolytes give the promising gel technology for VRLA battery and other technology applications.

4.5 Oxygen recombination reaction of gelled electrolyte

Type I and type II of all gelled electrolytes were selected to study in this stage due to their high conductivity and compared with the H_2SO_4 solution (35 %w/v). In Fig. 4.14 and 4.15 show the cyclic voltammograms of the type I and type II systems of all gelled electrolytes and H_2SO_4 solution. The results show similar redox peaks in the potential range -1.8 V–2.4 V, indicating that the addition of Na_2SO_4 salt or conducting polymers did not change the redox reactions of gelled electrolyte and planar lead electrodes. The oxidation of PbSO_4 to PbO_2 appears at -0.5 V and the reduction of PbO_2 to PbSO_4 appears at -0.4 V. Therefore, the CV results confirm that the type I and type II of all gelled electrolytes are stable under the operating conditions of VRLA batteries.

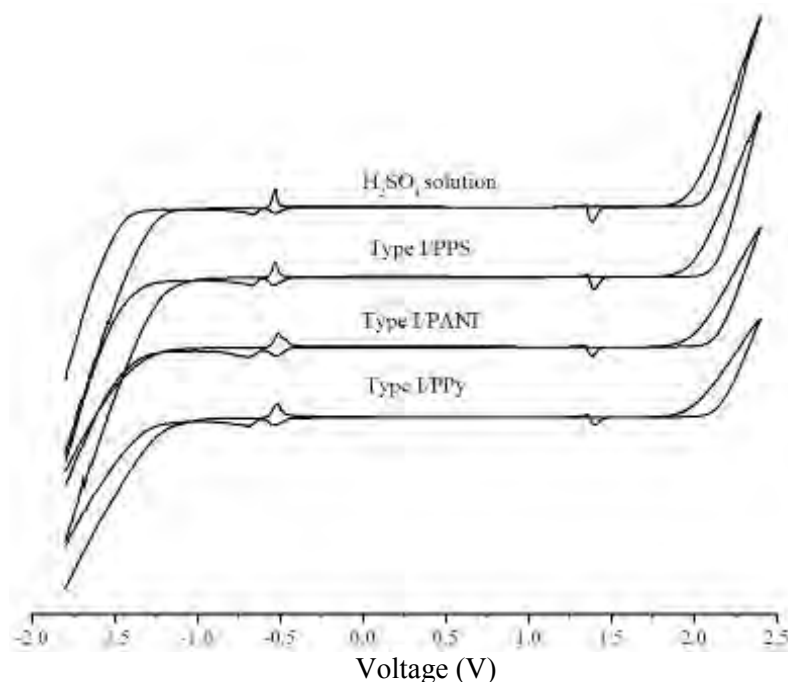


Figure 4.14 Cyclic voltammogram of type I of gelled electrolytes containing only conducting polymer as additive and acid solution at scan rate of 20 mV s^{-1} .

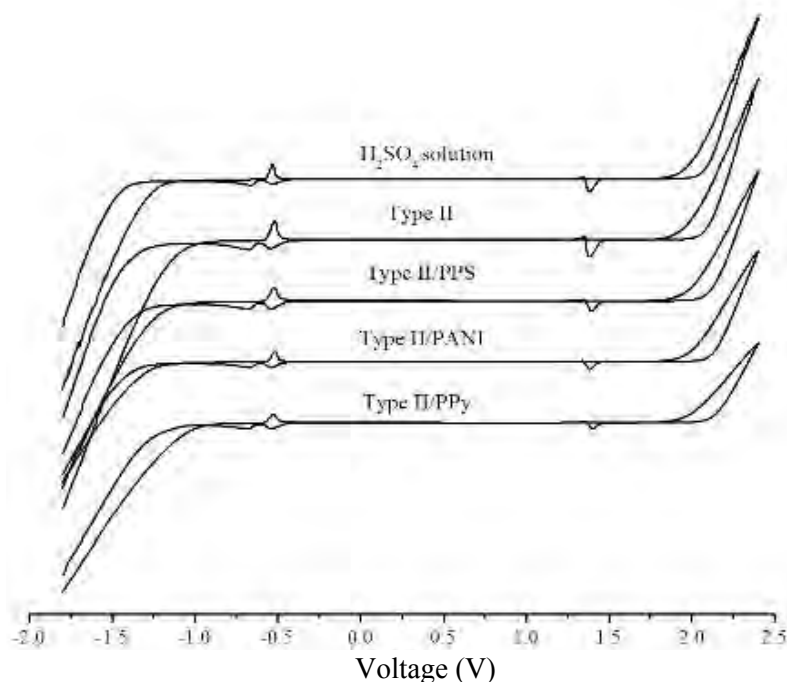


Figure 4.15 Cyclic voltammogram of type II of gelled electrolytes containing Na_2SO_4 and conducting polymer as additive and acid solution at scan rate of 20 mV s^{-1} .

The oxygen recombination studies allow for investigation from a more positive potential. In comparison with H_2SO_4 solutions, the type I and type II of gelled electrolytes containing a conducting polymer show diminished oxygen evolution peaks, leading to higher performance of the batteries. The lowest peak current of oxygen evolution was found in the gelled electrolyte containing PPy. This implies that the oxygen recombination process can be inhibited in the system of gelled electrolyte containing PPy. The decreasing of oxygen recombination process is probably due to the fact that the very thin passivation layer of conducting polymers adsorbed on plates make the transfer of oxygen between plates and electrolyte interface more difficult. In addition, the peak currents of oxygen evolution of the gelled electrolyte containing Na_2SO_4 (type II) were not altered when compared to the type I of all gelled electrolytes or the H_2SO_4 solution.

CHAPTER V

CONCLUSIONS AND FUTURE PERSPECTIVE

5.1 Conclusions

In conclusion, a suspension (low viscosity) of the gelled electrolytes is preferable because it allows for easy battery filling. The electrical conductivity of the gelled electrolytes depended on the concentrations of fumed silica, H_2SO_4 , Na_2SO_4 , H_3PO_4 and conducting polymers. The gelled electrolyte containing 2 % (w/v) of fumed silica and, 35% (w/v) of H_2SO_4 provided the highest conductivity of 838 mS/cm and were chosen to screen additives. Moreover, fumed silica, H_2SO_4 , Na_2SO_4 , H_3PO_4 and conducting polymers affected the gelling time. The gelled electrolytes containing PPy or PPS together with Na_2SO_4 and/or H_3PO_4 as additive resulted in fast gelling times. The conductivity of the gelled electrolytes was related to the initial discharge and to the discharge capacity of gelled electrolytes. In particular, type I and type II of all gelled electrolytes had similar conductivity, initial discharge and discharge capacities. Type III of all gelled electrolytes had the lowest conductivity and similar initial discharge and discharge capacities. The high discharge efficiencies of type I/PPy and type II/PPy of gelled electrolytes performed better under the cycling of VRLA batteries than the others and behaved similarly to type I/PANI and type II/PANI of gelled electrolytes. Moreover, the type I and type II gelled electrolyte containing PPy inhibited oxygen more than the others. Hence, the type I and type II gelled electrolytes containing PPy had the lowest water loss.

In addition, the novel gelled electrolytes had surprising capacity results when compared to the standard capacity of 2.3 Ah at 1-hour rate (at 25°C) (supplied by N.V. Battery) [47]. The best capacities were obtained for type I and type II gelled electrolytes leading to higher than the standard capacity at all cycle numbers. Furthermore, all of the results of conductivity and capacity tests showed that the proposed gelled electrolytes give the promising gel technology for VRLA battery and other technology applications.

5.2 Future perspective

The novel gelled electrolytes consisting of PANI, PPy and PPS showed high performance in VRLA batteries. Hence, others conducting polymers may be similarly used to enhance the performance of VRLA batteries.

REFERENCES

- [1] Misra, S. S. Advances in VRLA battery technology for telecommunications. Journal of Power Sources 168 (2007): 40-48.
- [2] Martha, S. K.; Hariprakash, B.; Gaffoor, S. A.; and Shukla, A. K. Lead-acid cells with polyaniline-coated negative plates. Journal of Applied Electrochemistry 36 (2006): 711-722.
- [3] Vinod, M. P.; and Vijayamohanan, K. Effect of gelling on the impedance parameters of Pb/PbSO₄ electrode in maintenance-free lead-acid batteries. Journal of Power Sources 89 (2000): 88-92.
- [4] Lambert, D. W. H.; Greenwood, P. H. J.; and Reed, M. C. Advances in gelled-electrolyte technology for valve-regulated lead-acid batteries. Journal of Power Sources 107 (2002): 173-179.
- [5] Hu, J.; and Guo, Y. Effects of electrolyte stratification on performances of AGM valve -regulated lead-acid batteries. Electrochimica Acta 52 (2007): 6734-6740.
- [6] Guo, Y.; Hu, J.; and Huang, M. Investigations on self-discharge of gel valve-regulated lead-acid batteries. Journal of Power Sources 158 (2006): 991-996.
- [7] Park, J.; Park, S. B.; Yang, S.-M.; Hong, W. H.; Choi, C. R.; and Kim, J. H. Rheological characterization and optimization of gelled electrolyte for sealed lead-acid batteries by small amplitude dynamic oscillation measurement. Journal of Non-Crystalline Solids 351 (2005): 2352-2357.
- [8] Trinidad, F.; Sáez, F.; and Valenciano, J. High power valve regulated lead-acid batteries for new vehicle requirements. Journal of Power Sources 95 (2001): 24-37.
- [9] Cai, Z.; Geng, M.; and Tang, Z. Novel battery using conducting polymers: Polyindole and polyaniline as active materials. Journal of Materials Science 39 (2004): 4001-4003.

- [10] Zhijiang, C. Study on a Novel Polymer-based Secondary Battery System. Journal of Polymer Research 13 (2006): 207-211.
- [11] Soontornworajit, B.; Wannatong, L.; Hiamtup, P.; Niamlang, S.; Chotpattananont, D.; Sirivat, A.; and Schwank, J. Induced interaction between polypyrrole and SO₂ via molecular sieve 13X. Materials Science and Engineering: B 136 (2007): 78-86.
- [12] Linden, D. Handbook of batteries. United States of America: McGraw-Hill, 1995.
- [13] Berndt, D. Maintenance-free batteries lead-acid, nickel/cadmium, nickel/hydride a handbook of battery technology. Great Britain: John Wiley & Sons, 1993.
- [14] Bullock, K. R. Lead/acid batteries. Journal of Power Sources 51 (1994): 1-17.
- [15] Hehner, N.E. Storage battery manufacturing manual. United States of America: Independent battery manufacturers association, 1986.
- [16] Berndt, D. Maintenance-free batteries based on aqueous electrolyte lead-acid, nickel/cadmium, nickel/hydride a handbook of battery technology. Great Britain: John Wiley & Sons, 2003.
- [17] Chen, M. Q.; Chen, H. Y.; Shu, D.; Li, A. J.; and Finlow, D. E. Effects of preparation condition and particle size distribution on fumed silica gel valve-regulated lead-acid batteries performance. Journal of Power Sources 181 (2008): 161-171.
- [18] IEEE guide for selection of valve-regulated lead-acid (VRLA) batteries for stationary applications [online]. (n.d.). Available from: <http://ieeexplore.ieee.org/stamp/stamp.jsp?arnumber=00531501> [2008, September 23].
- [19] Rusch, W.; Vassallo, K.; Hart G. Understanding the real differences between gel and AGM batteries [online]. (n.d.). Available from: <http://www.battcon.com/paperfinal2007/rushpaper2007.pdf> [2007, September 23].

- [20] Billingham, N.C.; Calvert, P.D.; Kurimura, Y.; Litmanovich, A.A.; and Papisov, I.M. Advances in polymer science 90. Germany: Springer-Verlag Berlin Heidelberg, 1989.
- [21] Chew, S. Y.; Guo, Z. P.; Wang, J. Z.; Chen, J.; Munroe, P.; Ng, S. H.; Zhao, L.; and Liu, H. K. Novel nano-silicon/polypyrrole composites for lithium storage. Electrochemistry Communications 9 (2007): 941-946.
- [22] Skotheim, T.A.; and Reynolds, J.R. Conjugated polymers theory, synthesis, properties, and characterization. United States of America: CRC Press Taylor & Francis Group, 2007.
- [23] Raghavan, M.; and Trivedi, D. C. Use of polyaniline in lead acid battery. Synthetic Metals 119 (2001): 285-286.
- [24] Martha, S.; Hariprakash, B.; Gaffoor, S.; Trivedi, D.; and Shukla, A. A low-cost lead-acid battery with high specific-energy. Journal of Chemical Sciences 118 (2006): 93-98.
- [25] Grgur, B. N.; Ristic, V.; Gvozdenovic, M. M.; Maksimovic, M. D.; and Jugovic, B. Z. Polyaniline as possible anode materials for the lead acid batteries. Journal of Power Sources 180 (2008): 635-640.
- [26] Mi, H.; Zhang, X.; Yang, S.; Ye, X.; and Luo, J. Polyaniline nanofibers as the electrode material for supercapacitors. Materials Chemistry and Physics 112 (2008): 127-131.
- [27] Cho, M. S.; Choi, H. J.; and Ahn, W.-S. Enhanced Electrorheology of Conducting Polyaniline Confined in MCM-41 Channels. Langmuir 20 (2004): 202-207.
- [28] Wu, A.; Venancio, E. C.; and MacDiarmid, A. G. Polyaniline and polypyrrole oxygen reversible electrodes. Synthetic Metals 157 (2007): 303-310.

- [29] Tang, Q.; Wu, J.; Sun, H.; Lin, J.; Fan, S.; and Hu, D. Polyaniline/polyacrylamide conducting composite hydrogel with a porous structure. Carbohydrate Polymers 74 (2008): 215-219.
- [30] Al-Mashat, L.; Tran, H. D.; Wlodarski, W.; Kaner, R. B.; and Kalantar-zadeh, K. Polypyrrole nanofiber surface acoustic wave gas sensors. Sensors and Actuators B: Chemical 134 (2008): 826-831.
- [31] Lu, Q.; and Li, C. M. One-step co-electropolymerized conducting polymer-protein composite film for direct electrochemistry-based biosensors. Biosensors and Bioelectronics 24 (2008): 767-772.
- [32] Dutta, K.; and De, S. K. Transport and optical properties of SiO₂-polypyrrole nanocomposites. Solid State Communications 140 (2006): 167-171.
- [33] Cheng, Q.; Pavlinek, V.; Li, C.; Lengalova, A.; He, Y.; and Saha, P. Synthesis and characterization of new mesoporous material with conducting polypyrrole confined in mesoporous silica. Materials Chemistry and Physics 98 (2006): 504-508.
- [34] Sharma, R. K.; Rastogi, A. C.; and Desu, S. B. Nano crystalline porous silicon as large-area electrode for electrochemical synthesis of polypyrrole. Physica B: Condensed Matter 388 (2007): 344-349.
- [35] Spires, J. B.; Peng, H.; Williams, D. E.; Wright, B. E.; Soeller, C.; and Travas-Sejdic, J. The effect of the oxidation state of a terthiophene-conducting polymer and of the presence of a redox probe on its gene-sensing properties. Biosensors and Bioelectronics 24 (2008): 928-933.
- [36] Wang, J.-Z.; Chou, S.-L.; Chen, J.; Chew, S.-Y.; Wang, G.-X.; Konstantinov, K.; Wu, J.; Dou, S.-X.; and Liu, H. K. Paper-like free-standing polypyrrole and polypyrrole-LiFePO₄ composite films for flexible and bendable rechargeable battery. Electrochemistry Communications 10 (2008): 1781-1784.
- [37] Skotheim, T.A. Handbook of conducting polymers. United States of America: Marcel Dekker, 1986.

- [38] Wang, J. Analytical electrochemistry. United States of America: John Wiley & Sons, 2006.
- [39] Introduction to conductivity [online]. (n.d.). Available from: <http://www.eutec.hinst.com/techtips/tech-tips25.htm> [2008, September 23].
- [40] Conductivity theory and practice [online]. (n.d.). Available from: http://www.analytical_chemistry.uoc.gr/pdf/Agwgimometria_2.pdf [2008, September 23].
- [41] Torcheux, L.; and Lailier, P. A new electrolyte formulation for low cost cycling lead acid batteries. Journal of Power Sources 95 (2001): 248-254.
- [42] Wu, L.; Chen, H. Y.; and Jiang, X. Effect of silica soot on behavior of negative electrode in lead-acid batteries. Journal of Power Sources 107 (2002): 162-166.
- [43] Martha, S.; Hariprakash, B.; Gaffoor, S.; and Shukla, A. Performance characteristics of a gelled-electrolyte valve-regulated lead-acid battery. Bulletin of Materials Science 26 (2003): 465-469.
- [44] Tang, Z.; Wang, J.; Mao, X.-x.; Shao, H.; Chen, Q.; Xu, Z.; and Zhang, J. Investigation and application of polysiloxane-based gel electrolyte in valve-regulated lead-acid battery. Journal of Power Sources 168 (2007): 49-57.
- [45] Tang, Z.; Wang, J.-M.; Mao, X.-X.; Chen, Q.-Q.; Shen, C.; and Zhang, J.-Q. Application of a novel gelled-electrolyte in valve-regulated lead-acid batteries with tubular positive plates. Journal of Applied Electrochemistry 37 (2007): 1163-1169.
- [46] Sodium sulfate [online]. (n.d.). Available from: http://en.wikipedia.org/wiki/sodium_sulfate [2008, September 23].
- [47] HGL4.0-12 Valve Regulated Sealed Lead-Acid Battery Lion [online]. (n.d.). Available from: <http://www.nvbattery.com/products.asp?page=2&ParentID=228> [2008, October 27].

APPENDICES

APPENDIX A

HGL4.0-12

HGL4.0 -12

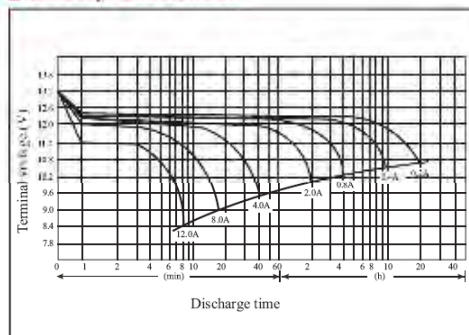
Valve Regulated Sealed Lead-Acid Battery



Specifications

| | | |
|--------------------------------|----------------------------------|--------|
| Nominal Voltage | | 12V |
| Rated Capacity (20 hours rate) | | 4.0Ah |
| Dimensions (= 2mm) | Total Height (with terminals) | 105mm |
| | Length | 91mm |
| | Width | 71mm |
| Approx. Weight | | 1.64kg |
| Standard Terminal | | F1 |

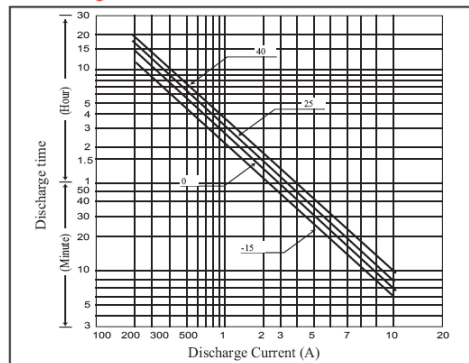
Discharge Characteristics



Characteristics

| | | | |
|---|----------------------------------|-----------------|----------------------|
| Capacity (25°C) | 20 hour rate (200mA) | 4.0AH | |
| | 10 hour rate (372mA) | 3.7AH | |
| | 5 hour rate (680mA) | 3.4AH | |
| | 1 hour rate (2.3A) | 2.3AH | |
| Internal Resistance | Fully charged Battery 25°C | Approx. 35m | |
| Capacity affected by temperature (20 hour rate) | 40°C | 102% | |
| | 25°C | 100% | |
| | 0°C | 85% | |
| Self Discharge (25°C) | Capacity after 3 months storage | 92% | |
| | Capacity after 6 months storage | 83% | |
| | Capacity after 12 months storage | 65% | |
| Charge Method (Constant Voltage) | Cycle use | Initial Current | 1.20A or smaller |
| | | Control Voltage | 14.4 to 15.0V (25°C) |
| | Standby use | Initial Current | 1.20A or smaller |
| | | Control Voltage | 13.5 to 13.8V (25°C) |

Discharge current & Duration Time



* The above data are average and obtained within three charge/discharge cycles. Cycles not the minimum values.

APPENDIX B

GELLING TIME

Table B1 The gelling time of gelled electrolytes providing highest conductivity with different concentrations of fumed silica and H₂SO₄

| Fumed silica (%w/v) | H ₂ SO ₄ (%w/v) | Gelling time (min) |
|------------------------|--|-----------------------|
| 1 | 35 | >60 |
| 2 | 35 | 10 |
| 3 | 35 | 10 |
| 4 | 35 | 10 |
| 5 | 30 | 20 |
| 6 | 30 | 20 |
| 7 | 40 | 10 |
| 8 | 25 | 20 |
| 9 | 15 | 25 |

Table B2 The gelling time of gelled electrolytes providing highest conductivity with different concentrations of Na₂SO₄ and H₃PO₄

| Na ₂ SO ₄ (g L ⁻¹) | H ₃ PO ₄ (%) | Gelling time (min) |
|---|---------------------------------------|-----------------------|
| 1.0 | 1.4 | 10 |
| 1.5 | 1.4 | 10 |
| 2.0 | 1.2 | 10 |
| 2.5 | 1.2 | 10 |
| 3.0 | 1.2 | 10 |
| 3.5 | 1.2 | 10 |
| 4.0 | 1.4 | 10 |

APPENDIX C

CHARGE AND DISCHARGE CHARACTERISTIC

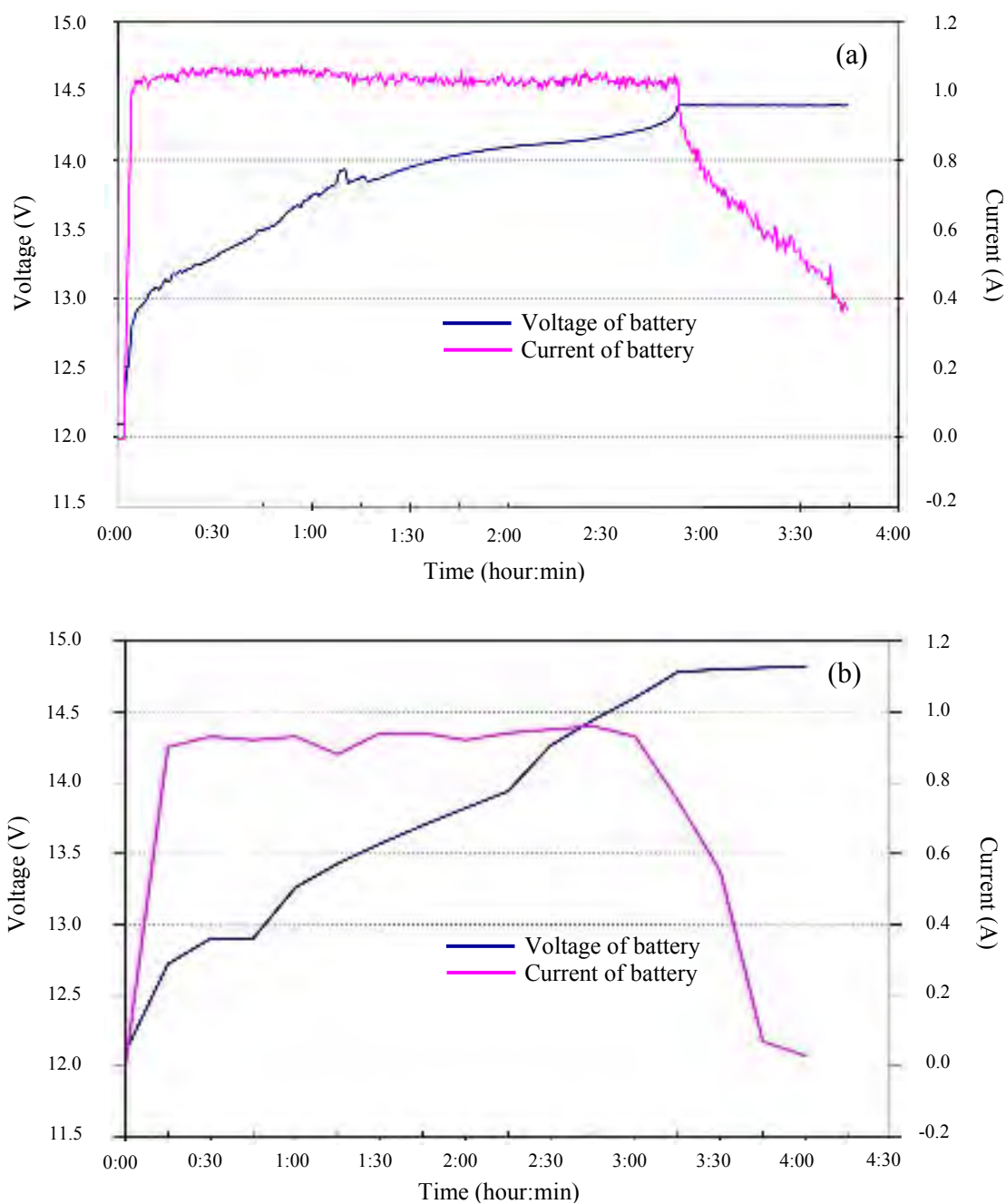


Figure C1 Charge characteristic of cycle 1 of VRLA battery containing 2%(w/v) of fumed silica and 35%(w/v) of H_2SO_4 (B1) for 1-hour rate at room temperature ($25^\circ C \pm 1$), which were measured by (a) universal battery analyzer version 0.9.9.0A3 and (b) manual method.

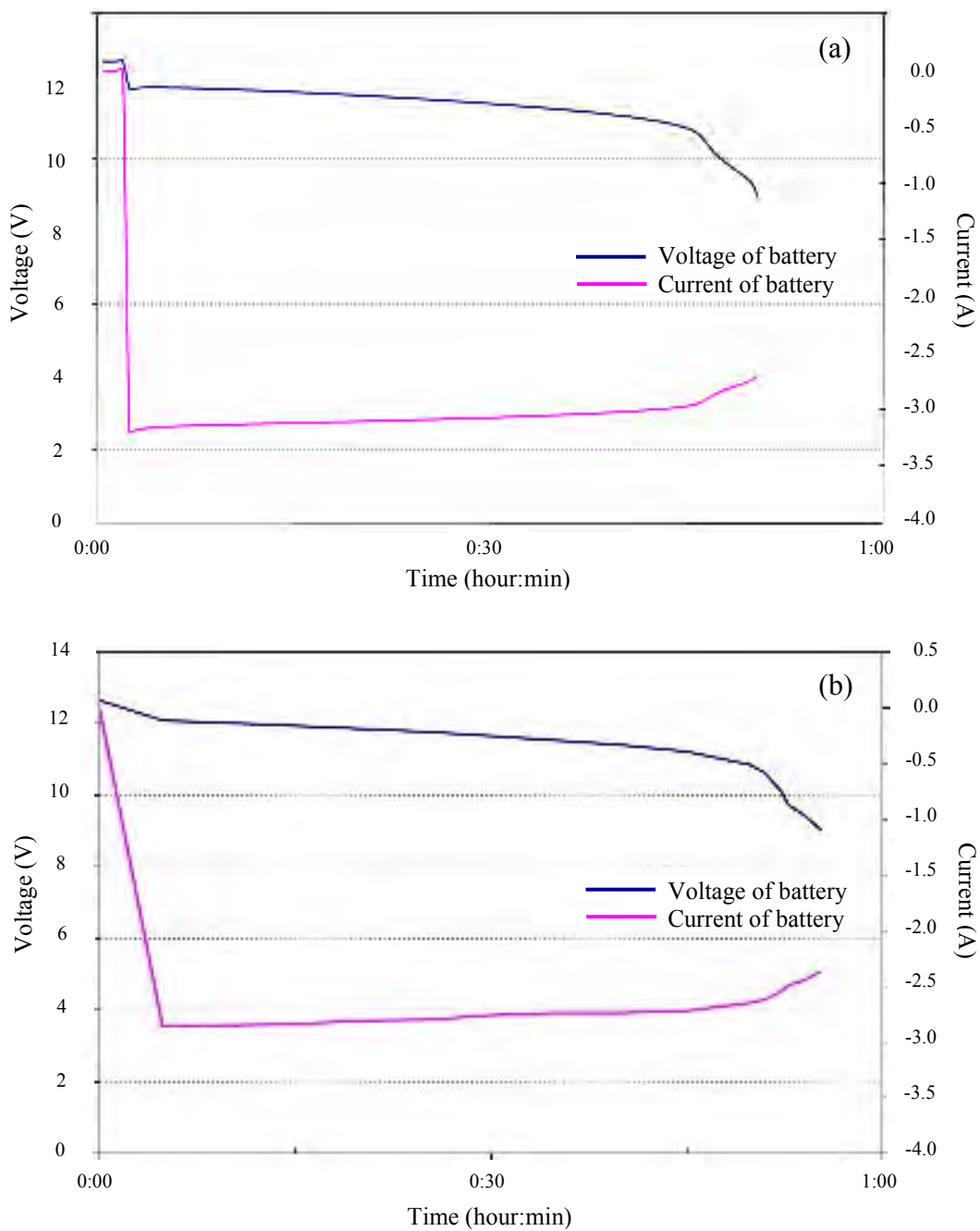


Figure C2 Discharge characteristic of cycle 1 of VRLA battery containing 2%(w/v) of fumed silica and 35%(w/v) of H_2SO_4 (B1) for 1-hour rate at room temperature ($25^\circ\text{C}\pm 1$), which were measured by (a) universal battery analyzer version 0.9.9.0A3 and (b) manual method.

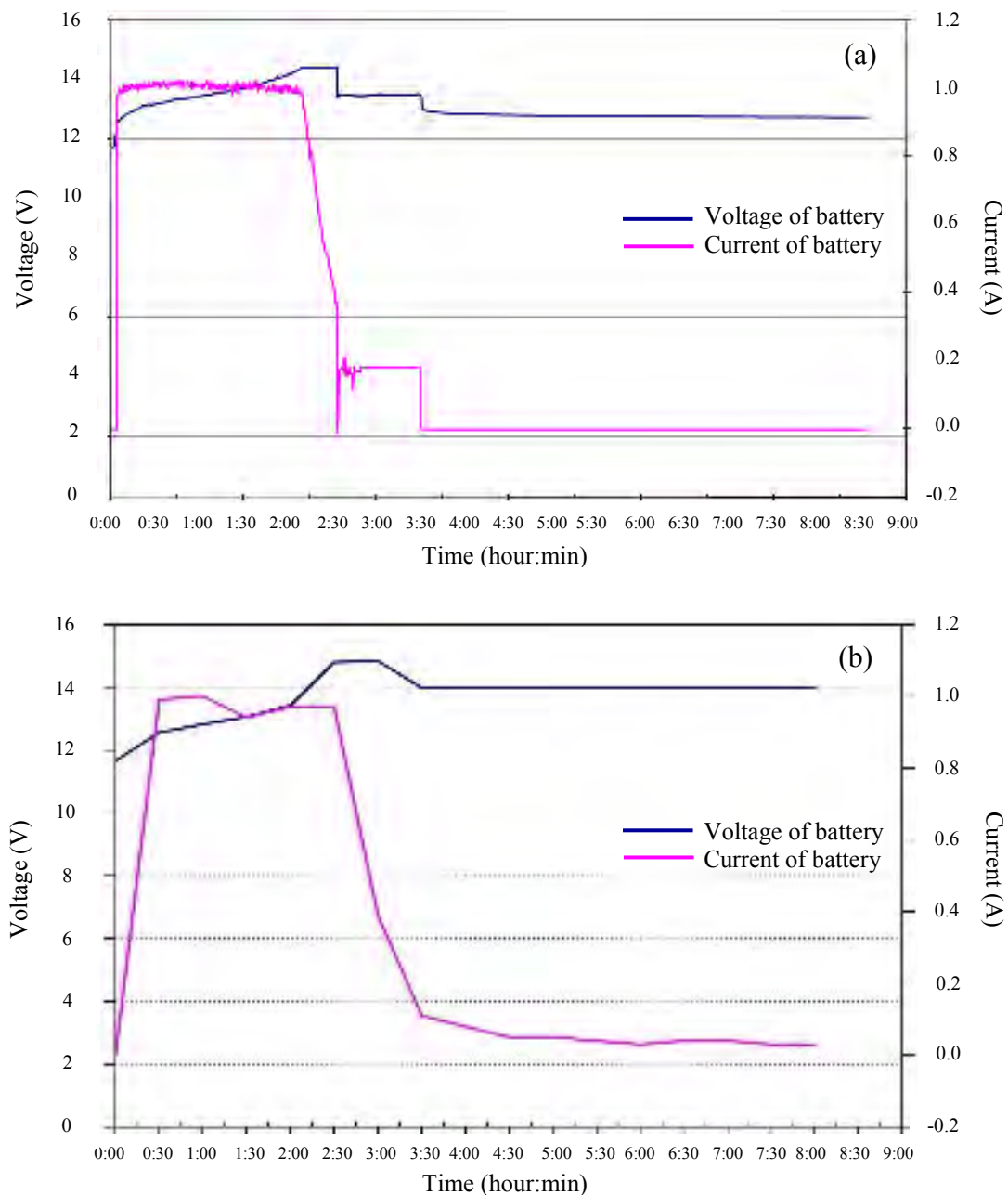


Figure C3 Charge characteristic of cycle 2 of VRLA battery containing 2%(w/v) of fumed silica and 35%(w/v) of H_2SO_4 (B1) for 1-hour rate at room temperature ($25^\circ C \pm 1$), which were measured by (a) universal battery analyzer version 0.9.9.0A3 and (b) manual method.

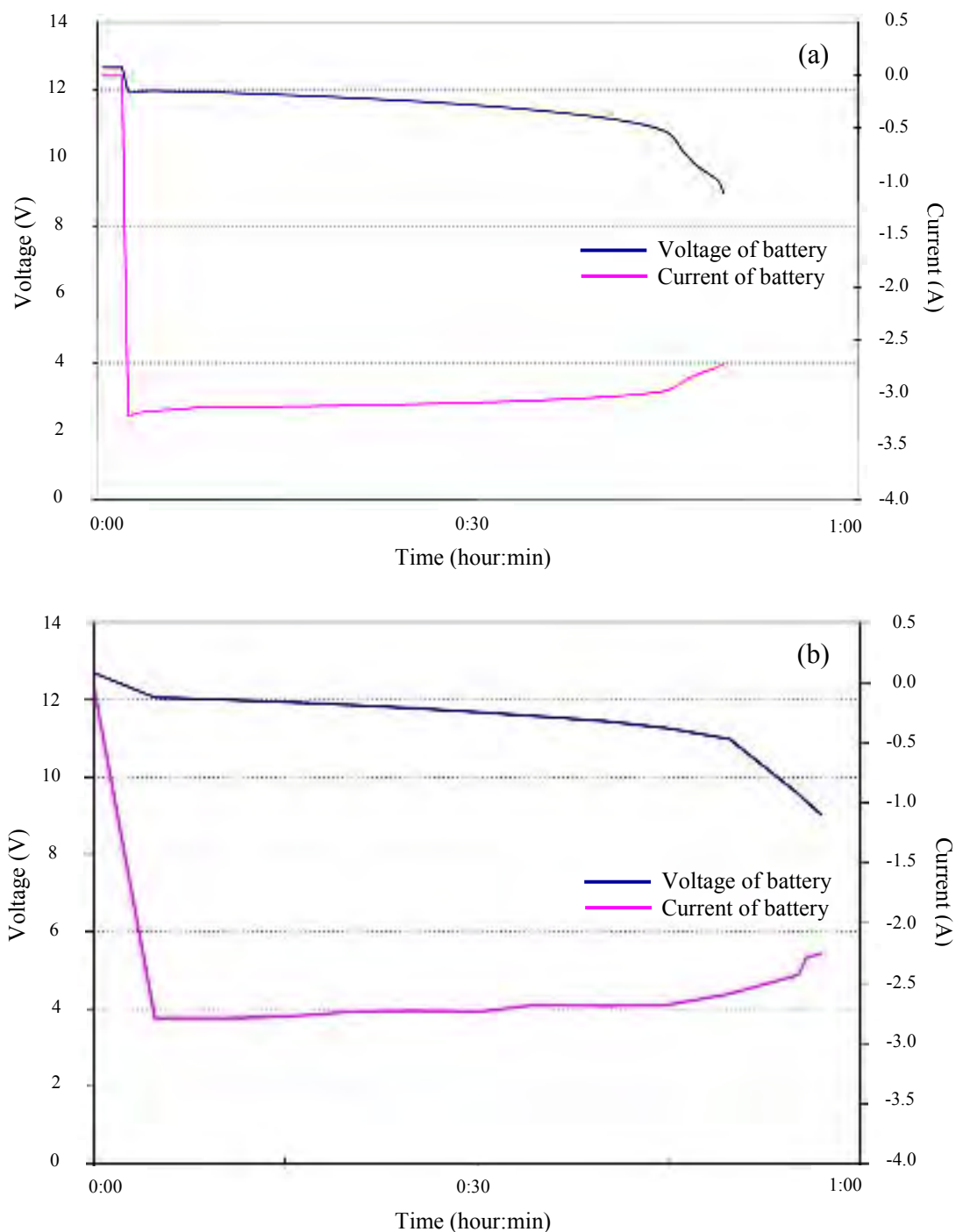


Figure C4 Discharge characteristic of cycle 2 of VRLA battery containing 2%(w/v) of fumed silica and 35%(w/v) of H_2SO_4 (B1) for 1-hour rate at room temperature ($25^\circ\text{C}\pm 1$), which were measured by (a) universal battery analyzer version 0.9.9.0A3 and (b) manual method.

APPENDIX D

PROCEEDING

ผลของสารเติมแต่งต่อประสิทธิภาพของเจลอิเล็กโทรไลต์ในแบตเตอรี่ชนิดตะกั่ว-กรดแบบมีวาล์ว

EFFECT OF ADDITIVES ON PERFORMANCE OF GELLED-ELECTROLYTE FOR VALVE-REGULATED LEAD-ACID BATTERIES

อมรรัตน์ ชัยสิทธิ์¹ และ อรวรรณ ชัยลาภกุล^{2*}

Amornrat Chaiyasit¹ and Orawon Chailapakul^{2*}

¹Program in Petrochemistry and Polymer Science, Faculty of Science, Chulalongkorn University, Bangkok 10330

²Department of Chemistry, Faculty of Science, Chulalongkorn University, Bangkok 10330 Phone 0-2218-7615, E-Mail: corawon@chula.ac.th

บทคัดย่อ: ผลของสารเติมแต่งต่อประสิทธิภาพของเจลอิเล็กโทรไลต์สำหรับใช้ในแบตเตอรี่ชนิดตะกั่ว-กรดแบบมีวาล์วถูกตรวจสอบด้วยการวัดค่าการนำไฟฟ้า (σ) เจลอิเล็กโทรไลต์ที่ประกอบด้วยฟumedซิลิกา ร้อยละ 2 โดยมวลต่อปริมาตร ของกรดซัลฟิวริก ร้อยละ 35 โดยมวลต่อปริมาตร ให้ค่าการนำไฟฟ้าที่สูงที่สุด ณ อุณหภูมิ 25 องศาเซลเซียส เท่ากับ 838 มิลลิซีเมนต์ต่อเซนติเมตร นอกจากนี้ ปริมาณฟumedซิลิกาและความเข้มข้นของกรดซัลฟิวริกส่งผลต่อค่าการนำไฟฟ้า และเวลาในการเกิดเจล สารเติมแต่งที่ใช้ในงานวิจัยนี้ คือ โซเดียมซัลเฟต และกรดฟอสฟอริก เพื่อปรับปรุงอายุการใช้งานและสารกระตุ้นบนแผ่นบวก เจลอิเล็กโทรไลต์ที่ประกอบด้วยโซเดียมซัลเฟต 2.5 กรัมต่อลิตร และกรดฟอสฟอริก ร้อยละ 1.2 แสดงค่าการนำไฟฟ้าที่สูงที่สุด ณ อุณหภูมิ 25 องศาเซลเซียส เท่ากับ 840 มิลลิซีเมนต์ต่อเซนติเมตร และพบว่าความเข้มข้นของกรดฟอสฟอริกมากกว่า ร้อยละ 1.2 โดยปริมาตรต่อปริมาตร จะให้ค่าการนำไฟฟ้าลดลง นอกเหนือจากสารเติมแต่งสองชนิดนี้แล้ว ในงานวิจัยได้ใช้พอลิแอนิไลน์ซึ่งเป็นพอลิเมอร์นำไฟฟ้า สำหรับเพิ่มความสามารถในการนำไฟฟ้าของเจลอิเล็กโทรไลต์ จากนั้นได้ทำการศึกษาความสามารถในการคายประจุของแบตเตอรี่ที่ประกอบด้วยเจลอิเล็กโทรไลต์ในส่วนผสมต่างๆกันอีกด้วย

Abstract: The effect of additives on the performance of gelled-electrolyte by measuring the conductivity values was investigated for valve-regulated lead-acid batteries. The gelled-electrolyte obtaining 2%(w/v) of fumed silica and 35%(w/v) of sulfuric acid provided the highest of specific conductivity (σ) of 838 mS/cm at 25°C. Moreover, fumed silica contents and concentration of sulfuric acid effected on the gelling time. Sodium sulphate and orthophosphoric acid have been also used in this work to improve the cycle life and positive active material. The additive of 2.5 g l⁻¹ of sodium sulphate and 1.2% of phosphoric acid provided a maximum conductivity of 840 mS/cm at 25°C. It also was found that increasing the concentration of phosphoric acid (>1.2%) reduced the conductivity values. Furthermore, polyaniline as a conducting polymer has been used in this research to increase the specific conductivity of gelled-electrolyte. In addition, the discharge capacity of different gelled-electrolytes was investigated.

Introduction: Gel technology for valve-regulated lead-acid (VRLA) battery is now extensively used in several application including energy storage, emergency power and

electric vehicles. VRLA battery has been developed from flooded lead-acid battery to improve the water loss and electrolyte leaked out of battery. Due to overcharging, the oxygen gas and hydrogen gas can leak from the cells of flooded lead-acid battery, which results in water loss. This problems are rectified by using the gel technology and oxygen-recombination principle [1]. The gel technology is immobilization of electrolyte within the cells of VRLA battery. There are two types:

- (i) AGM technology, absorptive glass-mat and a highly porous;
- (ii) GEL technology, gelled-electrolyte, thixotropic and including fumed silica.

The gelled-electrolyte consists of fumed silica, sulfuric acid, deionized water and some additives. An advantages of VRLA batteries include no acid stratification, no leakage of sulfuric acid, no maintenance and long life cycle [2]. Therefore, there is growing interest in developing gelled-electrolyte by using fumed silica.

The purpose of this work is to investigate the effect of additives on the performance of gelled-electrolyte for VRLA batteries. The specific conductivity has been investigated to indicate how well to maintain high power output of batteries [3]. The effect of fumed silica contents and H_2SO_4 concentrations was studied. An additives using in these gelled-electrolyte are Na_2SO_4 and H_3PO_4 . They are used for improvement of cycle life and positive active material [4,5]. Moreover, a conducting polymer such as polyaniline (PANI) has been used to increase the conductivity of gelled-electrolyte, which is used to indicate the performance of batteries.

Methodology:

1. Gelled-Electrolyte Preparation

The gelled-electrolyte were prepared by mixing (1-4%w/v) fumed silica (Degussa) with (15-55%w/v) H_2SO_4 , deionized water and additives, respectively. First additive was added including 2.0-3.5 $g\ l^{-1}$ of Na_2SO_4 together with 1.0-3.0% of H_3PO_4 . Second additive was (0.01-0.10%w/v) PANI (Aldrich). The suspension was stirred at room temperature for 10 min with 3000 rpm of speed. Finally, a slurry of gelled-electrolyte was obtained.

2. Specific Conductivity Testing

The specific conductivity of gelled-electrolyte was measured at 25°C by using S70-K SevenMulti conductivity meter with inlab 730 conductivity probe 0-1000 $mS.cm^{-1}$.

3. Study of Gelling Time

The gelled-electrolytes with various conditions were added into lead-acid batteries (12V) to observe gel formation by the time. These gelled-electrolytes contained 1-9 %(w/v) of fumed silica and 15-40%(w/v) of H_2SO_4 .

4. Battery Testing

The different gelled-electrolytes, which provided the maximum conductivity were transferred into lead-acid batteries (12V) to study discharge performance at 25°C and 1 hour rate. Potential values were measured with the time.

Results, Discussion and Conclusion:

1. Specific Conductivity

Fig.1 Shows the specific conductivity (at 25°C) of gelled-electrolyte with different concentrations of fumed silica and sulfuric acid. At concentrations of H_2SO_4 lower than 35%(w/v), the conductivity values increase and begin to decrease at higher concentrations of H_2SO_4 more than 35%(w/v) [6]. The maximum conductivity of 838 mS/cm was obtained from using 2%(w/v) of fumed silica and 35%(w/v) of H_2SO_4 . Na_2SO_4 and H_3PO_4 were added as the first additive into the gelled-electrolyte. The results are shown in Fig.2. It was found that an addition of Na_2SO_4 more than 3.0 g l^{-1} decreased the conductivity values. The conductivity values obviously decreased after adding H_3PO_4 more than 1.2% of concentration. The maximum conductivity of 840 mS/cm was obtained from the gelled-electrolyte containing 2.5 g l^{-1} of Na_2SO_4 and 1.2% of H_3PO_4 . The decreasing of conductivity of these gelled-electrolyte was shown in Fig.3 (a) and (b).

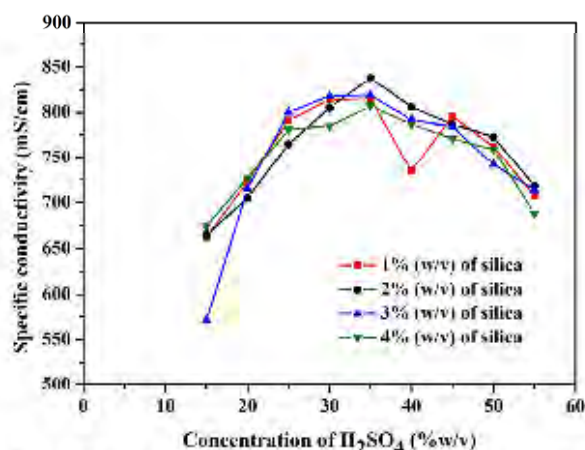


Figure 1 Variation of specific conductivity with different concentrations of fumed silica and sulfuric acid.

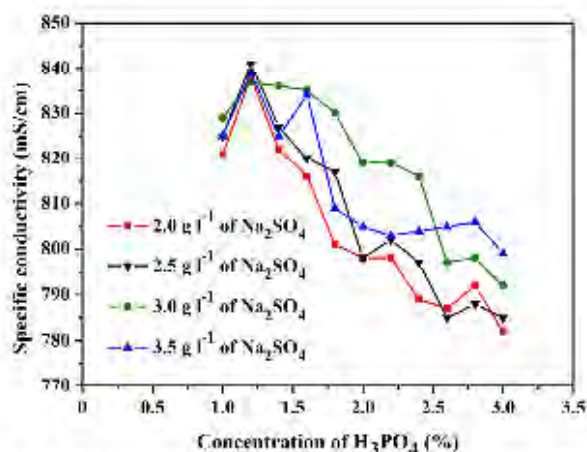


Figure 2 Variation of specific conductivity with different concentrations of Na_2SO_4 and H_3PO_4

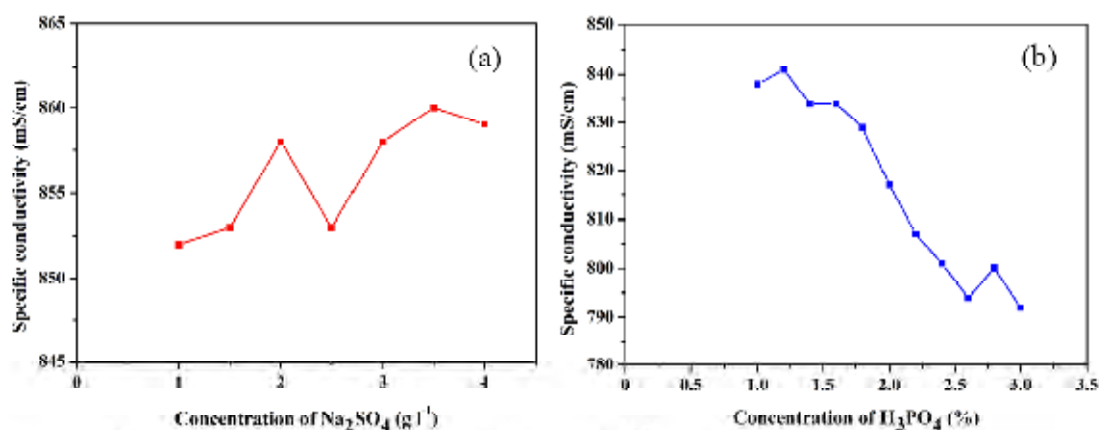


Figure 3 Variation of specific conductivity with different concentrations of (a) Na₂SO₄ and (b) H₃PO₄.

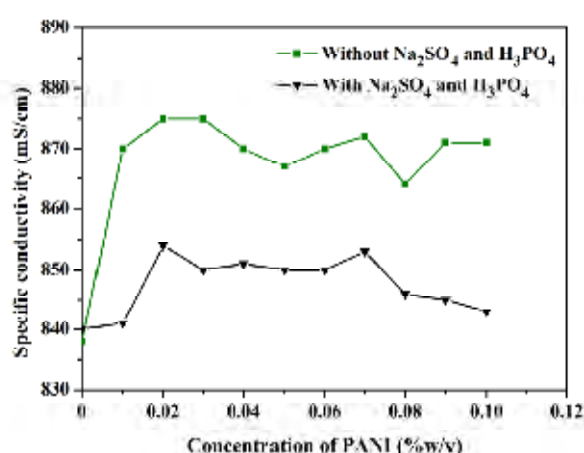


Figure 4 Variation of specific conductivity with different concentrations of PANI.

The addition of only Na₂SO₄ increased the conductivity, which can be explained by dissociation property of this salt. In contrast, the addition of only H₃PO₄ showed the decreasing of specific conductivity. This can explain why the gelled-electrolyte consisting of Na₂SO₄ and H₃PO₄ exhibit the decreasing of conductivity values. Thus, it can be concluded that the decreasing of conductivity values obtained due to adding H₃PO₄ (Fig.2). It may be presumed that there is the interaction between H₃PO₄ and silanol groups (Si-O-H) on the surface of fumed silica [7], resulting in decreasing of conductivity values.

To obtain higher conductivity, PANI as the second additive was added into the gelled-electrolyte containing 2%(w/v) of fumed silica, 35%(w/v) of H₂SO₄, 2.5 g l⁻¹ of Na₂SO₄ and 1.2% of H₃PO₄. The results are shown in Fig.4. There were two results: one was gelled-electrolyte without addition of Na₂SO₄ and H₃PO₄ and the other was gelled-electrolyte with addition of Na₂SO₄ and H₃PO₄. A considerable increase in the specific conductivity was observed at all concentrations of PANI. It is inferred from the structure of PANI that contains conjugated double bonds. The gelled-electrolyte without adding Na₂SO₄ and H₃PO₄ shows the conductivity values obviously higher than the gelled-electrolyte with adding Na₂SO₄ and H₃PO₄. Both gelled-electrolyte containing Na₂SO₄ and H₃PO₄ and gelled-electrolyte without adding Na₂SO₄ and H₃PO₄ show the maximum conductivity when using 0.02%(w/v) of PANI. The maximum

conductivity was 854 mS/cm and 875 mS/cm of the gelled-electrolyte with adding Na_2SO_4 and H_3PO_4 and without adding Na_2SO_4 and H_3PO_4 , respectively.

2. Effect of Gelling Time

The gelling time of gelled-electrolyte with different concentrations of fumed silica and H_2SO_4 was observed at ambient temperature as shown in Table 1. The results depended not only on fumed silica contents but also on the H_2SO_4 concentrations. The increasing in H_2SO_4 concentrations and fumed silica (1-4%w/v) provided the short gelling time.

Table 1 The gelling time of gelled-electrolyte with different concentrations of fumed silica and H_2SO_4 .

| Fumed silica %(w/v) | H_2SO_4 %(w/v) | Gelling time (min) |
|---------------------|--------------------------------|--------------------|
| 1 | 35 | > 60 |
| 2 | 35 | 10 |
| 3 | 35 | 10 |
| 4 | 35 | 10 |
| 5 | 30 | 20 |
| 6 | 30 | 20 |
| 7 | 40 | 10 |
| 8 | 25 | 20 |
| 9 | 15 | 25 |

3. Battery Performance

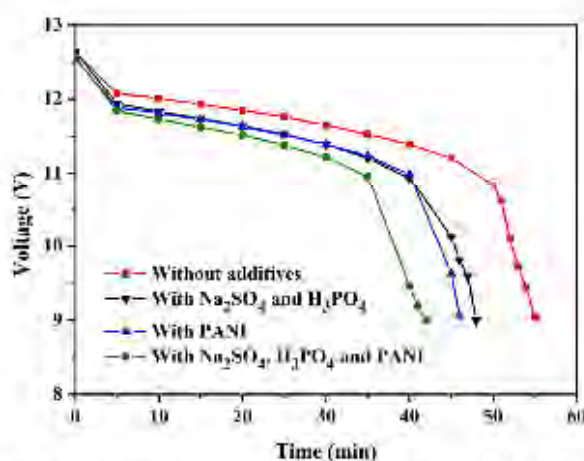


Figure 5 Initial discharge curve for lead-acid batteries (12V) at 25°C and 1-h rate.

The usage of different gelled-electrolyte in lead-acid batteries (12V) is presented in Fig.5. The discharge performance of batteries can be obtained from initial discharge at 1-h rate. Similarly, performance characteristics of different gelled-electrolyte were found. The lead-acid battery using 2%(w/v) of fumed silica and 35%(w/v) of H_2SO_4 presented higher discharge voltage and longer discharge capacity than the others. The

effect of discharge capacity may be due to active material on plates, gel filling and battery components [6].

In conclusions, the specific conductivity depended on concentrations of fumed silica, H_2SO_4 , Na_2SO_4 and H_3PO_4 . The fumed silica contents and concentrations of H_2SO_4 effected on gelling time. The gelled-electrolyte consisting of 2%(w/v) of fumed silica, 35%(w/v) of H_2SO_4 and 0.02%(w/v) of PANI provided the maximum conductivity of 875 mS/cm. Discharge capacity of the gelled-electrolyte consisting of 2%(w/v) of fumed silica, 35%(w/v) of H_2SO_4 and 0.02%(w/v) of PANI was not significant different to the gelled-electrolyte containing Na_2SO_4 and H_3PO_4 (840 mS/cm). The gelled-electrolyte without any additives provided the highest of discharge voltage and longest of discharge capacity. However, the gelled-electrolyte containing additives may be given the long life cycle and improved the positive active material more than the gelled-electrolyte without addition of some additives.

References:

1. Culpin B, Peters K. Study of transport of oxygen and water vapour between cells in valve regulated lead-acid batteries. *J. Power Sources* 2006; 158: 1077-1083.
2. Tang Z, Wang J, Mao et al. Investigation and application of polysiloxane-based gel electrolyte in valve-regulated lead-acid battery. *J. Power Sources* 2007; 168: 49-57.
3. Pavlov D, Naidenov V, Ruevski S. Influence of H_2SO_4 concentration on lead-acid battery performance II-type and P-type batteries. *J. Power Sources* 2006; 161: 658-665.
4. Hernández J C, Soria M I, González et al. Studies on electrolyte formulations to improve life of lead acid batteries working under partial state of charge conditions. *J. Power Sources* 2006; 162: 851-863.
5. Torcheux I, Lailier P. A new electrolyte formulation for low cost cycling lead acid batteries. *J. Power Sources* 2001; 95: 248-254.
6. Berndt D. Maintenance-free batteries: Lead-Acid, Nickel/Cadmium, Nickel/Hydride: A Handbook of Battery Technology, 1st edition. Taunton: Research Studies Press 1993; 50, 165-170.
7. Chen M Q, Chen H Y, Shu et al. Effects of preparation and particle size distribution on fumed silica gel valve-regulated lead-acid batteries performance. *J. Power Sources* 2008; 181: 161-171.

Keywords: gelled-electrolyte, valve-regulated lead-acid (VRLA) battery, gelling time, additive, specific conductivity

Acknowledgments: The authors would like to thank Krisana Watakeyanon, Plant Manager of N.V. Battery Ltd., Part. for supporting part of this research, National Center of Excellence for Petroleum, Petrochemicals, and Advanced Materials, NCE-PPAM and Chulalongkorn University.

The new gelled electrolyte for valve regulated lead acid batteries

Amornrat Chaisasit¹ and Orawon Chailasakul²

¹Department of Electrochemistry and Polymer Science, Faculty of Science, Chulalongkorn University, Bangkok, 10532

Phone: 66-2218-7615, Fax: 66-2218-7615, E-Mail: amornrat@mai.sru.ac.th

²Department of Chemistry Faculty of Science, Chulalongkorn University, Bangkok, 10530

Phone: 66-2218-7615, Fax: 66-2218-7615, E-Mail: orawon@mai.sru.ac.th

Abstract

The new gelled electrolyte has been studied in this work for valve regulated lead acid (VRLA) batteries. The new gel, which was optimized and prepared by means of acrylamidate is a mixture of sulfuric acid, fumed silica and other additives including sodium sulphate and phosphoric acid. In this work, the conductivity values of gelled electrolyte were measured to indicate how well it maintain high power output of batteries. It was found that fumed silica content, sulfuric acid concentration and amount of added additives affected on gel formation and the specific conductance (σ). There were disadvantages when increasing amount of fumed silica and sulfuric acid including shorter gelling time and lower specific conductivity. Moreover, it was found that increasing the concentration (10^{-3} to 10%) of phosphoric acid caused the reducing of the specific conductance. The specific conductivity results obtained from using 3.5 g.l^{-1} of sodium sulphate as the additive showed that the new gelled electrolyte provided a maximum conductivity value of 40 mS.cm^{-1} at 25°C.

Keywords: gelled electrolyte, VRLA batteries, specific conductivity, gelling time

1. Introduction

In recent years, gelled electrolyte was studied extensively due to the ever widely used of valve regulated lead acid (VRLA) batteries as the current applications, including energy storage, emergency power, and electric vehicles and owing to the continued growth of automobiles, boats and planes for which its overvoltage starting, lighting and ignition (MLI) VRLA batteries was developed from flooded electrolyte lead acid batteries because it was many disadvantages such as low maintenance, low cycle life, big ventilation and some loss [1]. The electrolyte of VRLA batteries is immobilized in two ways:

- (1) Absorbed electrolyte, a highly porous and absorbent microfiber glass mat
- (2) Gelled electrolyte, fumed silica is added to the electrolyte for harden into gel

Advantages of VRLA batteries include no acid stratification, no leakage of sulfuric acid, no maintenance and long life cycle [2]. However, it is very important to develop high performance and maintenance free batteries using the oxygen recombination principle to reduce water loss problem [3]. The gelled electrolyte consists of fumed silica, sulfuric acid, deaerated water and some additives. In this research, additives used in gelled electrolyte are sodium sulphate and phosphoric acid. They are used for the improvement of cycle life and

terminal evolution of the positive active material during cycling [4,5]. The increasing of conductivity of gelled electrolyte is useful for increasing high power output and indicate the performance of batteries. No previous work was reported about the specific conductivity measurement and optimization of gelled-electrolyte for VRLA batteries using sodium sulphate and phosphoric acid.

The aim of this work is to develop the new gelled-electrolyte which have high conductivities for VRLA batteries. The gelled electrolytes are prepared and measured by means of conductivity and gel formation which is observed by the time. The results obtained from conductivity gelled electrolyte containing sodium sulphate and orthophosphoric acid as additives will be discussed.

2. Experimental

Gelled electrolyte was prepared by mixing fumed silica with sulfuric acid, deionized water and additives respectively. Particle size of fumed silica (Degussa) is about 12 nm. The suspension consisted of 1.4 gwt% of fumed silica, 13.55 gwt% of sulfuric acid. In this work additives are 2.0 g/dm³ of Na₂SO₄ and 1.0 g/dm³ of H₃PO₄. The suspension was stirred for 10 min at 3000 rpm and room temperature. After study was homogeneous, the specific conductivity value was measured at 25°C by using SCAK SevenStar II conductivity meter with Tekel 730 conductivity probe G-1000 mS/cm. Finally, the homogeneous slurry, which has the maximum specific conductivity was transferred into lead acid battery case to investigate the gelling time.

3. Results and discussion

Fig. 1 shows the specific conductivities of gelled-electrolyte with different concentrations of fumed silica and sulfuric acid after optimized at room temperature. It is found that at lower the concentration of H₂SO₄ (3.35 gwt%), the specific conductivities increase, but these conductivities decrease at higher the concentrations of H₂SO₄ (13.55 gwt%).

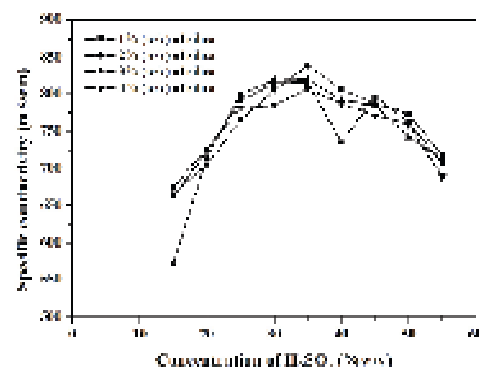


Fig. 1. Variation of specific conductivity with different concentrations of fumed silica and sulfuric acid.

The gelled electrolyte containing 2%wt% of fumed silica and 3%wt% of H₂SO₄ shows the maximum conductivity of 858 mS/cm at the gelling time of 10 min as shown in Table 1. These gelled-electrolyte was used to study the addition of sodium sulphate and orthophosphoric acid.

Table 1

The specific conductivities and gelling time of gelled electrolyte with different concentrations of fumed silica

| Fumed silica (gwt%) | H ₂ SO ₄ (gwt%) | σ (mS/cm) | Gelling time (min) |
|---------------------|---------------------------------------|------------------|--------------------|
| 1 | 35 | 815 | 15 |
| 2 | 35 | 858 | 10 |
| 3 | 35 | 815 | 15 |
| 4 | 35 | 807 | 10 |

Fig. 2 shows the specific conductivities of gelled electrolyte measured at 25°C with different concentrations of sodium sulphate and orthophosphoric acid. It was found that the addition of Na₂SO₄ more than 5.0 g/dm³ resulted in decreasing of the specific conductivities. The results from addition of H₃PO₄ is analogous to those of addition of Na₂SO₄. The specific conductivities decrease when the addition of the concentrations of H₃PO₄ are more than 1.25%.

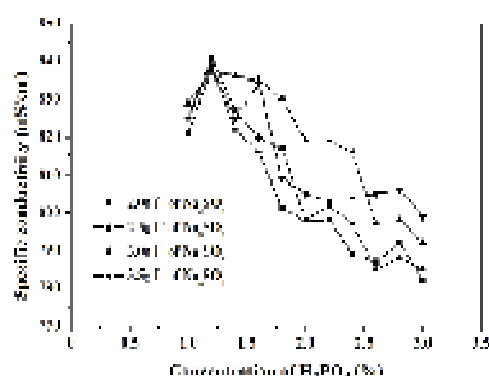


Fig. 2. Variation of specific conductivity with different concentrations of sodium sulfate and orthophosphoric acid

It was reported that high conductivity of gelled electrolyte maintain high power output for longer [6]. Therefore in this work we investigate the condition to obtain the maximum conductivity. Results (in Table 2) show the maximum conductivity obtained from gelled electrolyte containing 2.5 g L⁻¹ and 1.2% (1.0%) (340 mS/cm) at the gelling time of 10 min as shown in Table 2.

Table 2

The specific conductivities and gelling time of gelled electrolyte with different concentrations of sodium sulphate

| Na ₂ SO ₄ (g L ⁻¹) | H ₃ PO ₄ (%) | σ (mS/cm) | Gelling time (min) |
|--|------------------------------------|------------------|--------------------|
| 2.0 | 1.2 | 838 ± 2.3 | 10 |
| 2.5 | 1.2 | 873 ± 1.7 | 10 |
| 3.0 | 1.2 | 857 ± 3.8 | 10 |
| 1.5 | 1.2 | 830 ± 1.5 | 10 |

In our future work, the gelled electrolyte, which give the highest conductivity will be used for further study by the addition of polymer additive such as polyacrylamide to decrease gel time and polyacrylamide as a conductive polymer for improvement of conductivity of gelled electrolyte. The relationship of the specific conductivity, discharge volume and cycle life will be studied.

6. Conclusions

Effect of gel formation and specific conductivities depends on concentrations of fumed silica, sulfuric acid and additives including sodium sulfate and orthophosphoric acid. The addition of fumed silica at 2% (w/w) and sulfuric acid at 85% (w/w) provides the maximum conductivity. The increase of fumed silica and sulfuric acid will give long and cheap specific conductivity values. The addition of Na₂SO₄ and H₃PO₄ at 2.5 g L⁻¹ and 1.2%, respectively resulted in the maximum conductivity. It was also found that the specific conductivity values decreased when increasing the concentrations of H₃PO₄ (>1.2%).

Acknowledgements

The authors would like to thank Krisna Widiyayanti, Plant Manager of SOE Battery Ltd, and for supporting part of his research, and Ulsungjeon University.

References

- [1] Rode, H. Lead-acid batteries, A Wiley-Interscience, New York, 1977.
- [2] Landon, D.W.H., Greenwood, P.H.J., Reed, M.C., J. Power Sources 107 (2002) 173-176.
- [3] Chidari, B., Pezara, K., J. Power Sources 158 (2006) 1077-1083.
- [4] Taramakan, J.C., Soria, M.T., Gonzalez, M., Garcia-Quintero, J., Munoz, A., Trinidad, F., J. Power Sources 187 (2008) 351-357.
- [5] Taramakan, J., Lillo, P., J. Power Sources 95 (2001) 248-254.
- [6] Pacheco, D., Nobiletti, W., Pavesi, S., J. Power Sources 161 (2000) 658-667.

VITA

- Name** : Miss Amornrat Chaiyasit
- Date of birth** : November 11, 1982
- Gender** : Female
- Education** : 1998-2001 M.6 at Wat Songtham School, Major of Science-Mathematic
- 2001-2005 Bachelor's Degree of Science at King Mongkut's University of Technology Thonburi, Major of Chemistry
- 2006-2008 Master's Degree of Science at Chulalongkorn University, Major of Petrochemistry and Polymer Science
- Home Address** : 21, Moo 2, Tambol Banghuasau, Amphur Phrapradang, Samutprakarn 10130, Thailand
- Proceedings** :
1. **Chaiyasit, A.;** and Chailapakul, O. (31 October-2 November, 2008) Effect of Additives on Performance of Gelled-Electrolyte for Valve-Regulated Lead-Acid Batteries. Proceeding of STT34, Bangkok, Thailand.
 2. **Chaiyasit, A.;** and Chailapakul, O. (16-19 September, 2008) The New Gelled-Electrolyte for Valve-Regulated Lead-Acid Batteries. Proceeding of MSAT-5, Bangkok, Thailand.